Modeling of human vitreous as viscoelastic fluid considering the orientation of collagen fibers

DISSERTATION

zur Erlangung des akademischen Grades

Doktor der Naturwissenschaften (Dr. rer. nat.)

im

Fachbereich Mathematik und Naturwissenschaften

der

Universität Kassel

vorgelegt von

Judith Stein

Heidelberg, November 2021

First advisor: Prof. Dr. Elfriede Friedmann, Universität Kassel
Second advisor: Prof. Dr. Vít Průša, Charles University Prague

Day of the disputation: April 11, 2022

Abstract

For the most common treatment of retinal diseases worldwide by drug distribution in the human vitreous we developed the mathematical model of the vitreous. Compare to previous works we focus on the vitreous as a viscoelastic fluid including its heterogeneous property due to the orientation of collagen fibers. By using the incompressible viscoelastic Burgers-type model based on experimental data as the specific constitutive equation in the setting of continuum mechanics we considered its non-Newtonian nature. This viscoelastic response is derived from the interaction between hyaluronan, aqueous humor and elastic collagen fibers. The stability analysis of the spatially inhomogeneous non-equilibrium steady state for the incompressible heat conducting viscoelastic Burgers-type fluid was proven. The steady state is asymptotically stable irrespective of the initial conditions and of the shape of the domain. To investigate the influence of the rheology of the vitreous we analyzed its mechanical behavior in a deforming eye ball leading to a fluid-structure-interaction problem. We found that the healthy vitreous predicted by the Burgers-type model showed twice as high stress as the liquefied one predicted by the Navier–Stokes model. The coupling of the viscoelastic Burgers-type model with the drug distribution through the stress driven diffusion provides a fully coupled system of partial differential equations in contrast to the proposed models in the literature. The diffusion in the vitreous depends on the viscoelastic properties of the vitreous which act as a barrier to the drug distribution. The extension to an anisotropic stress driven diffusion reflects the tendency to follow the preferential direction along the collagen fibers depending on the molecule size. As an innovative approach we derived a thermodynamically consistent model for the vitreous as a viscoelastic fluid whose elastic reaction is anisotropic and took into account the heterogeneous property of the vitreous and its orientated collagen fibers. Our developed models about the mechanical behavior of the human vitreous and its influence on the drug distribution give a better understanding of the physiological and pathological processes in the eye.

Zusammenfassung

Für die weltweit häufigste Behandlung von Netzhauterkrankungen durch Wirkstoffverteilung im menschlichen Glaskörper haben wir das mathematische Modell des Glaskörpers entwickelt. Im Vergleich zu früheren Arbeiten konzentrieren wir uns auf den Glaskörper als viskoelastische Flüssigkeit einschließlich seiner heterogenen Eigenschaften aufgrund der Ausrichtung der Kollagenfasern. Durch die Verwendung des inkompressiblen viskoelastischen Burgers Modells, das auf experimentellen Daten basiert, als spezifische konstitutive Gleichung im Rahmen der Kontinuumsmechanik haben wir die nicht-Newtonsche Natur des Glaskörpers berücksichtigt. Diese viskoelastische Reaktion ergibt sich aus der Wechselwirkung zwischen Hyaluronsäure, Kammerwasser und elastischen Kollagenfasern. Die Stabilitätsanalyse des räumlich inhomogenen Nichtgleichgewichtszustandes für die inkompressible wärmeleitende viskoelastische Burgers Flüssigkeit wurde nachgewiesen. Der stationäre Zustand ist asymptotisch stabil, unabhängig von den Anfangsbedingungen und der Form des Gebiets. Um den Einfluss der Rheologie des Glaskörpers zu untersuchen, analysierten wir sein mechanisches Verhalten in einem sich verformenden Augapfel, was zu einem Fluid-Struktur-Interaktionsproblem führte. Wir fanden heraus, dass der gesunde Glaskörper, der durch das Burgers Modell vorhergesagt wurde, eine doppelt so hohe Spannung aufwies wie der verflüssigte Glaskörper, der durch das Navier-Stokes Modell beschrieben wurde. Die Kopplung des viskoelastischen Burgers Modells mit der Medikamentenverteilung durch die spannungsgesteuerte Diffusion liefert ein vollständig gekoppeltes System von partiellen Differentialgleichungen, im Gegensatz zu den in der Literatur vorgeschlagenen Modellen. Die Diffusion im Glaskörper hängt von den mechanischen Eigenschaften des Glaskörpers ab, die als Barriere für die Medikamentenverteilung wirken. Die Erweiterung auf eine anisotrope spannungsgesteuerte Diffusion spiegelt die Tendenz wider, abhängig von der Molekülgröße der Vorzugsrichtung entlang der Kollagenfasern zu folgen. Als neuartigen Ansatz haben wir ein thermodynamisch konsistentes Modell für den Glaskörper als viskoelastische Flüssigkeit hergeleitet, deren elastische Reaktion anisotrop ist und die heterogenen Eigenschaften des Glaskörpers und seiner orientierten Kollagenfasern berücksichtigt. Die von uns entwickelten Modelle über das mechanische Verhalten des menschlichen Glaskörpers und seinen Einfluss auf die Medikamentenverteilung ermöglichen ein besseres

Verständnis der physiologischen und pathologischen Prozesse im Auge.

Contents

1 Introduction

The development of mathematical models describing the drug distribution in the human vitreous after an intravitreal injection used for the treatment of retinal diseases play nowadays an important role in the drug development and optimization of personalized therapies. In this context the appropriate modeling of the vitreous is crucial and the concentration distribution depends on the properties of the vitreous. Key aspects are its *non-Newtonian viscoelastic nature* and the heterogeneous structure of the *elastic collagen fibers* inside the vitreous [159].
The retinal disease, wet aged-related macular degeneration, is the leading cause of vision loss in people aged 50 years or older and involves damage to the area responsible for sharp central vision due to abnormal blood vessel growth. The therapy consists of intravitreal injections which are administered over a period of time depending on the pathology. Thereby an active ingredient is injected in the vitreous that diffuse to the retina and effect there locally through molecular mechanism.

A first diffusion model to describe dispersion of drugs in the vitreous of a rabbit is written in [62] where they assumed that the vitreous is stagnant. Later studies extended the simple diffusion by a convection term which arises because of aqueous humor flow through the vitreous driven by a pressure drop between the anterior and the posterior surfaces [75]. But all of the previous studies model the vitreous humor as an incompressible Newtonian fluid ignoring the non-Newtonian property capable of describing its complex behavior seen in experiments [180, 164] and its influence on the drug distribution. The most common model in the literature uses the Darcy equation [75, 170]. In [2, 153] the incompressible Navier-Stokes equation describes the liquefied vitreous in age where they focus on the motion of the vitreous. Considering the drug distribution the drug is transported by convection of the induced flow field of the vitreous. The influence of the mechanical properties of the vitreous on the distribution rate of the drug as well as the effect of the spreading of the medicine molecules on the vitreous are not considered in the literature.

Motivation of the Thesis In this work and the parameters contained therein we focus on the most common retinal disease, especially aged-related macular degeneration. In 2013 it was the fourth most common cause of blindness [34] and affected in 2015 around 6.2 million people globally [1]. To date, there is no therapy response in 10.1-45 % of the patients [15], only a small drug concentration range is effective and higher concentrations may be toxic. In order to assess the effectiveness of the injected drug, it is of fundamental and therapeutic interest to model the physiology of the human vitreous. The motivation of this thesis is the improvement of the administered ophthalmic therapy through a better understanding of the properties of the vitreous humor provided by the ability to model its mechanical behavior and its influence on the drug distribution.

Objective and Method of the Thesis The contribution of this thesis is the development of our mathematical models describing the human vitreous as a viscoelastic fluid. The proposed models consider the heterogeneous structure of collagen fibers inside the vitreous and couple its induced flow field to the drug distribution for the treatment of retinal diseases. They are systems of coupled partial differential equations completed with initial and mixed boundary conditions, considering the complex biology of the vitreous and the surrounding tissues in the human eye. They are fully coupled in which the drug diffusion and flow of the vitreous can effect each other.
To our knowledge, we are the first considering the non-Newtonian nature of the vitreous body by using a thermodynamically derived *viscoelastic Burgers-type fluid* in the modeling of drug transport. We extend it to an *anisotropic viscoelastic fluid* taking into account the preferred direction of the elastic collagen fibers. Since the available experimental data in the literature do not coincide in their mechanical analog with our preferable model for the human vitreous, we converted the set of parameters characterizing the viscoelastic response by solving a nonlinear system of equations.
Further, we propose fully coupled systems extended by the Korteweg stress or *stress driven diffusion* in which the drug diffusion and flow inside the vitreous can effect each other. The vitreous acts as a barrier to the diffusion which has not yet been addressed in its modeling before. We generalize the existing approaches for stress driven diffusion by constructing an *anisotropic stress driven diffusion* tensor including the heterogeneous structure of collagen fibers inside the vitreous and introduce a possible generalization to three space dimensions.
In Section 4.5 also presented in the publications [173, 182], we analyzed the mechanical behavior of the vitreous in a deforming eye ball leading to a *fluid-structure-interaction problem*. In contrast to other studies, the geometry of the

vitreous is not fixed and does not take the spherical shape but a realistic geometrical setting in which the deformations of the sclera and lens induce the flowing of the vitreous. The focus on the interplay between the rheology of the vitreous and the stress field in it is of interest in the study of retinal pathologies and can answer clinically relevant questions.
In Section 4.4 published in [172], we examined the *stability of the rest state* of viscoelastic models with temperature dependent material coefficients to find the additional restrictions on the energetic equation of state which are well-known in the case of compressible Navier-Stokes fluid but not in the case of complex viscoelastic fluids. In our publication [38] the stability of a spatially inhomogeneous non-equilibrium steady state is investigated for incompressible *heat conducting viscoelastic rate-type fluids* occupying a mechanically isolated domain but allowing heat exchange with the surrounding. In this thesis we further extend the results to the more complex Burgers-type fluid characterizing the human vitreous. In this case, the standard methods for thermodynamically isolated systems or systems immersed in a thermal bath can not be used since the steady state is a non-equilibrium (entropy producing) steady state due to the constant spatially nonuniform temperature at the domain's walls. We proved that the steady state is asymptotically stable irrespective of the initial conditions and of the shape of the domain.

Structure of the Thesis This thesis is structured as follows: The first part deals with the biological and mathematical introduction. In Chapter 3, the well known models from the literature of drug distribution within the vitreous are presented and theoretical questions in analysis of existence and uniqueness of these models are explored. Section 3.1 gives an overview of the used geometry and the considered distinguishable boundaries. In Section 3.2 and 3.3, the modeling of the vitreous is introduced and coupled with the drug distribution in Section 3.4. The last Section includes the gravitational force to the introduced models. As a novel approach Chapter 4 is devoted to the viscoelastic approach for modeling the healthy vitreous using the Burgers-type model. The full system of governing equations is introduced in Section 4.1 and mechanically and thermodynamically derived in Section 4.2. Section 4.3 is about the setting of the parameter based on experimental data. Considering temperature changes in Section 4.4 we examine the stability of the rest for the incompressible heat conducting Burgers-type fluid.To investigate the influence of the rheology of the vitreous we analyze its mechanical behavior in a deforming eye ball leading to a fluid-structure-interaction problem in Section 4.5. Here, the sclera and the lens are modeled as hyperelastic solids. Section 4.6 presents the more realistic models of drug distribution within the vitreous

including the surface tension and stress driven diffusion due to viscoelastic properties of the vitreous. Corresponding numerical simulations in Section 4.7 are performed with the finite element method to compare the different rheological models of the vitreous and their influence on the drug distribution. Finally in Section 4.8, we consider the heterogeneous structure of the collagen fibers by extending the drug distribution to an anisotropic approach and deriving a thermodynamically consistent model for the vitreous as a viscoelastic fluid whose elastic reaction is anisotropic. A conclusion and outlook for future projects is given in Chapter 5.

2 Biological and Mathematical Background

2.1 Biological Background

The eye is an organ of the visual system with its anatomy divided into an anterior and posterior segment [110]. The anterior segment is composed of the cornea, lens, iris, ciliary body and aqueous humor, while the posterior segment consists of the retina, posterior sclera, choroid and vitreous humor (see Figure 2.1).

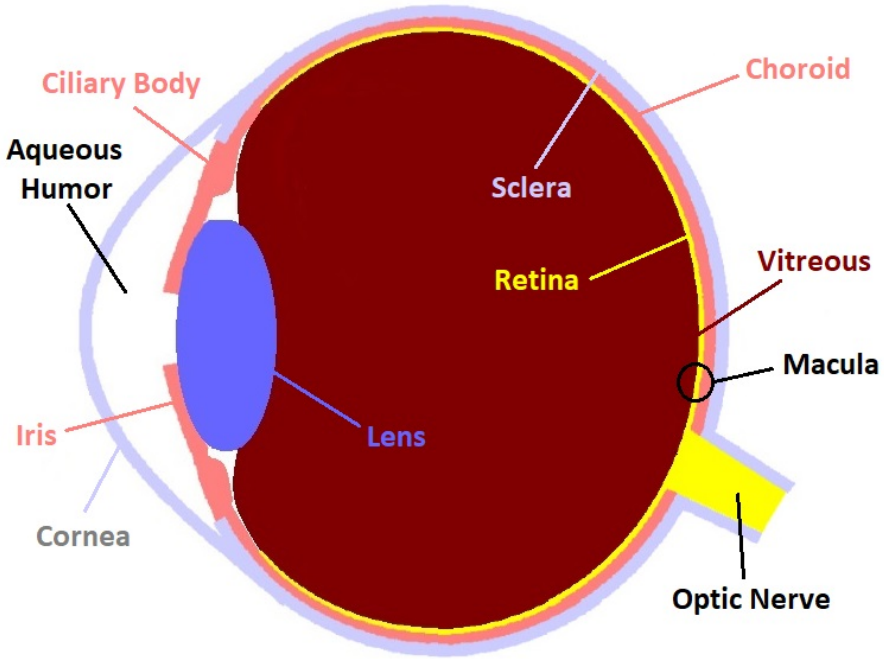

Figure 2.1: Structure of the eye

2.1.1 Aqueous humor

The aqueous humor is a transparent, watery fluid produced by the ciliary body (a structure supporting the lens) that flows into the anterior chamber, the space between the cornea and iris, through the pupil and leaves the posterior eye through the retina [159]. A major function of the aqueous humor is to provide nutrients for the cornea and lens. The production rate of aqueous humor is approximately 2.5 μl/min [132], which results in the intraocular pressure (IOP) of the eye.

2.1.2 Lens

The lens is the transparent biconvex tissue in the eye that is responsible for accommodation and refraction of light to be focused on the retina. The lens, by changing shape, can focus objects at various distances which is known as accommodation. Therefore, it is elastic, made up of elongated lens fiber cells.

2.1.3 Sclera

The sclera is the white colored part and the outer layer of the eye. This tissue is composed mainly of collagen and elastic fibers. The main function of the sclera is to provide a protective layer for the internal components of the eye.

2.1.4 Retina

The retina is the light-sensitive tissue of the eye. It contains the light sensing cells and supporting cells that are needed for the vision. The light entering the eye is transmitted to the brain with electrical neural impulses via the optic nerve and creates visual perception. The retina is supplied with blood by the choroid layer. It represents a barrier to drug delivery from the vitreous.
Near the center of the retina there is an oval-shaped area called the macula. It is responsible for the central, high-resolution, color vision and leads to loss of central vision if it is damaged, for example in age-related macular degeneration.

2.1.5 Vitreous Humor

The vitreous humor, also called the vitreous body or just vitreous, fills more than 2/3 of the eye volume and is situated between the lens and the retina, see Figure 2.1. In [159] the several functions of the vitreous are summarized in different categories: (1) developmental - mediating proper growth of the eye,

(2) optical - maintaining a clear path to the retina, (3) mechanical - supporting the various ocular tissues during physical activity (serving as a damper for the eye and absorbing impacts) and (4) metabolic - providing a repository of various small molecules for the retina.
It is transparent and contains of 98 % water and 2 % proteins, yet it behaves like a viscoelastic gel. This is due to a meshwork of collagen fibrils that are suspended in a network of hyaluronan/ hyaluronic acid (HA) [160]. In [160] a transmission electron micrograph taken from the central vitreous shows that parallel collagen fibrils are packed into bundles that aggregate and form visible fibers. Hyaluronic acid and water molecules fill the interfibrillar spaces. The presence of both hyaluronic acid and collagen together determine the viscoelastic properties of the vitreous. They provide strength and resistance to tractional forces.
Further the vitreous body is not completely homogeneous [67]. Anatomically, the vitreous is subdivided into different regions including the central, cortical vitreous and vitreous base as shown in Figure 2.2. These regions have different rheological properties as a result of differences in collagen fibers concentration and orientation. In the central vitreous parallel collagen fibers run with

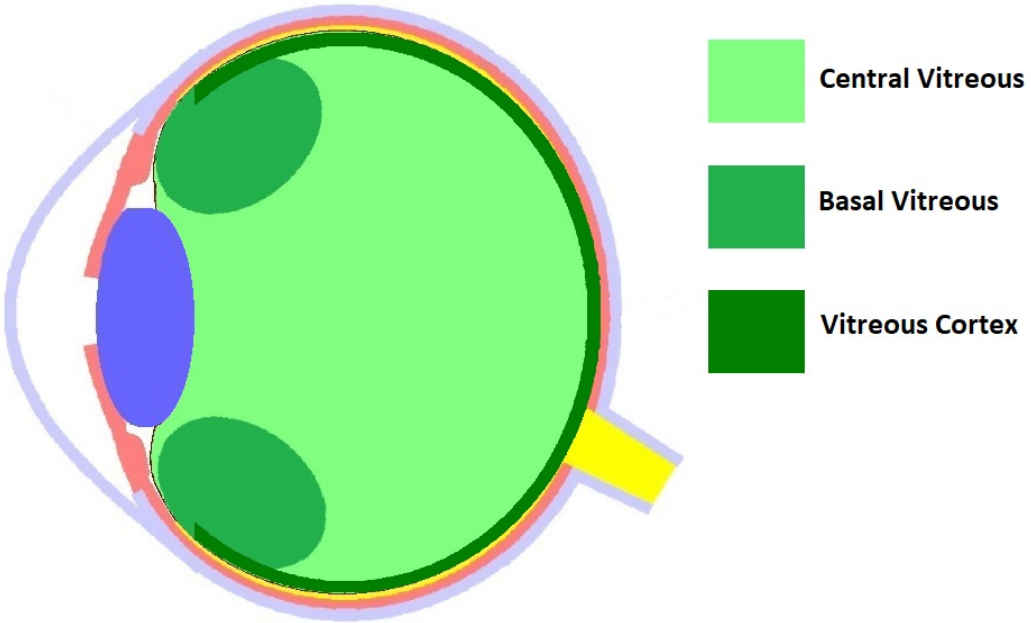

Figure 2.2: Regions within the vitreous

an anterior-posterior orientation attached to vitreous base and macula in the vitreous cortex [159]. Here is the lowest collagen concentration, 52 μg/ml, see [6]. A denser collagen fibrillar network is formed in the outer layer of the

vitreous, the so-called vitreous cortex. It can be seen in freeze etching/rotary shadowing electron microscopy images of the fibrillar network of a bovine vitreous in [25]. The cortex runs from the pars plana to the posterior lens, where it shares its attachment with the posterior zonule via Wieger's ligament, also known as "Egger's line" [155]. Specially, the anterior part is called the anterior hyaloid membrane, a highly porous membrane that separates the front of the vitreous from the anterior segment of the eye. In this region the aqueous humor can flow into the vitreous and can be degraded at the retina through the choroid [159]. The densest collagen fibrillar network is in the basal vitreous, 112 μg/ml [6], in which the fibers are arranged in thicker bundles inserting into the posterior ciliary body (pars plana) and the anterior retina [25]. The highest concentrations of hyaluronan are in the posterior vitreous cortex and the central vitreous is more liquid than the cortical vitreous [67]. An S-shaped channel free of collagen fibrils is an embryologic vascular remnant, referred as the Cloquet's chanal, running through the vitreous from the optic disc to the posterior lens [155]. It is visualized by dark-field slit microscopy in [159].

A diagram of the concept of the vitreous body anatomy can be found in [161]. It proposes cisternal systems from top to bottom identified by injecting with colored India ink. Light brown from Jongebloed and Worst [89].

Aging change

With aging the rheological properties of the vitreous change and tend towards a more liquid form, especially notable in the center of the vitreous where the collagen concentration is lowest. This disintegration of the gel structure is called liquefaction.
The young and healthy vitreous at birth is entirely gelatinous. Collagen fibrils are packed in bundles and form an extended interconnected network by branching between these bundles [67]. The fibrils run closely together in parallel, but are not fused. With increasing age thiner collagen fibrils fuse together which results in collagen fibrillar aggregation due to the degradation of collagen type IX preventing the collagen fibrils from adhering to each other. The aggregation of collagen fibrils results in the collapse of the vitreous and expulsion of the hyaluronic acid inside the collagen-hyaluronan network. The once homogeneous gel separates into heterogeneous phases.
From a diagram showing the liquefaction of the human vitreous in age in [110] you can see that more than half of the vitreous is liquid by the age of 80–90 years. The network density of collagen decreases and is replaced with pockets of liquid vitreous (lacunae), which melt together over time [159]. This results in an increasing heterogeneity.

The inhomogeneities created by these pockets and the total liquefaction in old age or after a vitrectomy effect the rate of diffusion of intravitreally applied medications. Therefor, it is important to study the mechanical properties of the vitreous to gain insight into diseases and the release and transport profile of intraocular drugs injected into the vitreous humor and understanding of the pathological conditions of the vitreous humor.

2.2 Mathematical Background

To describe physical processes like the drug distribution in the human vitreous we need a system of mathematical equations capable of modeling the behavior of complex situations. In the setting of continuum mechanics the balance equations (for mass, linear and angular momentum and energy), completed by the formulation of the second law of thermodynamics form the basis to describe various physical phenomena.

At the beginning of this chapter short mathematical preliminaries and basic notations are introduced. After that, the required theory of continuum mechanics is briefly stated. At the end, we give an overview of the derivation of the balance equations for mass, momentum, angular momentum, total energy and concept of entropy. They describe the general behaviour of the considered process and can be seen as reformulations of fundamental physical laws (e.g. Newton's law) which are universally valid for any continuous medium. But the critical and most difficult part in formulating the system of governing equations for a given material in the considered process is the specification of the response of the material to the given stimuli. An extra set of material specific equations is necessary, the so-called constitutive relations.

2.2.1 Basic Notation

In order to understand the derivation of the models, the main notation and function spaces are introduced.

In this thesis, let Ω be a domain of $\mathbb{R}^d, d \in \{2,3\}$. The spaces $L^p(\Omega)$ denote the Lebesgue spaces of order $1 \leq p \leq \infty$ and $H^s(\Omega)$ are the usual Sobolev spaces of order $s \geq 0, s \in \mathbb{R}$ with their corresponding norms. The space of continuous, real-valued functions on Ω which admit continuous partial derivatives up to order $m \in \mathbb{N}$ is denoted by $C^m(\Omega)$. $C^\infty(\Omega)$ describes the space of smooth functions on Ω. $L^p(0,T;X)$ defines the time involving Leray-Hopf

space for any Banach space X and time $0 < T < \infty$. For a bounded domain the space $C^{0,1}(\Omega)$ is called the space of Lipschitz continuous functions.
$(\cdot, \cdot)$ is the scalar product on $L^2(\Omega)$ and for the corresponding norm we will use the notation $\| \cdot \|_{L^2(\Omega)}$ and sometimes skip the space index if it is clear from the context.
A detailed introduction into the definition of these spaces and the theory of partial differential equations can be found in [48, 191, 156].

2.2.2 Continuum Mechanics

Before deriving the balance equations and constitutive relations we briefly introduce the theory of continuum mechanics. We assume that the material of interest entirely fills the whole space and we ignore the micro-structure of it like the fact that the fluid is made of atoms and molecules. Therefor, continuum mechanics can be used only on scales that are much greater than the distances between molecules. The reader who is not yet familiar with the field of continuum mechanics and thermodynamics is referred to [74].

Let $\Omega \subset \mathbb{R}^3$ be the continuous body which initially occupies a typical region $\kappa_0(\Omega)$ at a fixed reference time $t = t_0$ (usually $t_0 = 0$). This region is called the reference configuration of that body Ω. At a later time $t > t_0 > 0$ the continuous body is in a deformed position known as the current configuration $\kappa_t(\Omega)$. The function χ describes the motion of the body that maps the positions $X \in \kappa_0(\Omega)$ of points to their respective positions $x \in \kappa_t(\Omega)$, such that $x = \chi(X, t)$. Concerning a suitable framework for the description

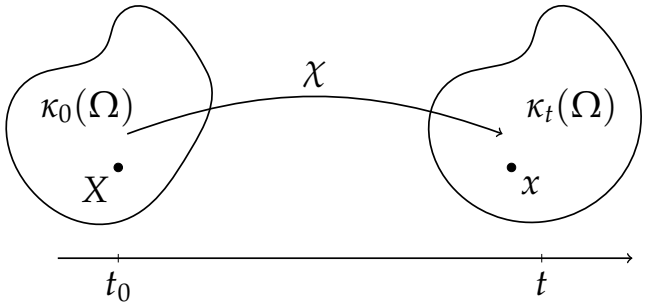

Figure 2.3: Motion of a continuous body

of processes in a continuous medium there are two choices. The Lagrangian description is suitable for the description of change of shape where in order to specify the change a reference point is needed. Here we consider the change with respect to the initial state $\kappa_0(\Omega)$ and it is chosen to study the motion of

solids. In contrast, the Eulerian framework focus on the rate of change (the time derivative) and refers to the state of the material at the current time $\kappa_t(\Omega)$ and in its infinitesimally small time neighborhood. It means one is interested in the velocity and there is no need to know the complete trajectories of the individual points. Hence the Eulerian description is used in the theory of fluids.

The Lagrangian velocity V defined on the reference configuration is the time derivative of the mapping

$$V(X,t) := \frac{\partial \chi(X,t)}{\partial t}$$

and the relation between V and the Eulerian velocity v living on the current configuration is given by

$$v(x,t) = v(\chi(X,t),t) := V(X,t).$$

The symmetric part of its gradient $\frac{\partial v(x,t)}{\partial x}$ is

$$\mathbb{D} := \frac{1}{2}\left(\nabla v + (\nabla v)^T\right)$$

and

$$\mathbb{F} := \frac{\partial \chi(X,t)}{\partial X}$$

defines the deformation gradient. Another important relation is

$$\begin{aligned} \frac{dv(x,t)}{dt} :&= \frac{\partial v}{\partial t} + \frac{\partial v(\chi(X,t),t)}{\partial x}\frac{\partial \chi(X,t)}{\partial t} = \frac{\partial v}{\partial t} + (\nabla v)v \\ &= \frac{\partial v}{\partial t} + (v\cdot\nabla)v \end{aligned} \tag{2.1}$$

which denotes the material time derivative in Eulerian description. The relation between the deformation gradient and the velocity gradient is the following

$$\frac{d\mathbb{F}}{dt} = \frac{d}{dt}\left(\frac{\partial \chi}{\partial X}\right) = \frac{\partial}{\partial X}\left(\frac{dx}{dt}\right) = \frac{\partial v}{\partial X} = \frac{\partial v}{\partial x}\frac{\partial x}{\partial X} = (\nabla v)\mathbb{F}. \tag{2.2}$$

Let $\mathbb{A}^T$ denote the transpose of a tensor $\mathbb{A}$. Then the left and right Cauchy–Green tensors are defined through

$$\mathbb{B} := \mathbb{F}\mathbb{F}^T, \qquad \mathbb{C} := \mathbb{F}^T\mathbb{F}. \tag{2.3}$$

2.2.3 Balance Equations

The balance equations used in the study of fluids are derived by applying the classical laws of Newtonian physics and classical thermodynamics. Thereby, the main mathematical tool is the Reynolds transport theorem [74].

Balance of mass

One classical law of Newtonian physics is the conservation of mass, i.e. mass can not de created or destroyed during physical processes. A generalization of this law to the continuum mechanics setting is given by:

$$\frac{d\rho}{dt} + \rho \operatorname{div} v = 0 \tag{2.4}$$

where ρ is the fluid density.

Balance of linear momentum

The generalization of Newton's second law provides the balance of linear momentum:

$$\rho \frac{dv}{dt} = \operatorname{div} \mathbb{T} + \rho f \tag{2.5}$$

with the body force $f(x,t)$ (like gravitational force) and the Cauchy stress tensor $\mathbb{T}(x,t)$ describing interaction between the given volume of the material and its surrounding.

Balance of angular momentum

The balance of angular momentum is the consequence of Newton's laws of motion which provides the symmetry of the Cauchy stress tensor:

$$\mathbb{T} = \mathbb{T}^T. \tag{2.6}$$

Balance of energy

The balance of energy and entropy are only needed for thermal effects in thermodynamics compare to mechanics (neglecting them). Repeating the same steps like in thermodynamics (multiplying the balance of momentum by v) with the non-mechanical energy exchange through the volume boundary (energy is transferred from the volume into the surrounding) we derive the balance of total energy

$$\rho \frac{de_{\text{tot}}}{dt} = \operatorname{div}(\mathbb{T}v) - \operatorname{div} j_e + \rho f \cdot v + \rho r$$

where $e_{\text{tot}}(x,t)$ is the total energy. It is the sum of internal (non-mechanical) and kinetic (mechanical) energy:

$$e_{\text{tot}} = e + \frac{1}{2}|v|^2.$$

j_e is the energy flux and r is the density of external energy sources. In the simplest setting, the energy flux tantamount to the heat flux.
The balance of the internal energy $e(x,t)$ (like thermal energy) reads

$$\rho\frac{de}{dt} = \mathbb{T} : \mathbb{D} - \operatorname{div} j_e + \rho r \tag{2.7}$$

where the symbol : denotes the scalar product of tensors and is defined by

$$\mathbb{A} : \mathbb{B} := \operatorname{tr}(\mathbb{A}\mathbb{B}^T)$$

and since the Cauchy stress is symmetric we have the relation

$$\mathbb{T} : \mathbb{D} = \mathbb{T} : \nabla v = \operatorname{div}(\mathbb{T}v) - \operatorname{div}(\mathbb{T}) \cdot v.$$

The term $\mathbb{T} : \mathbb{D}$ in (2.7) is called the stress power and plays a fundamental role in thermodynamics of continuous medium.

Balance of entropy

The entropy $\eta(x,t)$ is a fundamental state variable in thermodynamics and measures the degree of disorder in a system. The balance of entropy is

$$\rho\frac{d\eta}{dt} + \operatorname{div} j_\eta =: \xi \tag{2.8}$$

where ξ is the entropy production and $j_\eta := \frac{j_e}{\theta}$ describes the entropy flux.
Note that the balance of entropy is not necessary for a complete system of equations, because it can be specified as a function of the internal energy and the other state variables, i.e. $e = e(\eta, \rho, \dots)$.
But it is needed to show if the second law of thermodynamics is fulfilled (total entropy of an isolated system can never decrease over time). It says the entropy production has to be positive, i.e.

$$\xi \geq 0. \tag{2.9}$$

2.2.4 Material Specific Constitutive Equations

The motion of any single continuous medium in the Eulerian framework is governed by the following system of partial differential equations:

$$\frac{d\rho}{dt} + \rho \operatorname{div} v = 0, \tag{2.10a}$$

$$\rho \frac{dv}{dt} = \operatorname{div}\mathbb{T} + \rho f, \tag{2.10b}$$

$$\mathbb{T} = \mathbb{T}^T, \tag{2.10c}$$

$$\rho \frac{de}{dt} = \mathbb{T} : \mathbb{D} - \operatorname{div} j_e. \tag{2.10d}$$

where the conservations of mass (2.4), linear (2.5) and angular momentum (2.6) describe the whole mechanics in a physical process. Concerning thermal effects the balance of internal energy (2.7) characterizes the thermodynamics. Additionally, we need boundary and initial conditions to specify the considered process. The unknown quantities are the density ρ, the velocity field v, the specific internal energy e, the Cauchy stress $\mathbb{T}$ and heat flux j_e. The equations (2.10) remain valid in all branches of continuum mechanics but do not distinguish between different materials. They are insufficient for the description of the evolution of the quantities of interest. The Cauchy stress tensor and the heat flux are not specified because they are a priori unrelated to the rest of the unknowns. Therefore, in order to get a closed system of governing equations, we need extra equations relating the stress and the heat flux to the other quantities based on the assumptions on the behavior of the material.

$$\mathbb{T} = \mathbb{T}(\rho, v, e), \qquad j_e = j_e(\rho, v, e)$$

These relations are called the constitutive relations. They depend on two things: the given material and the considered process. For example the same material can show different properties in different processes (heating, cooling, ...). It is a simplified description of the physical reality and a critical and difficult part in formulating the system of governing equations.

Liquids and gases are characterized by the fact that the Cauchy stress tensor is always spherically symmetrical at rest, i.e.

$$\mathbb{T} = -p\mathbb{I}$$

for $v = 0$. Therefore in all fluid models we consider $\mathbb{T}$ in the form:

$$\mathbb{T} = -p\mathbb{I} + \mathbb{S}, \tag{2.11}$$

where $p\mathbb{I}$ is the spherical part with p called the pressure and $\mathbb{I}$ is the unit tensor. The deviatoric part $\mathbb{S}$ is called the extra stress tensor which measures the frictional tension (or also called shear stress). Now, $\mathbb{S}$ is the only part which has to be further specified by an extra evolutionary equation (the constitutive relation depending on the other quantities).

The approach is based on mechanical and thermodynamical considerations, such as the symmetry of the material and the requirement of the invariance of the constitutive relations with respect to the change of the observer, coordinate system and the conformance of the second law of thermodynamics. In particular, the relative rotation of the fluid should not affect its internal stress which is called material frame indifference and leads to the conclusion that $\mathbb{S}$ only depends on the symmetric part of the gradient of v, i.e. $\mathbb{D}$. From the balance of angular momentum it can be seen that the Cauchy stress $\mathbb{T}$ and so $\mathbb{S}$ should be symmetric. Further, for a homogeneous fluid it is assumed that $\mathbb{S}$ does not depend explicitly on time or position.

Compressible/incompressible fluids

Incompressible Fluids First, we divide into compressible and incompressible fluids where incompressibility means that the density of any given material point X is constant in time:

$$\frac{d\rho}{dt} = 0.$$

But note that the density can still vary in space (inhomogeneous material). Using the balance of mass (2.4), it follows

$$\operatorname{div} v = \operatorname{tr}(\nabla v) = \operatorname{tr} \mathbb{D} = 0 \tag{2.12}$$

which means that the material can undergo only isochoric (volume preserving) motions. The consequence is that the material can sustain arbitrary spherical stress and the pressure p in equation (2.11) is the force that guarantees the incompressibility. It is an additional unknown and can not be determined experimentally.

If the fluid is also homogeneous (counterpart of inhomogeneous), it follows from (2.4) and (2.12) that the density is constant in space and time.

Compressible Fluids Compressibility is the counterpart of incompressibility and measures the relative volume change of a fluid as a response to a pressure (or mean stress) change. It is described by the additional term $\lambda(\rho, \theta)(\operatorname{div} v)\mathbb{I}$

in the constitutive equation (2.11) for the stress, where λ is the bulk viscosity depending on the density and thermodynamical temperature θ.
Here the pressure is not an additional unknown like in the incompressible case and is labeled by p_{th} for the purpose of distinction. It is the so-called thermodynamic pressure which is a function of the density and the temperature/entropy. It is defined by the form

$$p_{\text{th}} := \rho^2 \frac{\partial e(\rho, \eta)}{\partial \rho}. \tag{2.13}$$

Newtonian Fluids

The Newtonian fluids or often called the Navier–Stokes fluids are named after the French engineer and physicist Claude-Louis Navier and Anglo-Irish physicist and mathematician George Gabriel Stokes. They describe the motion of viscous fluids. Their constitutive equations are based on Isaac Newton's second law to fluid motion that viscous stresses are proportional to rates of change of the fluid's velocity. It means that $\mathbb{S} = 2\mu\mathbb{D}$.
Newtonian fluids describe pure viscous flows:

$$\mathbb{T} = -p_{\text{th}}\mathbb{I} + \lambda(\operatorname{div} v)\,\mathbb{I} + 2\mu\mathbb{D} \qquad \text{(compressible)}$$
$$\mathbb{T} = -p\mathbb{I} + 2\mu\mathbb{D} \qquad \text{(incompressible)}$$

where μ is the dynamic shear viscosity which can depend on the density and temperature or can be a constant in the case of a homogeneous incompressible fluid ignoring thermal effects.

Due to the linear relation between $\mathbb{T}$ and $\mathbb{D}$ the Cauchy stress can be expressed in terms of the velocity and the constitutive equations can be inserted in the balance equations which will be shown in the Chapter 3.3.

The Navier–Stokes equations describe the physics of many phenomena of scientific and engineering interest and can model water flow in a pipe, air flow around an aircraft wing or blood flow.

Viscoelastic Fluids (Non-Newtonian fluids)

The models presented in the previous section are not suitable for all materials, especially for viscoelastic materials. They do not behave as Newtonian fluids described by Navier-Stokes fluid and are called Non-Newtonian for this reason. Some examples are toothpaste or food such as butter and yogurt or natural substances such as lava and honey or biological fluids such as blood

and vitreous body.

Viscoelasticity refers to both viscous fluid as well as elastic solid reactions. Viscosity means that they flow like a Newtonian fluid but on the other hand they can store or release energy, like an elastic solid. In linear elasticity, the stress σ depends linearly on the strain ϵ, which is a dimensionless (ratio of two lengths) measure of the local deformation of the material due to stress, with respect to a reference state (Lagrange framework). In contrast, the total strain and reference state are not of interest in a fluid, since fluid particles have no preferential position relative to one another (Eulerian framework). In a viscous Newtonian fluid the stress depends on the rate of strain. In an elastic solid the stress depends on the strain. Viscoelastic materials exhibit both properties. Their stress depends on the strain and the rate of strain.

Such viscoelastic properties are expressed in Non-Newtonian phenomena like the presence of non-zero normal stress differences in the steady simple shear flow. Figure 2.4 shows the associated rod climbing (Weissenberg) and die swelling effect. The fluid pressed in one direction reacts usually in the perpendicular direction. Other properties of viscoelastic fluids are shear thickening

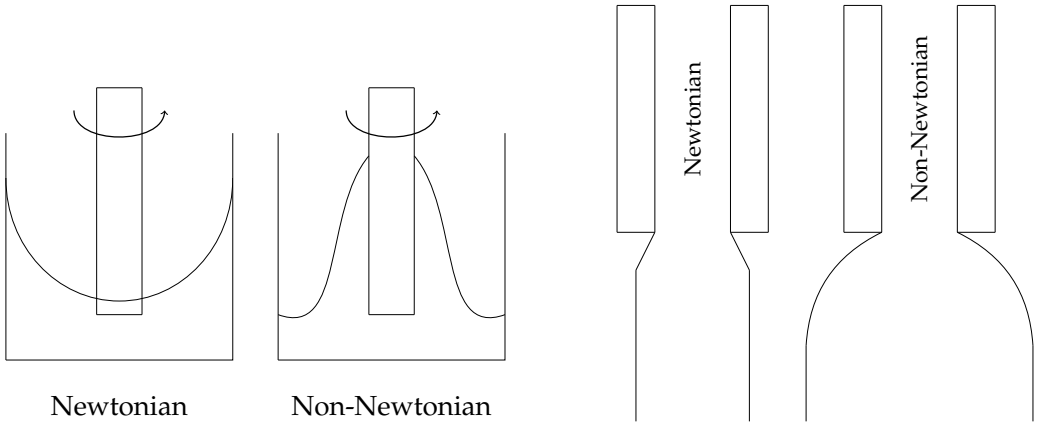

Figure 2.4: Rod climbing/Weissenberg effect (left) and die swelling (right)

and thinning. The shear rate is a shear component of the symmetric part of velocity gradient $\mathbb{D}$ and the shear stress is the corresponding component of the extra stress tensor, a part of the Cauchy stress $\mathbb{T}$. The difference to Newtonian fluids of these properties is graphically shown in Figure 2.5. For more details on the response of real viscoelastic materials see for example [190]. In contrast to Newtonian fluids, the stress in viscoelastic materials is not proportional to the velocity gradient but satisfy an additional evolutionary differential equation to be capable of characterizing the elastic response. Beside the velocity

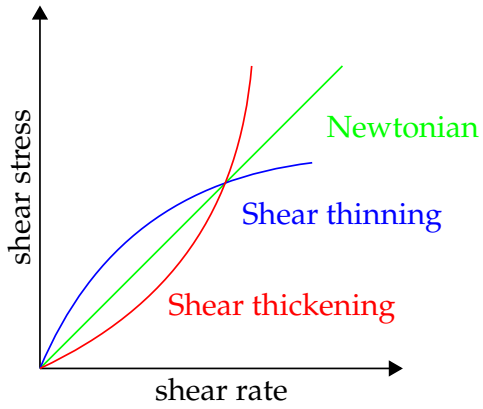

Figure 2.5: Comparison between Newtonian and Non-Newtonian fluids

and pressure the stress is treated as an unknown to be sought in mechanical processes. This is discussed in the section 4 below.

Derivation Viscoelastic rate-type models are motivated by a one-dimensional mechanical spring/dashpot analogue, see for example [181]. Here the linear elastic behavior is represented by a Hookean spring satisfying Hooke's law and the viscosity is described by a linear dashpot consisting of two concentric cylinders filled with a Newtonian fluid (see Figure 4.1). The relation between the stress and strain fulfills Newton's law. We use the combination by series

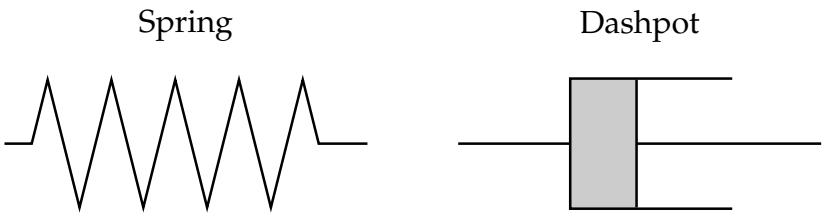

Figure 2.6: Linear spring and linear dashpot

and/or parallel connection of these two basic mechanical analogs for composing one-dimensional structure of viscoelastic fluids including Newtonian fluids as a special case, for more details on this topic see [181].

The constitutive equations are only approximations of the real material behavior and depend on the material and the considered processes but together with the balance equations which are exact and valid for any continuous medium they form a complete system of governing equations.

3 Well Known Models of Drug Distribution within Vitreous

The injection of a drug into the vitreous body for the treatment of retinal diseases like the wet aged-related macular degeneration, diabetic macular edema or diabetic retinopathy is the most common medical intervention worldwide. Drug delivery to the posterior eye is a challenge because of the physiological and anatomical barriers within the eye, which prevent drugs in the systemic circulation from entering the vitreous.
The aged-related macular degeneration is a medical condition which may result in vision loss at the macula due to abnormal blood vessel growth (choroidal neovascularization). The proliferation of abnormal blood vessels in the retina is stimulated by vascular endothelial growth factor (VEGF) which promotes the development of highly permeable vasculature in the retina and can be treated by drugs, Anti-VEGF recombinants, binding and inhibiting VEGF. The therapy consists of intravitreal injections which are administered over a period of time depending on the pathology. Specific treatment options and information on the spread of the drugs can be found in [50, 169]. Current drugs are Aflibercept from Eylea, Ranibizumab from Lucentis or Bevacizumab sold by Avastin which diffuse to the retina, effect there locally at the macula and subsequently are cleared by the choroidal blood flow. But there is no therapy response in 10.1-45 % of the patients [15], no quantitative predictions of the success of the therapy and the drug distribution in the vitreous is unknown. Additionally, personalized differences of the patients are not considered, especially the individual consistencies of the vitreous. Many of the used drugs have a small concentration range of effectiveness, and may be toxic at higher concentrations [170]. On the other hand, longer half-life of a drug means greater duration of the pharmacological response and allows less frequent dosing [42]. Therefore, the knowledge of drug distribution within the eye after intravitreal injection is important to avoid the tissue damage, caused by high concentrations of drug, while maximizing the therapeutic benefits.

In this Chapter, we present the well known models of drug distribution within the human vitreous after intravitreal injection for the treatment of retinal diseases from the literature. We introduce the used models for the description of

the vitreous distinguishing between the young healthy and liquefied vitreous in age. By emphasizing the corresponding properties of the vitreous, we derive the governing equations from the mathematical point of view and set the boundary conditions based on the complex biology in the eye. In Section 3.4 we exhibit the coupled system of convection-diffusion equation describing the drug distribution and flow equations characterizing the non-stagnant vitreous. Further, we extend the models to be more realistic by including the gravity and the surface tension, arising when fluids are mixed, in the case of the liquefied vitreous, modeled by the Navier-Stokes equation, that are lacking in literature.

3.1 Geometry

In the presented mathematical models the domain of interest is the vitreous body denoted by $\Omega \subset \mathbb{R}^d, d = 2, 3$ which is a bounded connected open set with a smooth, continuous boundary $\partial\Omega \subset C(\mathbb{R}^{d-1})$. Is is assumed that $0 < T < \infty$ is a fixed time and we consider the variables $x \in \Omega$ and $t \in [0, T]$ describing the d-dimensional space and time coordinates.

The boundary can be subdivided into $\partial\Omega = \Gamma_r \cup \Gamma_l \cup \Gamma_h$ with $\Gamma_r \cap \Gamma_l \cap \Gamma_h = \emptyset$ where Γ_r denotes the retina, Γ_l the lens and Γ_h defines the hyaloid membrane as introduced in the Chapter 2.1. A drawing of the boundaries is shown in Figure 3.1.

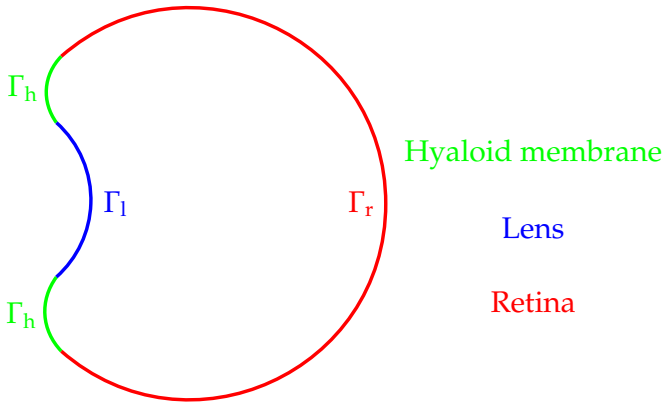

Figure 3.1: Drawing of the distinguishable boundaries

3.2 Modeling of Healthy Vitreous: Darcy Equation

The rheology of the individual vitreous body can influence the drug distribution and treatment outcome. Because of the biological given conditions, the complex composition and physical properties of the vitreous body can vary considerably from person to person. They also change with age and disease. The mathematical modeling of the vitreous will follow the phenomenological approach, describing the macroscopic nature as a continuum medium and fitting the equations to experimental data. Unless otherwise noted we study only mechanical processes, thermodynamic variables such as the entropy and the temperature are ignored.

The first approach for modeling the healthy vitreous is to describe the vitreous as a porous medium consisting of a solid skeleton (collagen fibers) and voids which are permeated by the aqueous humor flow entering the vitreous body from the hyaloid membrane and leaving the eye through the retina. The restrictions on a porous medium, like larger domain compared to the pore size or a connected void space, are fulfilled for the vitreous. In [19, 53] one can find an introduction to fluid dynamics in porous media. The steady aqueous humor flow is described by the incompressible Darcy equation driven by a pressure drop between the anterior and the posterior surfaces:

$$\nabla \cdot v = 0 \qquad \text{in } \Omega, \tag{3.1a}$$

$$-\frac{K}{\mu}\nabla p = v \qquad \text{in } \Omega, \tag{3.1b}$$

where $v(x) : \Omega \to \mathbb{R}^d$ is the velocity of the permeating aqueous humor, $p(x) : \Omega \to \mathbb{R}$ is the (hydrostatic) pressure and the material parameter $\frac{K}{\mu} > 0$ denotes the hydraulic conductivity, describing the characteristics of the porous medium and the properties of the fluid, namely the permeability K divided by the dynamic viscosity μ.

It is the most common model in the literature for the description of the flow in the vitreous, see [54, 75, 170] and many more. The nature of the vitreous and therein present collagen fibers justify the use of Darcy's equation (3.1) to describe the aqueous humor flow.

3.2.1 Boundary Conditions

To describe the biology of the vitreous in the human eye boundary conditions are needed capable to approximate the complicated real life. We distinguish

between two possible sets of boundary conditions varying only at the boundary of the hyaloid membrane.

With Dirichlet boundary

Following [75], we apply one Dirichlet boundary part at the hyaloid membrane Γ_{h} firstly, and prescribe the pressure which is considered to be the same as that of aqueous humor, $p_{\mathrm{in}} = 2000$ Pa for a healthy eye without glaucoma [139], which is close to the intraocular pressure (IOP) of the eye. The lens is assumed to be impermeable (no flow through but along) and the retina is considered as a membrane:

$$v \cdot n = 0 \qquad \text{on } \Gamma_l, \tag{3.2a}$$

$$p = p_{\mathrm{in}} \qquad \text{on } \Gamma_h, \tag{3.2b}$$

$$v \cdot n = \frac{K_{RCS}}{L}(p - P_v) \qquad \text{on } \Gamma_r, \tag{3.2c}$$

where K_{RCS} is the total hydraulic conductivity of retina, choroid and sclera (RCS), P_v is the pressure outwards of RCS and L denotes its thickness. n denotes the unit outward normal vector with respect to the corresponding boundary part. Since the retina is considered as a membrane the boundary condition there is derived by using Darcy's law and the difference quotient using porous media modeling:

$$n \cdot v = n \cdot (-K_{RCS} \nabla p) = K_{RCS} \frac{p - P_v}{L}.$$

No Dirichlet boundary

Second, not the Dirichlet boundary condition for the pressure is given at Γ_h but the Neumann condition prescribing the velocity:

$$v \cdot n = 0 \qquad \text{on } \Gamma_l, \tag{3.3a}$$

$$v \cdot n = v_{\mathrm{in}} \qquad \text{on } \Gamma_h, \tag{3.3b}$$

$$v \cdot n = \frac{K_{RCS}}{L}(p - P_v) \qquad \text{on } \Gamma_r. \tag{3.3c}$$

The hyaloid membrane operates as the area of inflow where v_{in} is computed by the total aqueous humor production at the ciliary body, which is 2.5 μl/min according to [55], considering that only 5% flows into the vitreous through the hyaloid membrane. v_{in} is defined as a parabolic Poiseuille inflow velocity profile with maximum velocity $v_{\max} = 1.58 \times 10^{-8}$ m/s.

To derive the right choice of boundary conditions characterizing the complex biology in the human eye is one of the main tasks. Only sparsely measured values from experiments are available.
The first variant of setting the pressure equal to the IOP is commonly used in the literature [54, 75], since the pressure in the anterior eye is practical to measure and well known, but it leads to singularities of the numerical solution of (3.1) on the boundary. Darcy's law can be seen as a Laplace equation and a smooth solution is expected. But the boundary conditions (3.2) lead to jumps across the different boundary parts. The change to prescribing the physically motivated inflow offers a continuous velocity profile between Γ_h and Γ_l.

3.2.2 Derivation of Governing Equations

Darcy's law is a physical law modeling the flow of fluids through porous media. Formulated by Henry Darcy in 1856 [32], based on experiments of flow of water through beds of sand, it is commonly viewed as a relationship between the fluid mass flux and pressure gradient in the medium.

One way to derive the momentum equation in (3.1) is based on the class-II mixture theory considering a two-component medium composed of solid porous matrix and a fluid where the two components not interact chemically (i.e. no mass transfer between the components) [84, 157]. In the context of mixture theory, we have the following forms of the balance equation for linear momentum:

$$\frac{d\rho_f v_f}{dt} = \nabla \cdot \mathbb{T}_f + I_f,$$
$$\frac{d\rho_s v_s}{dt} = \nabla \cdot \mathbb{T}_s + I_s.$$

We ignore the solid part, the second momentum balance, since the deformation of the solid resulting from the flow of the fluid through the pores is negligible and set $v_s = 0$. Furthermore, for small Reynolds numbers we can neglect the left-hand side of the balance equation for the fluid (steady case) and set the Cauchy stress $\mathbb{T}_f$ to be only the isotropic part, $\mathbb{T}_f := -p_f\mathbb{I} = -\phi_f p\mathbb{I}$, where the effective partial pressure exerted by the fluid on some surface of the porous medium p_f is equal to the mixture pressure p times volume fraction ϕ_f. For the interaction force I_f we keep only the drag term and the equilibrium term, i.e. $I_f := -\alpha v_f + p\nabla\phi_f$ with a constant $\alpha > 0$. Then the balance equation for linear momentum for the fluid has reduced to

$$0 = -\phi_f \nabla p - p\nabla\phi_f - \alpha v_f + p\nabla\phi_f$$

and we obtain Darcy's law:

$$\alpha v_f = -\phi_f \nabla p$$

by defining $\frac{K}{\mu} := \frac{\phi_f}{\alpha}$.

Another way to derive Darcy's law can be done by homogenization (rescaling from mirco- to macroscopic) of the steady incompressible (Navier-)Stokes fluid in a porous material [3, 124]. The ideas are to introduce a small parameter ϵ, to separate the macroscopic spatial scale described by x-dependence and the microscopic scale described by x/ϵ and to rewrite the macroscopic problem as a Stokes system in microscopic variable. Then Darcy's law can be obtained as the limit of the convergence of the microscopic problem (as ϵ tends to zero).

3.2.3 Existence and Uniqueness (Mixed Boundary Conditions)

In this section we prove the global existence and uniqueness of the weak solution of the Darcy equation (3.1) completed with mixed boundary conditions describing the human eye in the general d-dimensional setting. The application of the Lax-Milgram theorem leads to the desired result in the mathematical analysis.
First, we discuss the mathematical analysis of the Darcy equation (3.1) completed by the boundary conditions (3.2). Then we will consider the case of no Dirichlet boundary conditions (3.3) and it will clarify the influence of the definition of the boundary conditions on the mathematical analysis.
Known results about the theory of existence and uniqueness of weak solutions of elliptic partial differential equations can be found in [102] but the general case of mixed boundary conditions is not covered. In the modeling of the eye we have a complex biological system which requires complex boundary conditions. The developed boundary value problems need to be investigated in detail and they differ from the standard mathematical theory about existence and uniqueness. Further literature about existence and uniqueness results concerning incompressible flow in porous media can be found in [125, 158, 28].

As mentioned in the Section 3.1 where the geometry is stated the domain of the vitreous satisfies specific regularities. Additionally, we require a continuously differentiable boundary, i.e. $\partial\Omega \in C^1$. The distinguishable parts of it have non-vanishing Lebesgue measure, i.e. $|\Gamma_r|, |\Gamma_l|, |\Gamma_h| > 0$.

To be able to apply results from functional analysis, we have to consider the weak formulation of the Darcy equation but the two equations in (3.1)

are not in the preferable form for mathematical analysis. Thus, we derive a new variant, the so-called primal form whose structure allows one to apply standard results for Poisson equation and finally, existence of solutions for Darcy equation is shown.

The primal form can be written as

$$-\frac{K}{\mu}\nabla\cdot(\nabla p) = f, \tag{3.4}$$

received by the divergence of the second equation in (3.1), substituting the incompressibility constraint and including an external force $f : \Omega \to \mathbb{R}$ for generalization.

The Sobolev space of functions with L^2-integrable derivatives in Ω and the values vanishing on the Dirichlet boundary part $\Gamma_D \subseteq \partial\Omega$ is defined as

$$H_0^1(\Omega;\Gamma_D) := \{p \in H^1(\Omega) : p = 0 \text{ on } \Gamma_D\}. \tag{3.5}$$

With Dirichlet boundary

Considering the boundary conditions (3.2) we have $\Gamma_D = \Gamma_h$. Then by applying the lifting method and introducing $p_{hom} := p - p_{in}$ with $p \in H^1(\Omega)$ we can convert the problem to a system with homogeneous Dirichlet boundary condition on Γ_h. Green formula and integration by parts lead to the weak formulation of the Darcy equation.

Find $p_{hom} \in H_0^1(\Omega;\Gamma_h)$ such that

$$a(p_{hom},\phi) = l(\phi) \quad \forall\phi \in H_0^1(\Omega;\Gamma_h) \tag{3.6}$$

where

$$\begin{aligned} a(p_{hom},\phi) &:= \frac{K}{\mu}(\nabla p_{hom},\nabla\phi) + \frac{K_{RCS}}{L}(p_{hom},\phi)_{\Gamma_r} \\ l(\phi) &:= (f,\phi) - \frac{K}{\mu}(\nabla p_{in},\nabla\phi) + \frac{K_{RCS}}{L}(P_v,\phi)_{\Gamma_r} \\ &\quad - \frac{K_{RCS}}{L}(p_{in},\phi)_{\Gamma_r}. \end{aligned} \tag{3.7}$$

Remark 3.2.1: *Note that $p_{hom} := p - p_{in} \in H_0^1(\Omega;\Gamma_h)$ is well defined, since the existence of the extension of p_{in} into the interior of Ω is guaranteed due to the surjectivity of the trace operator.*

Theorem 3.2.2 (Existence and Uniqueness of weak solution)**:**
There exists only one solution to the problem (3.6) *with* $P_v \in H^{-1/2}(\Gamma_r)$, $p_{in} \in H^{1/2}(\Gamma_h)$ *and* $f \in H^{-1}(\Omega)$.

Proof. The proof can be given by the application of the Lax-Milgram theorem [105, 191] for the bilinear form $a(p_{\text{hom}}, \phi)$ and linear form $l(\phi)$ defined in (3.7) by using Cauchy-Schwarz inequality (CS) and Trace Theorem (TT) stated in [112].
Compared to the standard homogeneous Dirichlet boundary conditions in the literature we have to take care of the additional boundary terms describing the permeability at the retina and show that they fulfill all requirements of the Lax-Milgram theorem.
Due to the Poincaré inequality [150], we can equip the Hilbert space $H_0^1(\Omega; \Gamma_{\text{h}})$ with the H^1-semi norm which is in fact a norm on this space.

- The boundedness of $a(p_{\text{hom}}, \phi)$ for all $p_{\text{hom}}, \phi \in H_0^1(\Omega; \Gamma_{\text{h}})$ can be shown for a constant $\alpha := \frac{K}{\mu} + \frac{K_{RCS}}{L} c_1 c_2 > 0$. The first term is estimated in the same way as in the doctoral thesis of Vladislav Olkhovskiy [139]. The additional boundary term requires to apply twice the Trace Theorem with constants $c_1 > 0$ and $c_2 > 0$:

$$\begin{aligned}\left| \frac{K_{RCS}}{L} (p_{\text{hom}}, \phi)_{\Gamma_{\text{r}}} \right| &\overset{\text{CS}}{\leq} \frac{K_{RCS}}{L} \|p_{\text{hom}}\|_{L^2(\Gamma_{\text{r}})} \|\phi\|_{L^2(\Gamma_{\text{r}})} \\ &\overset{\text{TT}}{\leq} \frac{K_{RCS}}{L} c_1 c_2 \|p_{\text{hom}}\|_{H_0^1(\Omega;\Gamma_{\text{h}})} \|\phi\|_{H_0^1(\Omega;\Gamma_{\text{h}})},\end{aligned}$$

  where the assumptions of the Trace Theorem are fulfilled, since our domain Ω is bounded and $\partial\Omega \in C^1$.

- The proof for coercivity of $a(\cdot, \cdot)$ can also be found in [139] since the boundary term can be ignored due to its positive sign.

- The right hand side is bounded due to the specific choice of $P_v \in H^{-1/2}(\Gamma_{\text{r}})$, $p_{\text{in}} \in H^{1/2}(\Gamma_{\text{h}})$ and $f \in H^{-1}(\Omega)$ and the exemplary application of known results from the functional analysis as shown for the term:

$$\begin{aligned}|\frac{K_{RCS}}{L} (P_v, \phi)_{\Gamma_{\text{r}}}| &\overset{\text{CS}}{\leq} \frac{K_{RCS}}{L} \|P_v\|_{L^2(\Gamma_{\text{r}})} \|\phi\|_{L^2(\Gamma_{\text{r}})} \\ &\overset{\text{TT}}{\leq} \frac{K_{RCS}}{L} c_1 \underbrace{\|P_v\|_{L^2(\Gamma_{\text{r}})}}_{<\infty} \|\phi\|_{H_0^1(\Omega;\Gamma_{\text{h}})} \\ &= \beta \|\phi\|_{H_0^1(\Omega;\Gamma_{\text{h}})}\end{aligned}$$

with a constant $\beta := \frac{K_{RCS}}{L} c_1 \|P_v\|_{L^2(\Gamma_r)} > 0$.

□

No Dirichlet boundary

Now, we look at the Darcy equation (3.4) completed by the boundary conditions introduced in (3.3). Compared to the previous formulation, there is no Dirichlet boundary which leads to a new ansatz and test space, the whole $H^1(\Omega)$ without any restrictions. Hence, we have to prove the existence and uniqueness by the application of the Lax Milgram Theorem in the complete H^1-norm

$$\|p\|^2_{H^1(\Omega)} := \|p\|^2_{L^2(\Omega)} + \|\nabla p\|^2_{L^2(\Omega)}$$

instead only the semi-norm. The Poincaré inequality is not valid anymore. Additionally, the lifting with p_{hom} is not necessary and therefore it simplifies the concluded weak formulation which reads:

Find $p \in H^1(\Omega)$ such that

$$a(p, \phi) = l(\phi) \quad \forall \phi \in H^1(\Omega) \tag{3.8}$$

where

$$a(p, \phi) := \frac{K}{\mu}(\nabla p, \nabla \phi) + \frac{K_{RCS}}{L}(p, \phi)_{\Gamma_r},$$
$$l(\phi) := (f, \phi) + \frac{K_{RCS}}{L}(P_v, \phi)_{\Gamma_r} - (v_{\text{in}}, \phi)_{\Gamma_h}.$$

Theorem 3.2.3 (Existence and Uniqueness of weak solution)**:**
There exists only one weak solution to the problem (3.8) *with* $P_v \in H^{-1/2}(\Gamma_r)$, $v_{in} \in H^{-1/2}(\Gamma_h)$ *and* $f \in H^{-1}(\Omega)$.

Proof. Similar to the proof of Theorem 3.2.2 the proposition follows by the application of Lax-Milgram theorem. Since the H^1-seminorm can be estimated by the H^1-norm from above the results from the existence proof of (3.6) are adoptable. The linear form differs only in one missing and one extra term compare to (3.8) but the boundedness can be shown with the same proceeding by using the Cauchy-Schwarz inequality and Trace Theorem.
Thus, it suffices to show the coercivity condition of $a(\cdot, \cdot)$ for all $p \in H^1(\Omega)$ by using Friedrich's inequality [64, 156] with the constant $c > 0$:

$$\begin{aligned} a(p, p) &\geq \min(\frac{K}{\mu}, \frac{K_{RCS}}{L}) \left(\|\nabla p\|^2_{L^2(\Omega)} + \|p\|^2_{L^2(\Gamma_r)} \right) \\ &\geq \kappa \|p\|^2_{H^1(\Omega)} \end{aligned}$$

with a constant $\kappa := \min(\frac{K}{\mu}, \frac{K_{RCS}}{L})c > 0$. □

Regularity

The primal form (3.4) of the incompressible Darcy equation belongs to the class of elliptic partial differential equations with the general elliptic operator

$$Lu := -\sum_{i,j=1}^{n} (a_{ij}(x,t)u_{x_i})_{x_j} + \sum_{i=1}^{n} b_i(x,t)u_{x_i} + c(x,t)u \qquad \forall u \in H^1(\Omega)$$

and the coefficients $a_{ij} = \frac{K}{\mu}, b_i = c = 0 \in C^\infty(\Omega)$ for $i,j = 1,\ldots,3$ and right-hand side equal to zero. It is known that any possible singularities of the solution on the boundary do not propagate into the interior and therefore it holds for our weak solution of (3.6) and (3.8) that $p \in C^\infty(\Omega)$ (see Theorem 3 of Chapter 6.3.1 in [48]). Consequently, we obtain for the corresponding velocity,

$$v \in L^\infty(\Omega).$$

In the case of drug distribution within the human vitreous, the steady aqueous humor velocity field attains its maximum value at the hyaloid membrane, the inflow area, which is prescribed by a Poiseuille profile with maximum velocity of 1.58×10^{-8} m/s or constant pressure identical to the IOP, 2000 Pa, and decreases within the bounded vitreous due to permeable outflow at the retina. The flow patterns are slow in the biology of the vitreous in the human eye modeled as a porous medium with permeating aqueous humor flow completed with boundary conditions derived from experiments. Consequently, the flow is bounded.

$v \in L^\infty(\Omega)$ is the necessary assumption in the existence proof of the diffusion equation describing the drug distribution in the later Section 3.4.3.

3.3 Modeling of Liquefied Vitreous: Navier-Stokes Equation

Now, we look at the completely liquefied vitreous in age or after a vitrectomy which is a surgical procedure to remove the vitreous gel from the eye in order to decrease the vitreous related complications like posterior vitreous detachment or tractional retinal detachment. To model the pure viscous flow of the liquefied vitreous we use the incompressible Navier-Stokes equation introduced in the Section 2.2.4 as in the works [2, 153] where they focus on the

motion of the vitreous. The system of governing equations in the non-steady case reads as follows:

$$\nabla \cdot v = 0 \qquad \text{in } \Omega \times (0,T], \tag{3.9a}$$

$$\rho\left(\frac{\partial v}{\partial t} + (v \cdot \nabla)v\right) = \nabla \cdot \mathbb{T} \qquad \text{in } \Omega \times (0,T] \tag{3.9b}$$

$$\mathbb{T} = -p\mathbb{I} + 2\mu_0 \mathbb{D} \qquad \text{in } \Omega \times (0,T] \tag{3.9c}$$

where $v(x,t) : \Omega \times (0,T] \to \mathbb{R}^d$ is the velocity of the liquefied vitreous and $p(x,t) : \Omega \times (0,T] \to \mathbb{R}$ is the pressure. The material specific parameters $\rho > 0$ and $\mu_0 > 0$ are constants describing the density and dynamic viscosity, where μ_0 is set to be the dynamic viscosity of water at the corresponding temperature of the vitreous.

Since the Cauchy stress depends linear on the velocity the constitutive equation (3.9c) can be inserted into the balance equation of linear momentum (3.9b) and the whole system (3.9) can be rewritten as

$$\nabla \cdot v = 0 \qquad \text{in } \Omega \times (0,T], \tag{3.10a}$$

$$\rho\left(\frac{\partial v}{\partial t} + (v \cdot \nabla)v\right) = -\nabla p + \mu_0 \Delta v \qquad \text{in } \Omega \times (0,T]. \tag{3.10b}$$

Further, the positive constant density can be substituted into the pressure in the balance equation of linear momentum:

$$\frac{\partial v}{\partial t} + (v \cdot \nabla)v = -\frac{\nabla p}{\rho} + \nu_0 \Delta v$$

with the kinematic viscosity $\nu_0 := \frac{\mu_0}{\rho}$. Due to the relation

$$\frac{\nabla p}{\rho} = \nabla \tilde{p} + \frac{p}{\rho^2}\nabla \rho$$

where $\nabla \rho = 0$ if the density is constant we can rewrite the Navier-Stokes equation with the new pressure $\tilde{p} := \frac{p}{\rho}$ as

$$\frac{\partial v}{\partial t} + (v \cdot \nabla)v = -\nabla \tilde{p} + \nu_0 \Delta v.$$

As a special case one obtains the Stokes equation through linearization of the Navier–Stokes equations by neglecting the convection term. It describes the fluid flow where advective inertial forces are small compared with viscous forces and can be used in the modeling of aqueous humor flow in the anterior chamber of the eye [139]. For more details on incompressible Navier-Stokes equation see [178, 65].

3.3.1 Boundary and Initial Conditions

To get a closed system we need to set the initial and boundary conditions which are different compared to the previous Darcy case:

$$
\begin{aligned}
v &= v_0 && \text{on } \Omega \times \{t = 0\}, && \text{(3.11a)}\\
v &= 0 && \text{on } \Gamma_l \times (0, T], && \text{(3.11b)}\\
v &= v_{\text{in}} && \text{on } \Gamma_h \times (0, T], && \text{(3.11c)}\\
\mathbb{T} n \cdot n &= k_{\text{perm}} v \cdot n && \text{on } \Gamma_r \times (0, T], && \text{(3.11d)}\\
\mathbb{T} n \cdot \tau &= 0 && \text{on } \Gamma_r \times (0, T], && \text{(3.11e)}
\end{aligned}
$$

where v_0 and v_{in} are the initial and Poiseuille inflow velocity profile. τ denote the arbitrary unit outward tangential vector with respect to the retina.
In the case of a liquefied vitreous characterized by the Navier-Stokes equation, at the lens there is a non-slip boundary condition and v_{in} describes the same Poiseuille profile as for the porous medium approach for healthy vitreous in (3.3). The aqueous humor production at the ciliary body stays the same during the aging. Further, we assume at the retina that the flow can leave the vitreous only in normal direction which is a physical simplification due to the slow velocities in the eye. Here $k_{\text{perm}} < 0$ is a constant describing the permeability determined by considering the Beavers-Joseph-Saffman conditions on the interface between the vitreous, the fluid layer with lower index f and the retina modeled as a very thin porous medium described by Darcy's law denoted by the lower index p:

$$
\begin{aligned}
v_f \cdot n = v_p \cdot n = (-K_{RCS} \nabla p_p) \cdot n \quad & \text{(preservation of normal velocity)}\\
v_f \cdot \tau + \alpha \mathbb{T}_f n \cdot n = 0 \quad & \text{(behavior of tangential velocity)}\\
-\mathbb{T}_f n \cdot n = -\mathbb{T}_p n \cdot n = -(-p_p \mathbb{I}) n \cdot n = p_p \quad & \text{(continuity of normal stresses)}
\end{aligned}
$$

where the second equation is motivated by experiments conducted by Beavers, Joseph and Saffman [20, 154] and the factor α is the so-called slip coefficient which has to be determined experimentally. A mathematical justification of the Beavers-Joseph-Saffman condition can be found in [126].
In detail, we computed

$$
p_p = -\mathbb{T}_f n \cdot n = -k_{\text{perm}} v_f \cdot n = -k_{\text{perm}} v_p \cdot n
$$

using the continuity of normal stresses, preservation of normal velocity from the Beavers-Joseph-Saffman conditions and inserting our prescribed boundary condition. Applying the same procedure as for the boundary condition (3.2)

at Γ_r in the Darcy model and considering the retina as a membrane, we can approximate

$$-k_{\text{perm}} v_p \cdot n \approx -k_{\text{perm}} K_{RCS} \frac{p_p - P_v}{L}.$$

By assuming that p_p is equal to the IOP, we can calculate k_{perm}.
A perfectly permeable retina with free outflow would have $k_{\text{perm}} = 0$ which is equivalent to the traction-free boundary condition $\mathbb{T}n = 0$. In the commonly form (3.10) this condition is expressed with the replaced Cauchy stress known as the artificial do-nothing boundary condition, $\widehat{\mathbb{T}}n := \mu_0(\nabla v)n - pn = 0$.

3.3.2 Derivation of Governing Equations

Here, the thermodynamical derivation of the Navier-Stokes fluid (3.9c) is shown. The detailed classical thermodynamical procedure is outlined in the later Section 4.2.2.

First, we introduce the Helmholtz free energy

$$\psi := e - \theta\eta, \tag{3.12}$$

a thermodynamic potential, and use the definition $\eta := -\frac{\partial \psi}{\partial \theta}$ for the entropy. Its constitutive equation is assumed to be a function of the temperature θ and the density ρ, given in the following explicit form

$$\psi := \tilde{\psi}(\theta, \rho) = \psi_0(\rho) + \psi_1(\theta). \tag{3.13}$$

This is a straightforward generalization of the classical energetic equation of state known for the equilibrium thermodynamics [117]. One example for the definition of $\psi_1(\theta)$ can be seen later in (4.21). Applying the material time derivative of equation (3.13) yields,

$$\frac{d\psi}{dt} = \frac{\partial \psi}{\partial \theta}\frac{d\theta}{dt} + \frac{\partial \psi}{\partial \rho}\frac{d\rho}{dt}.$$

Recalling the definition of the thermodynamic pressure, see (2.13) but using the Helmholtz free energy instead of the internal energy,

$$p_{\text{th}}^{\text{NS}} := \rho^2 \frac{\partial \psi}{\partial \rho} = \rho^2 \frac{\partial \psi_0}{\partial \rho}, \tag{3.14}$$

and considering the relation (3.12) one can rewrite (3.13) as

$$\rho\theta\frac{d\eta}{dt} = \rho\frac{de}{dt} - \frac{p_{\text{th}}^{\text{NS}}}{\rho}\frac{d\rho}{dt}$$

to get the material time derivative of the entropy. Proceeding further and plugging in the balance equations for mass (2.4) and internal energy (2.7) one can substitute for $\frac{d\eta}{dt}$ and $\frac{d\rho}{dt}$ which yields

$$\begin{aligned}\rho\theta\frac{d\eta}{dt} &= \mathbb{T} : \mathbb{D} + p_{\text{th}}^{\text{NS}}\text{div } v - \text{div } j_e \\ &= \mathbb{T}_\delta : \mathbb{D}_\delta + \left(m + p_{\text{th}}^{\text{NS}}\right)\text{div } v - \text{div } j_e\end{aligned}$$

where

$$m := \frac{1}{3}(\text{tr } \mathbb{T}) \tag{3.15}$$

denotes the mean normal stress and

$$\mathbb{A}_\delta := \mathbb{A} - \frac{1}{3}(\text{tr } \mathbb{A})\mathbb{I}$$

is the traceless part of any tensor $\mathbb{A} \in \mathbb{R}^{d\times d}$. Since the thermodynamic temperature is positive (unit in Kelvin and absolute zero is the lowest limit of the thermodynamic temperature scale), we get a formula for the entropy production ξ defined in (2.8) with entropy flux $j_\eta = \frac{j_e}{\theta}$:

$$\theta\xi = \mathbb{T}_\delta : \mathbb{D}_\delta + (m + p_{\text{th}}^{\text{NS}})\text{div } v - j_e \cdot \frac{\nabla\theta}{\theta}. \tag{3.16}$$

The right-hand side of (3.16) shows that there exist three independent entropy producing mechanisms in the Navier-Stokes fluid. The first term is entropy production due to isochoric processes such as shearing, the second one is due to volume changes and the last part is due to heat transfer. Since we deal with isothermal processes in the eye (where the temperature is a constant), i.e. $\nabla\theta = 0$, the temperature is of no interest, and one can focus only on the mechanical part of the system. Further, the vitreous is incompressible, div $v = 0$, which reduces (3.16) to

$$\theta\xi = \mathbb{T}_\delta : \mathbb{D}_\delta.$$

The entropy production is a positive quantity if the constitutive relation is chosen as follows,

$$\mathbb{T}_\delta = 2\mu_0\mathbb{D}_\delta$$

with viscosity $\mu_0 > 0$. Note that since $\mathbb{D}_\delta$ is a symmetric tensor, $\mathbb{T}_\delta$ is also symmetric and the balance of angular momentum (2.6) is satisfied. The governing

equations for the incompressible Navier–Stokes fluid then take the form

$$\begin{aligned} \nabla \cdot v &= 0 \\ \rho\left(\frac{\partial v}{\partial t} + (v \cdot \nabla)v\right) &= \nabla \cdot \mathbb{T} \\ \mathbb{T} &= -p\mathbb{I} + 2\mu_0 \mathbb{D} \end{aligned}$$

where the relation $\mathbb{D} = \mathbb{D}_\delta$ has been exploited and we use the notation

$$p := -m$$

for the pressure in incompressible fluids compare to the thermodynamic pressure $p_{\text{th}}^{\text{NS}}$ in compressible fluids. Consequently, the notions of the mean normal stress and the pressure are often used interchangeably in the literature. Here the pressure is not a function of the local values of the state variables and the velocity field, it is understood as a new unknown quantity in the governing equations to be solved for because the corresponding flux div v identically vanishes.
Note that for the compressible Navier–Stokes fluid the term $(m + p_{\text{th}}^{\text{NS}})\text{div } v$ in (3.16) does not vanish and the constitutive relations are chosen as follows,

$$\begin{aligned} \mathbb{T}_\delta &= 2\mu_0 \mathbb{D}_\delta, \\ m + p_{\text{th}}^{\text{NS}} &= \frac{3\lambda + 2\mu_0}{3}\text{div } v, \end{aligned}$$

where the additional bulk viscosity $\lambda > 0$ is a given positive function of the state variables ρ and θ. It follows that the constitutive relation for the full Cauchy stress tensor $\mathbb{T} = m\mathbb{I} + \mathbb{T}_\delta$ is

$$\mathbb{T} = -p_{\text{th}}^{\text{NS}}\mathbb{I} + 2\mu_0 \mathbb{D} + \lambda(\text{div } v)\mathbb{I}.$$

3.3.3 Existence and Uniqueness

In this Section known results from the literature about existence and uniqueness are presented for the proposed mathematical model of the liquefied vitreous (3.9).
In [178] results related to the existence and uniqueness for weak solutions of the stationary and time-dependent incompressible Navier-Stokes equation with homogeneous Dirichlet boundary condition are presented. Despite its nonlinearity the stationary case possesses for any value of the Reynolds number $Re > 0$ at least one solution $v, p \in H_0^1(\Omega) \times L^2(\Omega)$ based on the Galerkin method. For sufficiently small data f this solution is unique but in general it is

not stable, i.e. physically not realized. By comparison with experiments you can see that for high Reynolds numbers it occurs a non-stationary up to chaotic behavior (turbulence flow). While increasing Re the non-linearity due to the transport term becomes more dominant and the flow gets faster which leads to singularities of the numerical solutions. In the human eye these problems do not arise. We have slow flow fields with average velocity $v_c = 5 \times 10^{-9}$ resulting in a very low Reynolds number, $Re \approx 1.5 \times 10^{-4} \ll 1$. Then the almost steady state situation together with the consideration, $f = 0$, may provide the existence and uniqueness of the solution for the discussed application.
In the non-stationary case there is a gap between the class of functions where existence is known and the smaller classes where uniqueness is proved for 3D due to the lack of information concerning the regularity of the weak solutions. Sufficient conditions under which a weak solution is unique in the class of weak solutions can be found in [65]. But in the class of all weak solutions the uniqueness stays an open problem (even in the case of trivial solution for trivial data) and without the requirement of small data (or for a small time interval) there is no proven existence and uniqueness of classical solutions in three space dimensions, see [66, 80] and the references therein.
No specific existence and uniqueness results for the liquefied vitreous (3.9) containing our mixed boundary conditions (3.11) have been given in the literature so far, to the best of our knowledge. We recall that our permeability boundary condition (3.11d) for our application is set such that we have nearly the do-nothing boundary condition. Herewith physiological processes of the aqueous humor in the eye can be described and the corresponding parameter values are partly measured. The amount of outflow is similar to the amount of inflow which correlates to the stationary state. Then the model can be approximated by the steady-state flow in Galdi et al. [66] for example. Here the existence and uniqueness for the do-nothing Neumann boundary condition is proven (for small data). As done in the thesis of Olkhovskiy [139] for the Stokes equation the analysis can be extended specifically to inhomogeneous boundary conditions.

3.4 Modeling of Drug Distribution: Convection-Diffusion Equation

A first diffusion model for drug distribution in the vitreous of a rabbit's eye is written in [62] where they assumed that the vitreous is stagnant. In [61] and [63] the model was developed for the human eye and they numerically evaluated the concentration distribution of intravitreal drug in stagnant vitreous.

Among other things the position of the injection is identified as an important parameter. Different injection positions cause variations of drug concentration level up to three magnitudes and the averaged concentration up to a scaling factor of four [61, 63]. Later studies considered aqueous humor flow taking into account convective drug transport within the vitreous [75, 10]. Missel [127] developed models of rabbit, monkey and human eyes to predict rate of clearance of intravitreal injected bolus. Repetto et al. [153] investigated the effects of saccadic eye rotations (rapid angular rotations of the eye) on the flow in the vitreous humor and consequent drug distribution. They predicted a significant reduction in the expected time for drug dispersal across the eye with fluid flow compared to the situation without fluid flow. Especially in the case of liquefied vitreous eye rotations produce effective fluid mixing influencing the dispersion of injected drugs [14]. Abouali et al. [2] studied the flow dynamics of vitreous resulting from saccadic movements following vitreous liquefaction or after vitrectomy. Xu et al. [192] showed that convection contributes to about 30% of intravitreal drug transport in humans which should be magnified for higher molecular-weight compounds like anti-VEGF drugs due to slower diffusion. Recently, more physiologic pharmacokinetic models have accounted for convection in the vitreous humor [142, 170, 127]. In [24] they showed that for liquefied vitreous advection plays a more significant role in the drug transport in the eye than diffusion.

For these reasons, in this thesis the drug transport in the human vitreous following intravitreal injection is modeled by the time-dependent convection-diffusion equation since it is caused by both diffusion through the vitreous and convection flow from the anterior to the posterior segment of the eye. The convection term arises because of the flow within the vitreous and depends on its physiology which changes with age and disease described by the previous models. The diffusion is driven by the drug concentration gradient. The diffusion speed depends on the properties of the drug itself and the vitreous' structure which constitute a barrier to the spreading of the drug.
Our model describing the drug distribution in the human vitreous body reads:

$$\frac{\partial C}{\partial t} + (v \cdot \nabla)C - \nabla \cdot (D \nabla C) = 0 \qquad \text{in } \Omega \times (0, T] \tag{3.17}$$

where $C(x,t) : \Omega \times (0,T] \to \mathbb{R}$ is the unknown concentration of the drug, $v(x,t) : \Omega \times (0,T] \to \mathbb{R}^d$ describes the velocity which model depends on the rheology of the vitreous and $D > 0$ is the diffusion coefficient depending on the rheology of vitreous and on the drug itself (or can be generalized to the diffusion tensor by the multiplication of D with the unit matrix $\mathbb{I}$).
In this study, the injection process is not modeled due to its slow impact

compare to the long-time diffusion behavior. Further, the saccadic eye motion is not considered since it is well examined in the literature and the time scale of seconds for saccadic eye movements does not match to the long time therapy of approximately one month for retinal diseases. This means that our following models describe the pharmacokinetics of a drug for a patient in rest, performing smooth pursuit eye movements and during the non-rapid eye movement of sleep.

3.4.1 Boundary and Initial Conditions

The governing equation (3.17) is completed with the following initial and boundary conditions according to [75],

$$C = C_0 \qquad \text{on } \Omega \times \{t = 0\}, \tag{3.18a}$$
$$(D\nabla C) \cdot n = 0 \qquad \text{on } \Gamma_l \times (0, T], \tag{3.18b}$$
$$C = 0 \qquad \text{on } \Gamma_h \times (0, T], \tag{3.18c}$$
$$-(D\nabla C) \cdot n - PC + (n \cdot v)(1 - k_{vr})C = 0 \qquad \text{on } \Gamma_r \times (0, T], \tag{3.18d}$$

where $C_0 : \Omega \to \mathbb{R}$ is the given initial concentration and P and k_{vr} are the positive material parameters characterizing the retinal permeability and the partition coefficient between vitreous and retina (ratio of drug concentration in a mixture of two immiscible solvents).
On the hyaloid membrane the concentration is set to zero, which is based on the assumption that there is the aqueous humor flow rate transporting the drug. Since the lens is assumed to be impermeable to the drug concentration, a no-flux boundary condition is applied at this surface. The retina is considered as a membrane acting as a barrier tissue to the diffusing drug and flow. The outer tissue of the retina, the choroid, acts as a perfect sink for drug transport. So, the active transport through the retina is described by the permeability boundary condition considering convective and diffusive transport of the drug, in particular it means that

$$J \cdot n \approx C$$

where $J = -D\nabla C + vC$ stands for the flux and n is the unit outward normal to the retina Γ_r. Following the Section 3.2.2 in [171] and apply Fick's law we get for one part of the flux across the retina:

$$-(D\nabla C) \cdot n = P(C_{\text{retina}} - C_{\text{choroid}}) = PC$$

where C_{retina} denotes the drug concentration on the retina at the vitreous side and C_{choroid} on the other side of the retina adjacent to the choroid. The choroid

is a highly vascularized layer, so it will act as a perfect sink for drug concentration across the retina. Therefore, a reasonable assumption is $C_{\text{choroid}} = 0$. The convective part of flux J is expressed as

$$(vC) \cdot n = (n \cdot v) k_{vr} C.$$

The typical intravitreal injection site is located at 3.5 mm posterior to the limbus (border of the cornea and the sclera) and 5.5 mm to either the left or right of the pupil axis and is modeled as a sphere with a radius of $r = 2.285$ mm, which was determined from the recommended dosage volume of 50 μl [111]. It is assumed that within this sphere the injected drug of 2 mg initially has a homogeneous distribution while there is no drug in the rest of the vitreous. In other words, the initial concentration C_0 is defined through:

$$C_0 := \begin{cases} 40a \cdot \cos(r_1) \cos(r_2) \cos(r_3), & x \in B_r(\hat{x}) \\ 0, & \text{else} \end{cases} \tag{3.19}$$

with the constant $a = 2.339$ and $r_i := \frac{0.5\pi}{r}(x_i - \hat{x}_i)$ for $i = 1, 2, 3$ in three-dimensions. The center of the sphere in our geometry is $\hat{x} = \begin{pmatrix} \hat{x}_1 & \hat{x}_2 & \hat{x}_3 \end{pmatrix}^T = \begin{pmatrix} 3.5 & -5.5 & 0 \end{pmatrix}^T$. Definition (3.19) yields a continuous transition from the injection sphere to the remaining area of the vitreous compare to the initial concentration profile in [75].

Diffusion Coefficient

The distribution of drug depends on multiple factors as the rheology of the vitreous humor, the type and severity of retinal disorders and the properties of the specific drug. One important parameter is the diffusion coefficient D, the proportionality constant between the molar flux due to molecular diffusion and the gradient in the concentration of the drug.
As the Table 3.1 shows, the current pool of diffusion data is based on vitreous of different species such as human, rabbit, porcine and on aqueous media. Diffusion coefficients were also measured using different experiment techniques based on different diffusion theories. The integrity of the vitreous humor is inevitably compromised to some degree due to the method of extraction from the eye, and as a result of being removed from its natural nurturing environment. The Table 3.1 is ordered by the molecular weight (MW) of the diffusing compound demonstrating an inverse relationship between D and MW since the diffusion of high molecular-weight molecules can be limited by the vitreous structure [144]. Most previous work on determination of diffusion coefficients in the vitreous has focused on methods, using fluorescein

Compound	MW [kDa]	Diffusion media	D [$\times 10^{-10}$ m^2/s]	References
Bevacizumab	149	Rabbit vitreous	0.4	[143]
Galbumin	74	Rabbit vitreous	0.8	[130]
Galbumin	74	Bovine vitreous	0.227	[151]
GFP	29	Porcine vitreous (gel)	1.2	[18]
GFP	29	Porcine vitreous (liquid)	1.4	[18]
FITC-Dextran	9.3	Rabbit vitreous	6.18	[33]
FITC-Dextran	4.4	Rabbit vitreous	7.56	[33]
DMSB	0.599	Rabbit vitreous	5.1	[137]
DMSB	0.599	Water	7	[137]
Dexamethasone	0.392	Porcine vitreous	18.06	[12]
Acid Orange 8	0.364	Bovine vitreous	3.4	[192]
Acid Orange 8	0.364	Water	6.5	[192]
Fluorescein	0.332	Human vitreous	8.91	[104]
Fluorescein	0.332	Human vitreous	9.6	[116]
Fluorescein	0.332	Human vitreous (diabetic)	7.4	[116]
Fluorescein	0.332	Human vitreous	4.91	[47]
Fluorescein	0.332	Human vitreous	13	[195]
Fluorescein	0.332	Water	6	[91, 135]
Fluorescein	0.332	Bovine vitreous	$4.8 - 6$	[91, 135]

Table 3.1: Measured diffusion coefficients in the literature

as a model compound. Kaiser and Maurice [91] measured the diffusivity of fluorescein of bovine eyes and water (agar gel) by using fluorophotometry. Even though they did not use human vitreous samples their data has been used in mathematical models [170, 8] to represent the diffusivity. But despite the fact that multiple studies have examined diffusion of fluorescein, there is significant variation in the reported diffusion coefficients. Further, even the rheological properties of bovine, porcine and human vitreous are similar, there are great differences in values following the rank order of diffusivity: human > bovine > porcine > ovine [162]. Overall, the conclusions about the diffusivity in the vitreous are: increased particle size decreases the mobility in the vitreous and liquefaction causes an increase in particle diffusion [6].
Due to the lack of experimental data of drug diffusion coefficients in human

vitreous, following [193, 6] the diffusion coefficient for the liquefied vitreous, $D = 0.83 \times 10^{-10}$ m^2/s, is calculated using the Stokes-Einstein equation in [12],

$$D := \frac{R\theta}{6\pi\mu_0 r N}$$

where $\theta = 307.05$ K is the constant temperature within the vitreous, μ_0 is the dynamic viscosity of the liquefied vitreous, r is the hydrodynamic radius of the diffusing Aflibercept listed in Table 5.1, R is the molar gas constant and N is the Avogadro's number. Since in vivo experiments often use young animal models with no alterations in the vitreous structure, as liquefactions or retinal diseases, the results of these experiments can overestimate drug efficacy and can not be extrapolate in general to humans. D characterizing the healthy vitreous is set to be 0.4×10^{-10} m^2/s according to experiments on rabbits' eyes with diffusing drug Bevacizumab in [143]. It is the closest value found in the literature to the real diffusion coefficient of Aflibercept in the human vitreous. The majority of available anti-VEGF pharmacokinetic data is from animal models but there are concerns about the extrapolation to human eyes due to anatomical and physiological differences. Due to the increased viscosity and porous/gel-like structure of the young vitreous it is assumed to be lower than for the liquefied one. In [123] they measured the apparent diffusion coefficient of water protons for human eyes of all ages showing decreasing values ($2.88 - 3.76 \times 10^{-3}$ mm^2/s) with decreasing age. The measurements in Xu et al. [192] exhibit changes up to 48% between diffusivity in water and bovine vitreous.
Intravitreal drug distribution depends on many parameters related to the specific drug used for the treatment and to the physiology of the eye. The parameters required to solve the models are summarized in Table 5.1.

3.4.2 Derivation of Governing Equations

The mathematical theory of diffusion can be found in [30]. Physically, diffusion is the spontaneous, natural process by which molecules spread from areas of high concentration to areas of low concentration as a result of random molecular motions. In the situation of drug diffusion through the vitreous it means that the high drug concentration gradients from the injection site provides the force for the drug-particles to move until a concentration balance is reached. It is the consequence of the conservation of mass which states that the change of concentration is equal to the accumulation due to net influx. Effectively, no material is created or destroyed:

$$\partial_t C = -\nabla \cdot J$$

where C is the concentration and J is the flux of the diffusing material. The diffusion equation (3.17) can be obtained easily from this equation by combining with the phenomenological Fick's first law. It states that the flux of the diffusing material in any part of the system is proportional to the local concentration gradient times the diffusion coefficient D, which means that flux always points in the direction from high to low concentration:

$$J := -D\nabla C + vC.$$

3.4.3 Existence and Uniqueness (Mixed Boundary Conditions)

In this section we prove the global existence and uniqueness of the weak solution of the convection-diffusion equation (3.17) describing the drug distribution. In particular, results from the literature are extended from homogeneous Dirichlet boundary conditions to our mixed boundary conditions (3.18) characterizing the human eye with the Galerkin's method using Cauchy-Schwarz inequality and trace theorem.

As mentioned in the previous Section 3.2.3, we require for the boundary of our domain Ω that $\partial\Omega \in C^1$. The distinguishable parts of it have non-vanishing Lebesgue measure, i.e. $|\Gamma_r|, |\Gamma_l|, |\Gamma_h| > 0$.

We generalize (3.17) by adding the gravity $\tilde{g} : \Omega \to \mathbb{R}, \tilde{g} := \frac{1}{\beta}\left(1 - \frac{\rho_f}{\rho_p}\right) g$ as introduced in Chapter 3.2 and a given external force $f : \Omega \times (0, T] \to \mathbb{R}$ which yields to

$$\partial_t C + (v + \tilde{g}) \cdot \nabla C - \nabla \cdot (D\nabla C) = f. \tag{3.20}$$

Literature about the analytical results for parabolic differential equations can be found in [101, 191]. But the mixed boundary conditions characterizing the drug distribution in the vitreous including Dirichlet, Neumann as well as Robin boundary conditions are new developed and therefore not examined before. We extend the existence and uniqueness proof of weak solutions of the parabolic problem in [48] from homogeneous boundary conditions to the general boundary conditions (3.18).
For further analysis including the variational form and energy estimates we assume now that

$$\begin{aligned} D, v, \tilde{g} &\in L^\infty(\Omega), \\ f &\in L^2(\Omega \times (0, T]), \\ C_0 &\in L^2(\Omega). \end{aligned}$$

For the gravity vector and initial concentration this is fulfilled by construction. Since the diffusion coefficient $0 < D < \infty$ is constant we also have $D \in L^\infty(\Omega)$. The velocity field v is modeled by an extra set of equations depending on the physiology of the vitreous. If there is no back-coupling between the diffusion equation and the flow model one can decouple the system and reduce the proof to results concerning the flow equations and parabolic equation describing the drug distribution. For the special case of the drug distribution within the healthy vitreous we consider the equation (3.17) generalized to (3.20) where v is described by Darcy's flow (3.1). Here, the velocity is bounded for almost all $x \in \Omega$, as shown in the previous Section 3.2.3 of the regularity of Darcy's flow. In the case of no external forces, $f = 0$, like in the developed model describing the drug transport (3.17), the condition $f \in L^2(\Omega \times (0,T])$ is trivially fulfilled.

We define by $[\mathbf{C}(t)](x) := C(x,t)$ for $x \in \Omega, t \in [0,T]$ a mapping

$$\mathbf{C} : [0,T] \to H_0^1(\Omega;\Gamma_\mathrm{h})$$

and consider C not as a function of x and t together, but as a mapping $\mathbf{C}$ of t into the space $H_0^1(\Omega;\Gamma_\mathrm{h})$ of functions of x. Similarly, we define $\mathbf{f} : [0,T] \to L^2(\Omega)$ by $[\mathbf{f}(t)](x) := f(x,t), x \in \Omega, t \in [0,T]$. Then the weak formulation states:

Find $\mathbf{C} \in L^2(0,T;H_0^1(\Omega;\Gamma_\mathrm{h}))$ such that

$$(d_t\mathbf{C},\varphi) + B[\mathbf{C},\varphi] = (\mathbf{f},\varphi) \qquad \forall \varphi \in H_0^1(\Omega;\Gamma_\mathrm{h}),\ \text{a.e. } t \in [0,T] \tag{3.21}$$

and

$$\mathbf{C}(0) = C_0$$

with the time-independent bilinear form

$$B[\mathbf{C},\varphi] := (D\nabla\mathbf{C},\nabla\varphi) + ((v+\tilde{g})\cdot\nabla\mathbf{C},\varphi) + (P\mathbf{C} + (n\cdot v)(k_{vr}-1)\mathbf{C},\varphi)_{\Gamma_\mathrm{r}} \tag{3.22}$$

and $d_t\mathbf{C} \in L^2(0,T;(H_0^1(\Omega;\Gamma_\mathrm{h}))^*)$ where $(H_0^1(\Omega;\Gamma_\mathrm{h}))^*$ denotes the dual space to $H_0^1(\Omega;\Gamma_\mathrm{h})$.

Remark 3.4.1: *We see that* $\mathbf{C} \in C([0,T];L^2(\Omega))$ *[48].*

We will use the Galerkin's method to build weak solutions of our parabolic problem (3.20) by first constructing solutions of finite-dimensional approximations $\mathbf{C}_m : [0,T] \mapsto H_0^1(\Omega;\Gamma_\mathrm{h})$ as a linear combination of the form

$$\mathbf{C}_m(t) := \sum_{k=1}^{m} d_{km}(t) w_k \tag{3.23}$$

for a fixed integer $m > 0$ and with the coefficients $d_{km}(t), t \in [0,T], k = 1,\dots,m$ such that

$$d_{km}(0) = (C_0, w_k) \qquad \forall k = 1,\dots,m. \tag{3.24}$$

Then the function $\mathbf{C}_m$ satisfies the projection of our problem onto the finite dimensional subspace spanned by smooth functions $\{w_k\}_{k=1}^m$:

$$(d_t\mathbf{C}_m, w_k) + B[\mathbf{C}_m, w_k] = (\mathbf{f}, w_k) \qquad t \in [0,T], k = 1,\dots,m \tag{3.25}$$

where $\{w_k\}_{k=1}^\infty$ is an orthogonal basis of $H_0^1(\Omega;\Gamma_\mathrm{h})$ and an orthonormal basis of $L^2(\Omega)$.
For each integer $m = 1, 2, \dots$ there exists a unique function $\mathbf{C}_m$ of the form (3.23) satisfying the equations (3.24) and (3.25) since the existence of the unique solution of the resulted linear system of ordinary differential equations can be proven by the Picard-Lindelöf existence theorem using Lipschitz-continuity [149].

To show that a subsequence of our solutions $\mathbf{C}_m$ of the approximate problems (3.24), (3.25) converges to a weak solution of (3.20) with the corresponding boundary conditions (3.18) we need energy estimates.

Theorem 3.4.2 (Energy estimates)**:**
There exists a constant c depending only on Ω, T and the coefficients $D, v, \tilde{g}$ such that

$$\max_{t\in[0,T]} \|\mathbf{C}_m(t)\|_{L^2(\Omega)} + \|\mathbf{C}_m(t)\|_{L^2(0,T;H_0^1(\Omega;\Gamma_h))} + \|d_t\mathbf{C}_m(t)\|_{L^2(0,T;(H_0^1(\Omega;\Gamma_h))^*)}$$
$$\leq c\left(\|f\|_{L^2(0,T;L^2(\Omega))} + \|C_0\|_{L^2(\Omega)}\right)$$

for $m = 1, 2, \dots$.

Proof. The proof of this theorem uses the same arguments as the proof of Theorem 2 in 6.2.2 in [48] and is therefore not carried out in detail. The restriction to the ansatz space $H_0^1(\Omega;\Gamma_\mathrm{h})$ instead of $H_0^1(\Omega;\partial\Omega)$ for pure Dirichlet boundary conditions has no influence. In contrast the definition (3.22) of $B[\cdot,\cdot]$ differs due to additional boundary terms considering the biology of the eye and hence we have to show the following two Lemmas to complete the proof. □

Lemma 3.4.3: *For all $\mathbf{C}_m \in H_0^1(\Omega;\Gamma_h)$ there exist constants $\beta > 0$ and $\gamma \geq 0$ such that*

$$\beta\|\mathbf{C}_m\|^2_{H_0^1(\Omega;\Gamma_h)} \leq B[\mathbf{C}_m, \mathbf{C}_m] + \gamma\|\mathbf{C}_m\|^2_{L^2(\Omega)} \qquad \forall t \in [0,T], m = 1,\dots$$

Proof. In view of the ellipticity condition, i.e. $\exists\theta > 0$ such that

$$\theta\|y\|^2_{L^2(\Omega)} \leq (Dy, y) \qquad \forall x \in \Omega, y \in \mathbb{R}^3,$$

and the definition of the bilinear form (3.22) we have

$$\begin{aligned}
\theta\|\nabla \mathbf{C}_m\|^2_{L^2(\Omega)} &\leq (D\nabla \mathbf{C}_m, \nabla \mathbf{C}_m) \\
&= B[\mathbf{C}_m, \mathbf{C}_m] - ((v + \tilde{g}) \cdot \nabla \mathbf{C}_m, \mathbf{C}_m) - (P\mathbf{C}_m, \mathbf{C}_m)_{\Gamma_r} \\
&\quad - ((n \cdot v)(k_{vr} - 1)\mathbf{C}_m, \mathbf{C}_m)_{\Gamma_r} \\
&\leq B[\mathbf{C}_m, \mathbf{C}_m] + \left(\|v\|_{L^\infty(\Omega)} + \|\tilde{g}\|_{L^\infty(\Omega)}\right)(|\nabla \mathbf{C}_m|, |\mathbf{C}_m|) \\
&\quad + \left(|P| + \|(n \cdot v)(k_{vr} - 1)\|_{L^\infty(\Omega)}\right)\|\nabla \mathbf{C}_m\|^2_{L^2(\Omega)}.
\end{aligned}$$

Using Cauchy's inequality with $\epsilon > 0$, see Appendix B.2 in [48], we observe

$$(|\nabla \mathbf{C}_m|, |\mathbf{C}_m|) \leq \epsilon\|\nabla \mathbf{C}_m\|^2_{L^2(\Omega)} + \frac{1}{4\epsilon}\|\mathbf{C}_m\|^2_{L^2(\Omega)}.$$

We choose $\epsilon > 0$ so small that

$$\epsilon\left(\|v\|_{L^\infty(\Omega)} + \|\tilde{g}\|_{L^\infty(\Omega)}\right) + |P| + \|(n \cdot v)(k_{vr} - 1)\|_{L^\infty(\Omega)} < \frac{\theta}{2}$$

and get

$$\beta\|\mathbf{C}_m\|^2_{H^1_0(\Omega;\Gamma_h)} = \frac{\theta}{2}\|\nabla \mathbf{C}_m\|^2_{L^2(\Omega)} \leq B[\mathbf{C}_m, \mathbf{C}_m] + \gamma\|\mathbf{C}_m\|^2_{L^2(\Omega)}$$

with the constants $\beta = \frac{\theta}{2} > 0$ and $0 \leq \gamma := \frac{1}{4\epsilon}\left(\|v\|_{L^\infty(\Omega)} + \|\tilde{g}\|_{L^\infty(\Omega)}\right)$.

□

Lemma 3.4.4: *There exists a constant $\alpha > 0$ such that*

$$|B[\mathbf{C}_m, \varphi]| \leq \alpha\|\mathbf{C}_m\|_{H^1_0(\Omega;\Gamma_h)}\|\varphi\|_{H^1_0(\Omega;\Gamma_h)} \qquad \forall\, \mathbf{C}_m, \varphi \in H^1_0(\Omega;\Gamma_h).$$

Proof.

$$
\begin{aligned}
|B[\mathbf{C}_m, \varphi]| &\leq D\|\nabla \mathbf{C}_m\|_{L^2(\Omega)}\|\nabla \varphi\|_{L^2(\Omega)} \\
&\quad + \left(\sum_{i=1}^{3} \|v_i\|_{L^\infty(\Omega)} + \|\tilde{g}\|_{L^\infty(\Omega)}\right) \|\nabla \mathbf{C}_m\|_{L^2(\Omega)}\|\varphi\|_{L^2(\Omega)} \\
&\quad + \left(|P| + \sum_{i=1}^{3} \|n_i v_i (k_{vr} - 1)\|_{L^\infty(\Omega)}\right) \|\mathbf{C}_m\|_{L^2(\Gamma_\mathrm{r})}\|\varphi\|_{L^2(\Gamma_\mathrm{r})} \\
&\leq D\|\nabla \mathbf{C}_m\|_{L^2(\Omega)}\|\nabla \varphi\|_{L^2(\Omega)} \\
&\quad + \left(\|v\|_{L^\infty(\Omega)} + \|\tilde{g}\|_{L^\infty(\Omega)}\right) \|\nabla \mathbf{C}_m\|_{L^2(\Omega)}\|\nabla \varphi\|_{L^2(\Omega)} \\
&\quad + \left(|P| + \|(n \cdot v)(k_{vr} - 1)\|_{L^\infty(\Omega)}\right) \|\nabla \mathbf{C}_m\|_{L^2(\Omega)}\|\nabla \varphi\|_{L^2(\Omega)} \\
&\leq \alpha \|\nabla \mathbf{C}_m\|_{L^2(\Omega)}\|\nabla \varphi\|_{L^2(\Omega)} \\
&= \alpha \|\mathbf{C}_m\|_{H_0^1(\Omega;\Gamma_\mathrm{h})}\|\varphi\|_{H_0^1(\Omega;\Gamma_\mathrm{h})}
\end{aligned}
$$

for a constant

$$
\alpha := D + \|v\|_{L^\infty(\Omega)} + \|\tilde{g}\|_{L^\infty(\Omega)} + |P| + \|(n \cdot v)(k_{vr} - 1)\|_{L^\infty(\Omega)} > 0.
$$

□

Next, we build a weak solution of our initial/boundary-value problem (3.21) by passing $m \to \infty$.

Theorem 3.4.5 (Existence of weak solution)**:**
There exists a weak solution $\mathbf{C} \in L^2(0, T; H_0^1(\Omega; \Gamma_h))$ *of problem* (3.21) *for* $D, v, \tilde{g} \in L^\infty(\Omega)$ *and* $f \in L^2(\Omega \times (0, T]$ *and* $C_0 \in L^2(\Omega)$*.*

Proof. The proof follows the idea in Theorem 3 in 7.1.2 in [48]. Since we consider different boundary conditions the corresponding function space and bilinear form $B[\cdot, \cdot]$ differ from the examined results in [48]. But by applying the Lemmas 3.4.3 and 3.4.4 the proof can be generalized.
First, we use previous energy estimates and weak compactness theorem to show the weakly convergence of subsequences $\{\mathbf{C}_{m_l}\}_{l=1}^{\infty} \subset \{\mathbf{C}_m\}_{m=1}^{\infty}$ to $\mathbf{C}$ in $L^2(0, T; H_0^1(\Omega; \Gamma_\mathrm{h}))$. Then we fix an integer M and choose a function

$$
\mathbf{v} \in C^1([0, T]; H_0^1(\Omega; \Gamma_\mathrm{h}))
$$

having the form $\mathbf{v}(t) = \sum_{k=1}^{M} d_k(t) w_k$ where $\{d_k\}_{k=1}^{M}$ are given smooth functions. By passing to the limits we get

$$
(d_t \mathbf{C}, \varphi) + B[\mathbf{C}, \varphi] = 0 \qquad \forall \varphi \in H_0^1(\Omega; \Gamma_\mathrm{h}), \text{ a.e. } t \in [0, T].
$$

Finally, we show that $\mathbf{C}(0) = C_0$.

□

Theorem 3.4.6 (Uniqueness of weak solution)**:**
A weak solution of problem (3.21) *is unique.*

Proof. Regarding the uniquenss of weak solution, it is straightforward to reuse the results by Theorem 4 in 7.1.2 in [48] which follows the generally known procedure. It suffices to check that the only weak solution of (3.21) with $C_0 \equiv 0$ is

$$\mathbf{C} \equiv 0$$

and set the test function $\varphi = C$ in the weak formulation. □

Summarized, we proved the global existence and uniqueness of the weak solution of the drug distribution (coupled with the Darcy equation modeling the healthy human vitreous by the porous medium approach) and showed that the developed mathematical model is well posed in its mathematical theory and biological derivation.

3.4.4 Convection-Diffusion Coupled with Darcy

As introduced in Section 3.2 the healthy vitreous is modeled as a porous medium with the steady permeating aqueous humor flow through the vitreous and active transport through the retina. Therefore to describe the drug distribution within the healthy vitreous for the treatment of retinal diseases, the diffusion equation (3.17) is coupled with Darcy's law (3.1). The global existence and uniqueness of the weak solution of the developed initial-boundary value problem is shown in the Sections 3.2.3 and 3.4.3.

As a starting point for further numerical simulations we derive the weak formulation by multiplying by suitable test functions, integrating over the domain Ω and applying integration by parts, since the strong formulation of the model is not convenient for numerical treatment.

If we consider the boundary conditions (3.2) for the Darcy flow the variational formulation reads:

We search for $v \in L^2_{\mathrm{div}}(\Omega;\Gamma_1)^d$, $p \in L^2(\Omega)$ and $C \in L^2(0,T;H^1_0(\Omega;\Gamma_{\mathrm{h}}))$ such that the initial condition $C(x,0) = C_0(x)$ is satisfied and for almost all time

steps $t \in (0, T]$ it holds:

$$
\begin{aligned}
(\nabla \cdot v, \xi) &= 0, \\
\frac{\mu}{K}(v, \phi) - (p, \nabla \cdot \phi) + (p_{\text{in}}, n \cdot \phi)_{\Gamma_{\text{h}}} + (P_v + \frac{L}{K_{RCS}}(v \cdot n), n \cdot \phi)_{\Gamma_{\text{r}}} &= 0, \\
\left(\frac{dC}{dt}, \varphi\right) + (D\nabla C, \nabla \varphi) + (PC + (n \cdot v)(k_{vr} - 1)C, \varphi)_{\Gamma_{\text{r}}} &= 0
\end{aligned}
$$

for all $(\xi, \phi, \varphi) \in L^2(\Omega) \times L^2_{\text{div}}(\Omega; \Gamma_{\text{l}})^d \times H^1_0(\Omega; \Gamma_{\text{h}})$ with the following function space:

$$L^2_{\text{div}}(\Omega; \Gamma_{\text{l}})^d := \{v \in L^2(\Omega)^d : \nabla \cdot v \in L^2(\Omega), v \cdot n = 0 \text{ on } \Gamma_{\text{l}}\},$$

and $H^1_0(\Omega; \Gamma_{\text{h}})$ is defined in (3.5) with $\Gamma_{\text{D}} = \Gamma_{\text{h}}$.

In the second case, we look at the boundary conditions (3.3) for the Darcy flow, then the corresponding weak formulation reads:

We search for $v \in L^2_{\text{div}}(\Omega; \Gamma_{\text{l}} \cup \Gamma_{\text{h}})^d$, $p \in L^2(\Omega)$ and $C \in L^2(0, T; H^1_0(\Omega; \Gamma_{\text{h}}))$ such that the initial condition $C(x, 0) = C_0(x)$ is satisfied and for almost all time steps $t \in (0, T]$ it holds:

$$(\nabla \cdot v, \xi) = 0, \tag{3.26a}$$

$$\frac{\mu}{K}(v, \phi) - (p, \nabla \cdot \phi) + (P_v + \frac{L}{K_{RCS}}(v \cdot n), n \cdot \phi)_{\Gamma_{\text{r}}} = 0, \tag{3.26b}$$

$$\left(\frac{dC}{dt}, \varphi\right) + (D\nabla C, \nabla \varphi) + (PC + (n \cdot v)(k_{vr} - 1)C, \varphi)_{\Gamma_{\text{r}}} = 0 \tag{3.26c}$$

for all $(\xi, \phi, \varphi) \in L^2(\Omega) \times L^2_{\text{div}}(\Omega; \Gamma_{\text{l}} \cup \Gamma_{\text{h}})^d \times H^1_0(\Omega; \Gamma_{\text{h}})$ with the function space

$$L^2_{\text{div}}(\Omega; \Gamma_{\text{l}} \cup \Gamma_{\text{h}})^d := \left\{ v \in L^2(\Omega)^d : \nabla \cdot v \in L^2(\Omega), v \cdot n = \begin{cases} 0 & \text{on } \Gamma_{\text{l}} \\ v_{\text{in}} & \text{on } \Gamma_{\text{h}} \end{cases} \right\}.$$

In our publications [41, 60] the corresponding numerical simulations for the drug distribution including the steady permeating aqueous humor flow are performed with the finite element method [26]. The position of injection is analyzed by functionals which measure the mean and relative amount of the drug in the vitreous and in the area of action, the macula. For an optimal treatment of the retinal disease the drug is supposed to stay as long as possible there. The results show that the maximal amount of drug is found in the area

of interest for the considered time period when the position of injection is located in the center of the vitreous body. Thus, the position of the injection is identified as an important parameter which is in agreement with previous studies [61].

3.4.5 Convection-Diffusion Coupled with Navier-Stokes

The liquefaction of the vitreous, the degeneration process of the vitreous humor associated with aging, causes an increase in the drug elimination and an increase in the convection flow due to the disruption of the fibers' mesh composing the vitreous humor [14, 177]. In [174] a simulated liquefaction caused a 12-fold faster distribution of fluorescein sodium compared to the simulated juvenile vitreous model without liquefaction, which was most likely caused by enhanced convective forces and mass transfer. Most animal models in the literature indicate that intravitreal drugs have reduced half-lives and increased clearance in vitrectomized eyes [44]. For example, Niwa et al. [136] measured the pharmacokinetic parameters in vitrectomized and non-vitrectomized monkey eyes. Here, the half-life of ranibizumab and aflibercept was shorter in vitrectomized eyes than in non-vitrectomized eyes.
The whole system of governing equations in the weak formulation describing the drug distribution in the liquefied vitreous by coupling the diffusion equation (3.17) with the Navier-Stokes equation (3.9) from the previous sections reads:

Find $p \in L^2(0,T;L^2(\Omega))$, $v \in L^2(0,T;\{v_{\text{in}} + H_0^1(\Omega;\Gamma_{\text{D}})^d\})$ and the drug concentration $C \in L^2(0,T;H_0^1(\Omega;\Gamma_{\text{h}}))$ such that the initial conditions $v(x,0) = v_0(x)$, $C(x,0) = C_0(x)$ are satisfied, $v_{\text{in}} \in H^1(\Omega)^d$ and for almost all time steps $t \in (0,T]$ with $T \in (0,\infty)$ it holds that

$$(\nabla \cdot v, \xi) = 0, \tag{3.27a}$$

$$\rho(\partial_t v, \phi) + \rho((v \cdot \nabla)v, \phi) + (\mathbb{T}, \nabla\phi) - (k_{\text{perm}}(v \cdot n)n, \phi)_{\Gamma_{\text{r}}} = 0, \tag{3.27b}$$

$$\left(\frac{dC}{dt}, \varphi\right) + (D\nabla C, \nabla\varphi) + (PC + (n \cdot v)(k_{vr} - 1)C, \varphi)_{\Gamma_{\text{r}}} = 0 \tag{3.27c}$$

for all $(\xi, \phi, \varphi) \in L^2(\Omega) \times H_0^1(\Omega;\Gamma_{\text{D}})^d \times H_0^1(\Omega;\Gamma_{\text{h}})$ where the Dirichlet boundary is defined as $\Gamma_{\text{D}} := \Gamma_{\text{l}} \cup \Gamma_{\text{h}} \subset \partial\Omega$.

Back Coupling Through Surface Tension

So far we considered in the previous models describing the drug distribution a coupling between the vitreous flow and the diffusion of the drug concentration

only through the velocity field. In particular, the convection-diffusion equation (3.17) is coupled by the transport term $(v \cdot \nabla)C$ with the fluid flow modeled either by Darcy's flow (3.1) or Navier-Stokes equation (3.9).
The following section will show a possible back-coupling through surface tension and extend the developed models to a fully coupled system in which the drug transport contains the transport term including the velocity field and the fluid flow model contains the drug concentration. Then the drug diffusion and fluid flow are closely related and can effect each other. The surface tension is represented by the so-called Korteweg stress based on the Van der Waals theory at the interface of two miscible fluids. It is the tendency of liquid surfaces to reduce into the minimum surface area possible and influences the drug transport in the human vitreous beside the rheology of the vitreous and its induced flow field.

Physical Meaning The liquefied vitreous humor fluid and the solution for injection containing the active ingredient are two miscible liquids. In contact they immediately start to diffuse in each other but if the diffusion is sufficiently slow like in the case of large drug molecules, a concentration gradient exists which relaxes through further diffusion. Then an effective interfacial tension appears which can lead to transient capillary phenomena in the case of liquefied vitreous. As stated in the literature [9, 78] the surface tension has an important impact on pharmaceutical sciences in general and especially in the eye it influences the drug distribution and could impact the performance of intravitreal therapy. The surface tension of liquefied vitreous should be taken into account when simulating drug dispersion following intravitreal injection [78].
For example, a drop of oil in water (immiscible liquids) becomes spherical because of the interfacial tension which acts to minimize its surface, contrary to that a drop of water on the surface of glycerin (miscible liquids), initially round, changes its shape in time [98]. To model this behavior, the classical approach used in immiscible cases is not suitable. Here it is supposed that the liquids are separated by a sharp interface described by a free-boundary formulation which specifies a jump condition at the surface separating fluids possessing different concentrations. Instead one describes the phase transition phenomena by the Korteweg model proposed in 1901 in [97]. Korteweg states that fluid stresses which arise as a result of concentration (or temperature, density) gradients at the interface between two miscible fluids (vitreous/drug) lead to the notion of surface tension between miscible fluids [7]. The key feature of the model is the additional contribution to the Cauchy stress tensor, the Korteweg stress (surface tension) in terms of the concentration and its spatial gradients. This

tensor is associated with the surface tension that relaxes with time due to the mass diffusion and takes into account the concentration changes [185].

In accordance to the assumptions of Kostin et al. [98] that the diffusion is sufficiently small, the vitreous and drug injection are incompressible and have the same density and viscosity which is fulfilled in our situation, we write the governing equations for the drug distribution concerning surface tension in the form:

$$\nabla \cdot v = 0 \qquad \text{in } \Omega \times (0,T], \tag{3.28a}$$

$$\rho\left(\frac{\partial v}{\partial t} + (v \cdot \nabla)v\right) = \nabla \cdot \mathbb{T} \qquad \text{in } \Omega \times (0,T], \tag{3.28b}$$

$$-p\mathbb{I} + 2\mu_0 \mathbb{D} + T(C) = \mathbb{T} \qquad \text{in } \Omega \times (0,T], \tag{3.28c}$$

$$\frac{\partial C}{\partial t} + (v \cdot \nabla)C - \nabla \cdot (D\nabla C) = 0 \qquad \text{in } \Omega \times (0,T], \tag{3.28d}$$

where the Korteweg stress associated with surface tension is defined as

$$T(C) := -k_{\text{kor}}(\nabla C \otimes \nabla C) + k_{\text{kor}}|\nabla C|^2\mathbb{I} \tag{3.29}$$

with the nonnegative material parameter k_{kor} called Korteweg's constant. The divergence of the Cauchy tensor including the Korteweg stress yields

$$\nabla \cdot \mathbb{T} = -\nabla p + \mu_0 \Delta v + \frac{k_{\text{kor}}}{2}\nabla|\nabla C|^2 - k_{\text{kor}}\Delta C \nabla C.$$

This system of equations is completed by the initial and boundary conditions (3.18) and (3.11) defined in the previous sections introducing the diffusion and Navier-Stokes equation.

Derivation of Governing Equations The above constitutive equation (3.28c) for the Cauchy stress tensor including the Korteweg stress (3.29) can be derived in a thermodynamically consistent manner in the setting of binary mixtures in the class I framework introduced in [84]. The mixture of the two incompressible fluids, drug injection (component 1) and liquefied vitreous (component 2), forms a typical representative of the class of the so-called diffuse interface models. Then the model for surface tension can be obtained by employing the classical thermodynamical framework and following the procedure for the Navier-Stokes fluid introduced in Section 3.3.2 in combination with the presence of the concentration gradient in the specific formula for the Helmholtz potential.

The system of balance equations for binary mixtures (neglecting for simplicity the energy sources) is the same as introduced in Chapter 2.2 plus the additional evolution equation for the concentration $C = C_1 = \rho_1/\rho$

$$\rho \frac{dC}{dt} = -\text{div } j$$

where $\rho = \rho_1 + \rho_2$ with the partial densities ρ_1, ρ_2 and j denotes the diffusive flux. Derived from it one obtains an evolution equation for the gradient ∇C:

$$\rho \frac{d\nabla C}{dt} = -(\nabla v)^T \nabla C - \nabla \left(\frac{\text{div } j}{\rho} \right).$$

In contrast to Section 3.3.2 we consider the constitutive equation for the specific Helmholtz free energy ψ in the following explicit form

$$\psi := \tilde{\psi}(\theta, \rho, \nabla C) = \psi_0(\rho) + \psi_1(\theta) + \frac{k_{\text{kor}}}{2\rho} |\nabla C|^2. \tag{3.30}$$

Compare to the specific form (3.13) for the Navier-Stokes fluid, the form (3.30) contains one additional term. This choice is motivated by the fact that one expects the concentration gradient ∇C to contribute to the energy storage mechanisms, and the fact that the norm of the gradient ∇C is the simplest possible choice if one wants the Helmholtz free energy to be a scalar isotropic function of ∇C. (By the principle of material frame indifference one concludes that $\psi = \tilde{\psi}(\theta, \rho, |\nabla C|)$ such that the resulting additional contributions to the Cauchy stress tensor are symmetric.) Introducing the new thermodynamic pressure and a variation of the chemical potential via

$$p_{\text{th}}^{\text{K}} := \rho^2 \frac{\partial \psi}{\partial \rho}, \qquad \mu_C := \rho \frac{\partial \psi}{\partial \nabla C} = k_{\text{kor}} \nabla C,$$

applying the material time derivative to equation (3.30),

$$\frac{d\psi}{dt} = \frac{\partial \psi}{\partial \theta} \frac{d\theta}{dt} + \frac{\partial \psi}{\partial \rho} \frac{d\rho}{dt} + \frac{\partial \psi}{\partial \nabla C} \frac{d\nabla C}{dt},$$

and considering the relation (3.12) we get the material time derivative of the entropy η:

$$\rho\theta \frac{d\eta}{dt} = \rho \frac{de}{dt} - \frac{p_{\text{th}}^{\text{K}}}{\rho} \frac{d\rho}{dt} - \mu_C \frac{d\nabla C}{dt}.$$

Notice that the thermodynamic pressure p_{th}^{K} for the Korteweg fluid is different from the thermodynamic pressure $p_{\text{th}}^{\text{NS}} := \rho^2 \frac{\partial \psi_0}{\partial \rho}$ for the Navier–Stokes fluid:

$$p_{\text{th}}^{\text{K}} = p_{\text{th}}^{\text{NS}} - \frac{k_{\text{kor}}}{2} |\nabla C|^2.$$

Proceeding further analog to the framework in Section 3.3.2 we get

$$\begin{aligned}
\rho\theta \frac{d\eta}{dt} &= \mathbb{T}_\delta : \mathbb{D}_\delta + (m + p_{\text{th}}^{\text{K}}) \text{div } v - \text{div } j_e + \mathbb{K} : (\nabla v)^T + \mu_C \cdot \nabla \left(\frac{\text{div } j}{\rho} \right) \\
&= (\mathbb{T}_\delta + \mathbb{K}_\delta) : \mathbb{D}_\delta + \left(m + p_{\text{th}}^{\text{K}} + \frac{\text{tr } \mathbb{K}}{3} \right) \text{div } v - \text{div } \left(j_e - \frac{\text{div } j}{\rho} \mu_C \right) \\
&\quad - \text{div } \left(\frac{\text{div } \mu_C}{\rho} j \right) + j \cdot \nabla \left(\frac{\text{div } \mu_C}{\rho} \right)
\end{aligned}$$

where we introduced the tensor $\mathbb{K} := \mu_C \otimes \nabla C$. After reformulations and requiring the linear relations between the fluxes and affinities it follows the constitutive relation for the Cauchy stress tensor as:

$$\begin{aligned}
\mathbb{T} &= -p_{\text{th}}^{\text{K}} \mathbb{I} + 2\mu_0 \mathbb{D} + \lambda (\text{div } v) \mathbb{I} - \mathbb{K} \\
&= -p_{\text{th}}^{\text{NS}} \mathbb{I} + 2\mu_0 \mathbb{D} + \lambda (\text{div } v) \mathbb{I} - k_{\text{kor}} (\nabla C \otimes \nabla C) + \frac{k_{\text{kor}}}{2} |\nabla C|^2 \mathbb{I}.
\end{aligned}$$

Since we consider only incompressible and isothermal processes it reduces to

$$\mathbb{T} = -p\mathbb{I} + 2\mu_0 \mathbb{D} - k_{\text{kor}} (\nabla C \otimes \nabla C) + \frac{k_{\text{kor}}}{2} |\nabla C|^2 \mathbb{I}.$$

By setting $k_{\text{kor}} = 0$ the contribution of the surface tension is neglected and we get the thermodynamic derivation of the Navier-Stokes fluid (3.9c).
In the general model proposed by Korteweg in [97] the Cauchy stress tensor is given by

$$\mathbb{T} = -p\mathbb{I} + 2\mu_0 \mathbb{D} \left(\alpha_0 (C \Delta C) + \alpha_1 |\nabla C|^2 \right) \mathbb{I} + \beta (\nabla C \otimes \nabla C)$$

where $\alpha_0, \alpha_1, \beta$ are constant material parameters. Motivated by the fact that α_1 and β do not need to match we set $\alpha_0 = 0, \alpha_1 = k_{\text{kor}}/2$ and $\beta = -k_{\text{kor}}$ according to [98] but the thermodynamic derivation would proceed analogously. The reader interested in more details concerning the derivation of the model (3.28) is referred to [77].

Existence and Uniqueness In [98] and [100] the authors prove the global existence and uniqueness of the solution and the longtime behavior for the mathematical model (3.28) consisting of the time-dependent convection-diffusion equation coupled with incompressible Navier-Stokes equations including the Korteweg stress tensor. They use the same specific parameters for the Korteweg stress but complete the problem with homogeneous Dirichlet and Neumann boundary conditions for the velocity or rather the concentration in a two-dimensional bounded domain $\Omega \subset \mathbb{R}^2$ with boundary $\partial\Omega \in C^2$ and time $0 < T < \infty$. The coupling through the Korteweg stress tensor is nonlinear and poses an additional challenge which can be solved because of the specific form of the Korteweg stress. Following the Galerkin procedure the a priori estimation becomes possible since the Korteweg stress tensor and terms from the convection-diffusion equation cancel each other out.
Since [98, 100] consider different boundary conditions for the velocity and the concentration they describe another situation than the drug elimination in the vitreous in this thesis. We illustrate at the retina an outflow for both and at the hyaloid membrane we have an inflow velocity profile and the impermeable condition for the drug concentration. So, referring to the Section 3.3.3 and the known problems concerning the Navier-Stokes equation this concept is not adoptable to our model with mixed boundary conditions set in the three dimensional domain of the vitreous.

3.5 Models Including Gravity

To reflect the reality as well as possible, we include the gravity which influences the drug transport within the vitreous after an intravitreal injection. The direction of the gravitational force is changed due to the position of the patient. In the literature, [56, 62, 75] and many more, the effect of gravity on the drug diffusion was neglected. In [95] they analyze the effect of the gravity on bevacizumab distribution in an undisturbed balanced salt solution in vitro after intraocular injection (not intravitreal). They showed a significant difference in concentration due to gravity, especially at the beginning of the injection.
So, to our knowledge we are the first considering the effect of gravity in the mathematical models describing the drug distribution in the human vitreous. We add the gravitational force to the vitreous models described in the previous sections and to the drug distribution model (3.17). But the gravity do not influence the fluid motion due to the constant density of the vitreous, only in the diffusion equation we have density changes and therefore a significant difference in concentration due to gravity [95].

3.5.1 Vitreous Models

Generally in fluid dynamics, the gravity is included by adding the gravitational vector g times the density in the corresponding balance equation of the linear momentum, see the general equation (2.5). For the liquefied vitreous (3.9), we get

$$\begin{aligned} \nabla \cdot v &= 0 && \text{in } \Omega \times (0,T], \\ \rho\left(\frac{\partial v}{\partial t} + (v\cdot\nabla)v\right) &= \nabla\cdot\mathbb{T} + \rho g && \text{in } \Omega \times (0,T], \\ \mathbb{T} &= -p\mathbb{I} + 2\mu_0\mathbb{D} && \text{in } \Omega \times (0,T]. \end{aligned}$$

In the case of the healthy vitreous described by Darcy's flow, it reads

$$\nabla \cdot v = 0 \qquad \text{in } \Omega, \tag{3.31a}$$

$$-\frac{K}{\mu}\left(\nabla p - \rho_a g\right) = v \qquad \text{in } \Omega \tag{3.31b}$$

with the density of the aqueous humor ρ_a, see [121, 188].

Nevertheless, in this study the gravity is not included in the mathematical models for the flow since steady body forces (like gravity) in homogeneous density fluids do not influence the fluid motion and are therefore commonly neglected from the governing equations.
The vitreous has constant density and the gravitational force has a potential, i.e. $g = -\nabla\tilde{g}$ where $\tilde{g}$ is a scalar function. Because of that, one can rewrite the general momentum balance equation (2.5) as

$$\rho\left(\frac{\partial v}{\partial t} + (v\cdot\nabla)v\right) = -\nabla p + \nabla\cdot\mathbb{S} - \rho\nabla\tilde{g}$$

using the general form (2.11) for the Cauchy stress tensor. When we assume that the density ρ is spatially homogeneous, i.e. $\rho\nabla\tilde{g} = \nabla(\rho\tilde{g})$, then the momentum equation reduces to

$$\rho\left(\frac{\partial v}{\partial t} + (v\cdot\nabla)v\right) = -\nabla\tilde{p} + \nabla\cdot\mathbb{S}.$$

For the incompressible vitreous the gravity term can be incorporated into the pressure gradient term by defining the modified pressure $\tilde{p} := p + \rho\tilde{g}$. Furthermore, the tilde on p is typically dropped in this situation. Consequently, the shape of the momentum balance equation does not change, and for that

reason the fluid flow is not effected. Only the pressure must be reinterpreted. The same result follows for the special case of the healthy vitreous (3.31) which can be rewritten as

$$-\frac{K}{\mu}\nabla\left(p+\rho_a\tilde{g}\right)=v.$$

However, when the flow includes a free surface, a fluid-fluid interface across which the density changes, or other variations in density, the gravity should be considered.

3.5.2 Drug Distribution Model

Assuming the drug as spherical particles of mass m and radius r there are three forces acting on each particle moving with velocity v: drag force f_{d}, gravity force $f_{\mathrm{g}} := mg$ and buoyant force $f_{\mathrm{b}} := \rho V_p g$ as shown in Figure 3.2. $g =$

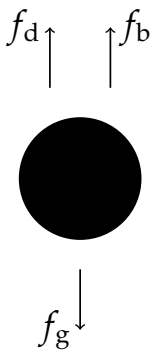

Figure 3.2: Forces acting on each drug particle

$g_{\mathrm{const}}e$ is the gravitational vector, i.e. gravitational constant g_{const} (acceleration of gravity) times the unit vector e in the direction of the gravitational field. $V_p := m/\rho_p$ is the solute particle volume and ρ, ρ_p are the respective densities of the surrounding fluid (vitreous) and diffusing drug particle. According to the Stokes formula for the drag on a sphere moving slowly in a fluid (valid for small Reynolds numbers) it holds that $f_{\mathrm{d}} := 6\pi\mu r v$ with the viscosity μ of the vitreous. At equilibrium all forces are balanced, i.e.

$$f_{\mathrm{g}} = f_{\mathrm{d}} + f_{\mathrm{b}}$$

and we get

$$6\pi\mu r v = m\left(1-\frac{\rho}{\rho_p}\right)g.$$

After rearranging, we obtain $v = \frac{m}{6\pi\mu r}\left(1 - \frac{\rho}{\rho_p}\right) g$ and can define the Mason–Weaver sedimentation coefficient $s := \frac{m}{6\pi\mu r}\left(1 - \frac{\rho}{\rho_p}\right)$. In three-dimensions the flux J at any point is given by

$$J = -D\nabla C + vC = -D\nabla C - sgC.$$

The first term describes the flux due to diffusion down a concentration gradient according to Fick's law, whereas the second term describes the convective flux due to the average velocity v of the particles. According to the conservation of mass a positive net flux out of a small volume produces a negative change in the local concentration within that volume

$$\partial_t C = -\nabla \cdot J.$$

Substituting the equation for the flux produces the Mason–Weaver equation:

$$\partial_t C = -\nabla \cdot J = \nabla \cdot (D\nabla C) + s\nabla \cdot (gC).$$

It may be written as

$$\partial_t C = \nabla \cdot (D\nabla C) + sg \cdot \nabla C.$$

This approach is fitting to the convective form of Smoluchowski's diffusion equation [133, 120, 5]:

$$\partial_t C + (v \cdot \nabla)C = \nabla \cdot (D\nabla C) + \nabla \cdot \left(\frac{F}{\beta} C\right)$$

with the external force $F := \left(1 - \frac{\rho}{\rho_p}\right) g$ per unit mass acting on the dispersed particle and the Stokes viscous drag parameter $\beta := \frac{6\pi\mu r}{m}$.

Summarized, including the gravity in the diffusion equation (3.17) describing the drug distribution we get

$$\partial_t C + (v \cdot \nabla)C = \nabla \cdot (D\nabla C) + \frac{1}{\beta}\left(1 - \frac{\rho}{\rho_p}\right) g \cdot \nabla C.$$

Here, the gravity has an effect on the drug distribution. As seen in the experiments the injected drug sinks in the direction of gravity [95].

4 Viscoelastic Approach for the Healthy Vitreous: Burgers Model

In order to assess the effectiveness of the injected drug into the vitreous for the treatment of retinal diseases, it is crucial to know the drug distribution within the eye. The results in [93] show that the concentration distribution depends on the properties of the vitreous. Therefore, it is important to analyze the properties of the vitreous like in [78, 179]. A better understanding of the properties of the vitreous humor will aid to develop more effective therapies such that drug concentration is maintained within the therapeutic range at the target site for the desired period of time. For this reason, we present a more realistic model considering the non-Newtonian nature of the vitreous body in the modeling of drug transport. We include the elastic collagen fiber network compared to the simpler models introduced in Chapter 3 used in the literature. For this application it is a new approach taking into account realistic parameters from measurements capable of describing the complex behavior of the human vitreous seen in experiments.
In this Chapter we model the healthy vitreous as an incompressible viscoelastic Burgers-type fluid. We derive the governing equations through the motivation of the one-dimensional mechanical analog and the well established thermodynamical framework. Experimental data from the literature is converted to our preferable formulation for further numerical simulations by solving a nonlinear system of equations. For simplicity, the stability of the rest state is examined for non-isothermal processes in a mechanically isolated domain instead of the vitreous body, but allowing heat exchange with the surrounding. The mixed boundary conditions characterizing the vitreous body would be to complex to analyze the rest state. In this case, the standard methods for thermodynamically isolated systems or systems immersed in a thermal bath can not be used since the steady state is a non-equilibrium (entropy producing) steady state due to the constant spatially nonuniform temperature at the domain's walls. Further, we analyze the mechanical behavior of the vitreous in a deforming eye ball leading to a fluid-structure-interaction problem. For the drug distribution we propose fully coupled systems extended by the surface tension or stress driven diffusion in which the drug diffusion and flow inside the vitreous can effect each other. The vitreous acts as a barrier to the diffusion

which has not yet been addressed in its modeling before. We extend the simple diffusion to an anisotropic ansatz taking into account the heterogeneous structure of collagen fibers which have a certain orientation in the vitreous body. Herewith we enlarge the considered drugs since the anisotropic ansatz depends on the molecule size of the drug. Finally, we introduce the thermodynamical derivation of the anisotropic viscoelastic vitreous where we consider the vitreous as a viscoelastic fluid whose elastic reaction is anisotropic in the preferred direction of the collagen fibers.

Another approach for modeling the healthy vitreous is using fluid dynamics and takes the elastic behavior of the collagen network into account. It is a purely phenomenological approach in the sense that it does not rely on the knowledge of the internal microscopic structure of the vitreous. All of the previous studies [62, 75, 10, 153, 170] model the vitreous humor as an incompressible fluid ignoring the non-Newtonian nature which is insufficient to describe the complex reality. The young and healthy vitreous is not liquefied but a gel that has both viscous and elastic properties. The viscous response is derived from the interaction between hyaluron and aqueous humor. The elastic property results from the collagen fibers. As a viscoelastic, Non-Newtonian fluid it can store energy and produce entropy in virtue of mechanisms. The rheological behavior of the vitreous body can be modeled by the incompressible viscoelastic Burgers-type model according to measurements from experiments on porcine eyes in [164] and on human autopsy eyes in [180]. It is an higher order rate-type viscoelastic fluid model capable of describing two different relaxation times observed by these experiments [164, 180] which excludes simpler models like the classical Maxwell model or the Oldroyd-B model [138]. The relaxation times roughly measure for how long a fluid will have some memory of the flow and relates to the Weissenberg number We which measures the grade of elasticity/viscosity in the fluid, i.e. the bigger the Weissenberg number, the more the fluid will behave like an elastic solid, the smaller it gets, the more it will be like viscous Newtonian flow.

4.1 Full System of Governing Equations

The full system of governing equations for the Burgers-type model characterizing the healthy viscoelastic vitreous reads:

$$\nabla \cdot v = 0 \qquad \text{in } \Omega \times (0,T], \tag{4.1a}$$

$$\rho\left(\frac{\partial v}{\partial t} + (v\cdot\nabla)v\right) = \nabla\cdot\mathbb{T} \qquad \text{in } \Omega \times (0,T], \tag{4.1b}$$

$$-p\mathbb{I} + 2\mu_3\mathbb{D} + G_1(\mathbb{B}_1 - \mathbb{I}) + G_2(\mathbb{B}_2 - \mathbb{I}) = \mathbb{T} \qquad \text{in } \Omega \times (0,T], \tag{4.1c}$$

$$-\frac{G_1}{\mu_1}(\mathbb{B}_1 - \mathbb{I}) = \overset{\nabla}{\mathbb{B}}_1 \qquad \text{in } \Omega \times (0,T], \tag{4.1d}$$

$$-\frac{G_2}{\mu_2}(\mathbb{B}_2 - \mathbb{I}) = \overset{\nabla}{\mathbb{B}}_2 \qquad \text{in } \Omega \times (0,T], \tag{4.1e}$$

where $\mathbb{B}_1$ and $\mathbb{B}_2$ are the left Cauchy–Green tensors associated to two natural configurations. The material parameters are the constant density ρ, $\mu_i, i = 1,2,3$ and $G_i, i = 1,2$, describing the dynamic viscosities and elastic shear moduli. Like before v, p and $\mathbb{T}$ denote the velocity, the pressure and the Cauchy stress tensor. The material time derivative is replaced by the upper convected Oldroyd derivative

$$\overset{\nabla}{\mathbb{A}} := \frac{\partial \mathbb{A}}{\partial t} + (v\cdot\nabla)\mathbb{A} - (\nabla v)\mathbb{A} - \mathbb{A}(\nabla v)^T \tag{4.2}$$

for any second order tensor $\mathbb{A}$. It is a time derivative from the family of Gordon-Schowalter objective time derivatives with $c \in [-1,1]$ given by

$$\overset{\circ}{\mathbb{A}} := \frac{\partial \mathbb{A}}{\partial t} + (v\cdot\nabla)\mathbb{A} + \mathbb{A}\mathbb{W} - \mathbb{W}\mathbb{A} - c\,(\mathbb{A}\mathbb{D} + \mathbb{D}\mathbb{A}) \tag{4.3}$$

with the skew-symmetric part of the velocity gradient $\mathbb{W} := \frac{1}{2}\left(\nabla v - (\nabla v)^T\right)$. When $c = 0$ we obtain the Jaumann derivative (co-rotational time derivative), while $c = -1$ is associated to the lower convected Oldroyd derivative and for $c = 1$ we get the upper convected Oldroyd derivative (4.2). Oldroyd showed in [138] that his model called Oldroyd-B with the upper convected Oldroyd derivative predicts rod climbing. While the same model with lower convected Oldroyd derivative predicts the opposite effect (the descend) and is named Oldroyd-A. Since most of the Non-Newtonian fluids like the vitreous show rod climbing we use the upper convected Oldroyd derivative. This is necessary to obtain a proper viscoelastic model since the partial time derivative and the material time derivative are not objective derivatives and the appropriate generalizations are not unique. For the definition of the objective tensor see

[181].

Note that the Navier-Stokes equation (3.9) is a special case of the Burgers-type model (4.1) with $G_1 = G_2 = \mu_1 = \mu_2 = 0$. The Navier-Stokes equation describes the liquefied vitreous and shows only viscous behavior compared to the Burgers-type model which is capable of characterizing viscous and elastic behavior.

4.1.1 Boundary and Initial Conditions

For the healthy viscoelastic vitreous we use the same boundary conditions for the velocity like in the Navier-Stokes model. At the boundary the elastic tensorial quantities $\mathbb{B}_i, i = 1,2$ are derived from the prescribed velocity using the evolution equations (4.1d), (4.1e) and the definition (4.2) by setting the material time derivative equal to zero. See Hron et al. [83] for detailed informations about the boundary conditions for the flow of a Burgers fluid. In our situation we have

$$v = 0 \qquad \text{on } \Gamma_\mathrm{l} \times (0,T], \tag{4.4a}$$
$$\mathbb{B}_i = \mathbb{I}, \quad i = 1,2 \qquad \text{on } \Gamma_\mathrm{l} \times (0,T], \tag{4.4b}$$
$$v = v_\mathrm{in} \qquad \text{on } \Gamma_\mathrm{h} \times (0,T], \tag{4.4c}$$
$$\mathbb{B}_i = \mathbb{B}_i^\mathrm{in}, \quad i = 1,2 \qquad \text{on } \Gamma_\mathrm{h} \times (0,T], \tag{4.4d}$$
$$\mathbb{T}n \cdot n = k_\mathrm{perm} v \cdot n \qquad \text{on } \Gamma_\mathrm{r} \times (0,T]. \tag{4.4e}$$

In detail, the inflow boundary condition at the hyaloid membrane Γ_h is:

$$\mathbb{B}_i^\mathrm{in} = \frac{\mu_i}{G_i}(\nabla v_\mathrm{in})\mathbb{B}_i + \frac{\mu_i}{G_i}\mathbb{B}_i(\nabla v_\mathrm{in})^T + \mathbb{I}, \qquad i = 1,2.$$

$\mathbb{B}_i, i = 1,2$ represent the deformation of the elastic collagen fibers inside the vitreous. Therefore, the initial state is undeformed and one sets:

$$v = v_0 \qquad \text{on } \Omega \times \{t = 0\}, \tag{4.5a}$$
$$\mathbb{B}_1 = \mathbb{I} \qquad \text{on } \Omega \times \{t = 0\}, \tag{4.5b}$$
$$\mathbb{B}_2 = \mathbb{I} \qquad \text{on } \Omega \times \{t = 0\}. \tag{4.5c}$$

Since the symmetric and positive definite setting at the beginning $t = 0$, one can show that $\mathbb{B}_i, i = 1,2$ remains to be symmetric positive definite for all times $t > 0$ with

$$\det \mathbb{B}_i \geq 1 \quad \forall t \geq 0, \quad i = 1,2$$

and

$$\operatorname{tr} \mathbb{B}_i \geq d, \qquad i = 1,2$$

where d denotes the space dimension, see [181].

Existence and Uniqueness It is necessary to recognize that even in the analysis of standard viscoelastic Oldroyd-type models (special case of the Burgers-type model with $G_2 = \mu_2 = 0$) there are open problems concerning long time and large data existence. For that reason, we present the state of research and outline a short overview of mathematical results from the literature.

In [21, 113] they proved global in time existence of weak solutions in dimension $d \leq 3$ for general initial data of the Oldroyd model with the corrotational (Jaumann) derivative (4.3). The proof is based on the L^2-norm energy estimate for velocity and stress fields. But this type of energy estimate does not hold for the Oldroyd-B model (with upper-convected Oldroyd derivative) and seems to be an open problem. Global existence for plane Couette (plane shear) and Poiseuille flows, i.e. one-dimensional motions, of Oldroyd-B fluids between two parallel planes is shown for arbitrary time and arbitrary initial data in [73]. For small data global existence of two-dimensional incompressible Oldroyd-type fluids was proven in [108, 109].
Concerning the original Burgers model with $\mu_3 = 0$ stability, uniqueness and continuous dependence on initial data were proved for the three-dimensional case in [145, 146] by Quintanilla and Rajagopal. In this paper they have studied qualitative aspects concerning the solutions to the flow of the linearized Burgers fluid. Higher-order non-linearities due to additional convective derivatives lead to a fully non-linear problem. Even within the context of linearization there are higher time derivatives of the velocity field.
In the case of the human vitreous these issues could be addressed, since the flow velocities are very low.

4.2 Derivation of Governing Equations

In this Section we present two different ways to derive the constitutive equations in the system (4.1). The first one is motivated by the one-dimensional mechanical analog representing the elasticity by one linear elastic spring and representing the viscosity by a dashpot filled with a viscous Newtonian fluid. The second way uses the thermodynamical framework and guarantees that the second law of thermodynamics is fulfilled for the derived model.

4.2.1 Mechanical Analog

Motivated by a one-dimensional mechanical spring/dashpot analogue introduced in Section 2.2.4 the Burgers-type model consists of two linear dashpots

and two linear springs with one additional dashpot to obtain a more convenient model (from the perspective of fitting the experimental data) than the original Burgers model (with $\mu_3 = 0$) derived in [181]. A draft of the Burgers-type model can be seen on the left side in Figure 4.1. This Figure shows the difference between the two constitutive equations for the healthy viscoelastic and the liquefied vitreous. The liquefied vitreous described by the Navier-Stokes equation (3.9) shows only viscous behavior motivated by one linear dashpot in the one-dimensional mechanical analogue compared to the Burgers-type model which contains two additional springs exhibiting elastic behavior. Since the springs satisfy Hooke's law and the dashpots fulfill Newton's law the

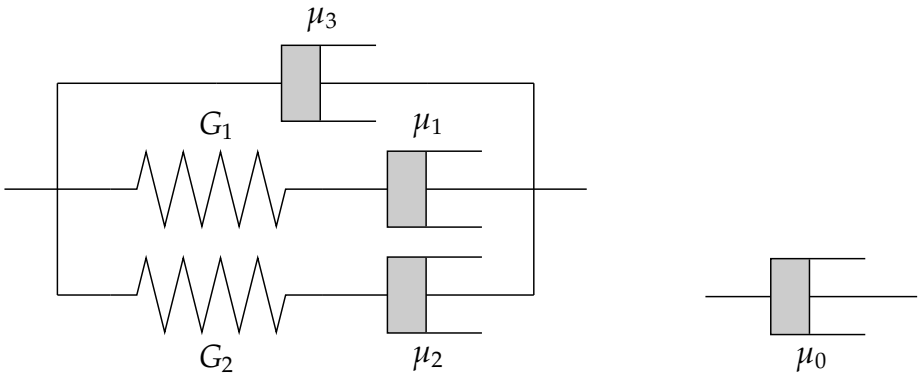

Figure 4.1: 1D-mechanical spring/dashpot analogue of viscoelastic Burgers-type model (left) and pure viscous Navier-Stokes model (right)

relation between the stress σ and the strain ϵ for this one-dimensional model satisfies the second order differential equation:

$$\sigma + \lambda_1 \frac{d\sigma}{dt} + \lambda_2 \frac{d^2\sigma}{dt^2} = \lambda_3 \frac{d\epsilon}{dt} + \lambda_4 \frac{d^2\epsilon}{dt^2} + \lambda_5 \frac{d^3\epsilon}{dt^3} \tag{4.6}$$

where the constant parameters $\lambda_i, i = 1, \ldots, 5$ are defined by

$$\begin{aligned}
\lambda_1 &:= \left(\frac{\mu_1}{G_1} + \frac{\mu_2}{G_2} \right), & \lambda_2 &:= \frac{\mu_1 \mu_2}{G_1 G_2}, \\
\lambda_3 &:= (\mu_1 + \mu_2 + \mu_3), & \lambda_4 &:= \left(\frac{\mu_1(\mu_2 + \mu_3)}{G_1} + \frac{\mu_2(\mu_1 + \mu_3)}{G_2} \right), \\
\lambda_5 &:= \frac{\mu_1 \mu_2 \mu_3}{G_1 G_2}
\end{aligned}$$

and G_1, G_2 and μ_1, μ_2, μ_3 are material parameters characterizing the elastic moduli and viscosities of the individual springs and dashpots respectively.

For numerical simulations and more realistic modeling we need to generalize the one-dimensional model into higher space dimensions. The evolution equation for the extra stress tensor $\mathbb{S}$ in equation (2.11) is obtained from (4.6) by replacing the one-dimensional stress σ by $\mathbb{S}$ and $\frac{d\epsilon}{dt}$ by two times the symmetric part of the velocity gradient $2\mathbb{D}$. The material time derivative defined in (2.1) is replaced by the objective upper convected Oldroyd time derivative (4.2). Then the generalization of (4.6) is

$$\mathbb{T} = -p\mathbb{I} + \mathbb{S}, \tag{4.7a}$$

$$\mathbb{S} + \lambda_1 \overset{\nabla}{\mathbb{S}} + \lambda_2 \overset{\nabla\nabla}{\mathbb{S}} = 2\lambda_3\mathbb{D} + 2\lambda_4 \overset{\nabla}{\mathbb{D}} + 2\lambda_5 \overset{\nabla\nabla}{\mathbb{D}}\,. \tag{4.7b}$$

This equation can be reformulated into a lower order differential equation by splitting the extra stress tensor as $\mathbb{S} = 2\mu_3\mathbb{D} + \tilde{\mathbb{S}}$,:

$$\mathbb{T} = -p\mathbb{I} + 2\mu_3\mathbb{D} + \tilde{\mathbb{S}},$$

$$\tilde{\mathbb{S}} + \left(\frac{\mu_1}{G_1} + \frac{\mu_2}{G_2}\right) \overset{\nabla}{\tilde{\mathbb{S}}} + \frac{\mu_1\mu_2}{G_1G_2} \overset{\nabla\nabla}{\tilde{\mathbb{S}}} = 2(\mu_1+\mu_2)\mathbb{D} + 2\left(\frac{\mu_1\mu_2}{G_1} + \frac{\mu_1\mu_2}{G_2}\right) \overset{\nabla}{\mathbb{D}}\,.$$

usually written using the relaxation times $\tau_1 := \frac{\mu_1}{G_1}$ and $\tau_2 := \frac{\mu_2}{G_2}$ as:

$$\mathbb{T} = -p\mathbb{I} + 2\mu_3\mathbb{D} + \tilde{\mathbb{S}}, \tag{4.8a}$$

$$\tilde{\mathbb{S}} + (\tau_1+\tau_2) \overset{\nabla}{\tilde{\mathbb{S}}} + \tau_1\tau_2 \overset{\nabla\nabla}{\tilde{\mathbb{S}}} = 2(\mu_1+\mu_2)\mathbb{D} + 2\left(\mu_2\tau_1 + \mu_1\tau_2\right) \overset{\nabla}{\mathbb{D}}\,. \tag{4.8b}$$

In the last step we show that the derived model (4.8) is indeed equivalent to the last three equations in (4.1). Starting with (4.1) we define $\tilde{\mathbb{S}} := \mathbb{S}_1 + \mathbb{S}_2$ with $\mathbb{S}_1 := G_1(\mathbb{B}_1 - \mathbb{I})$ and $\mathbb{S}_2 := G_2(\mathbb{B}_2 - \mathbb{I})$. Using (4.1d),(4.1e) and the relation $\overset{\nabla}{\mathbb{I}} = -2\mathbb{D}$, we have

$$\overset{\nabla}{\mathbb{S}} = \overset{\nabla}{\mathbb{S}}_1 + \overset{\nabla}{\mathbb{S}}_2 = -\frac{G_1}{\mu_1}\mathbb{S}_1 - \frac{G_2}{\mu_2}\mathbb{S}_2 + 2(G_1+G_2)\mathbb{D}. \tag{4.9}$$

Applying the upper convected Oldroyd derivative to (4.9) and using (4.1d) and (4.1e) again, we obtain

$$\begin{aligned}\overset{\nabla\nabla}{\mathbb{S}} &= -\frac{G_1}{\mu_1} \overset{\nabla}{\mathbb{S}}_1 - \frac{G_2}{\mu_2} \overset{\nabla}{\mathbb{S}}_2 + 2(G_1+G_2) \overset{\nabla}{\mathbb{D}} \\ &= \frac{G_1^2}{\mu_1^2}\mathbb{S}_1 + \frac{G_2^2}{\mu_2^2}\mathbb{S}_2 - 2\left(\frac{G_1^2}{\mu_1} + \frac{G_2^2}{\mu_2}\right)\mathbb{D} + 2(G_1+G_2) \overset{\nabla}{\mathbb{D}}\,.\end{aligned} \tag{4.10}$$

Multiplying the equation (4.9) by $\left(\frac{\mu_1}{G_1} + \frac{\mu_2}{G_2}\right)$ and adding the result to $\frac{\mu_1\mu_2}{G_1G_2}$ times equation(4.10), we get (4.8).

Even if the two models (4.8) and (4.1) are equivalent, they have different properties concerning further numerical simulations. The three-dimensional generalization (4.8) of the one-dimensional spring/dashpot model (4.6) is not a preferable formulation. It is a second order differential equation, which is difficult to numerically implement, and we would need to provide initial conditions for the parts of the Cauchy stress tensor and its derivative. The introduced model (4.1) is a more convenient equivalent with two symmetric first order differential equations for $\mathbb{B}_1$ and $\mathbb{B}_2$ which allow an easier numerical implementation. Additionally, the quantities $\mathbb{B}_1, \mathbb{B}_2$ correspond to the state of the springs in Figure 4.1, which makes it reliable to specify the initial conditions for the system. It is a well established viscoelastic model, derived and treated numerically in the literature, for example in our work [182]. But as written in the Section 2.2.4 of constitutive equations the relations should satisfy the second law of thermodynamics which is not obvious in this setting. In the following section we will derive (4.1) via the thermodynamical-based procedure introduced by [147] and show that it is a proper constitutive equation.

4.2.2 Thermodynamical Framework

In the previous section we derived the constitutive equation (4.8) for the viscoelastic vitreous in the human eye on the basis of the one-dimensional analog but it is not obvious that the generalization satisfy the second law of thermodynamics. Rajagopal and Srinivasa [147] proposed a framework based on the concept of evolving a natural configuration and the principle of maximal rate of entropy production to derive thermodynamically consistent viscoelastic rate-type fluid models to overcome this issue. This approach guarantees that the derived models satisfy the second law of thermodynamics.
By prescribing two constitutive relations: one for the Helmholtz free energy ψ (other thermodynamic potentials such as the internal energy e, Gibbs potential or the enthalpy can be used as well), describing the elastic response, and the second for the rate of entropy production ξ (see (2.8)) providing information how the energy dissipates, one obtains the needed constitutive equations, as the form of the Cauchy stress tensor $\mathbb{T}$ including its evolution equation, which fulfill automatically the laws of thermodynamics. This procedure has the advantage of prescribing only two scalars instead of six in three-space-dimensions by directly setting the constitutive equation for the symmetric Cauchy stress tensor. For more details see [117] or [181].

Viscoelastic models with two natural configurations

From Section 2.2.2 we already know the reference and current configuration of the continuous body Ω made from the viscoelastic material, here the vitreous body. In the reference configuration the system is in rest at the beginning. For the description of viscoelastic fluids we introduce the natural configuration associated with the current configuration $\kappa_t(\Omega)$. It is the situation that the fluid in the current configuration would take if the external stimuli are removed. The approach of defining the natural configuration is based on the idea that we split the total deformation gradient $\mathbb{F}$ into a purely dissipative/viscous and an elastic response.

On the example of the Maxwell element, one simple viscoelastic model which consists of one dashpot and one spring in series in the one-dimensional analogue, we motivate the existence of the natural configuration. At the beginning the element is at rest, relaxed, the spring and the dashpot are not stretched. This is the reference configuration. If we deform the element it goes to the current configuration. Now, you release the system, the spring shrinks back to its original length but the dashpot remains stretched. We have the natural configuration.

Our aim is to model the complex vitreous body. By assuming the co-existence of two natural configurations we are able to describe the vitreous' behavior of exhibiting two different relaxation mechanisms (see [106] and [164]). We define two natural configurations $\kappa_{n_1}(\Omega)$ and $\kappa_{n_2}(\Omega)$ shown in Figure 4.2 and virtually split the total deformation into purely elastic parts corresponding to the mappings $\mathbb{F}_1, \mathbb{F}_2$ and the dissipative parts $\mathbb{H}_1$ and $\mathbb{H}_2$. This decomposition is in agreement with the standard spring–dashpot analogue in Figure 4.1 and can be done in two ways, see Figure 4.2:

$$\mathbb{F} = \mathbb{F}_1\mathbb{H}_1, \qquad \mathbb{F} = \mathbb{F}_2\mathbb{H}_2. \tag{4.11}$$

In this setting , one can introduce left and right Cauchy-Green tensors corresponding to $\kappa_{n_1}(\Omega)$ and $\kappa_{n_2}(\Omega)$ in contrast to (2.3) corresponding to the total deformation. For $i = 1, 2$ they are defined through:

$$\mathbb{B}_i := \mathbb{F}_i\mathbb{F}_i^T, \qquad \mathbb{C}_i := \mathbb{F}_i^T\mathbb{F}_i. \tag{4.12}$$

Then one needs to find an expression for the material time derivative of $\mathbb{B}_i, i = 1, 2$ because this is the sought measure of the deformation associated with the instantaneous elastic part of the deformation. Next, we introduce the relation

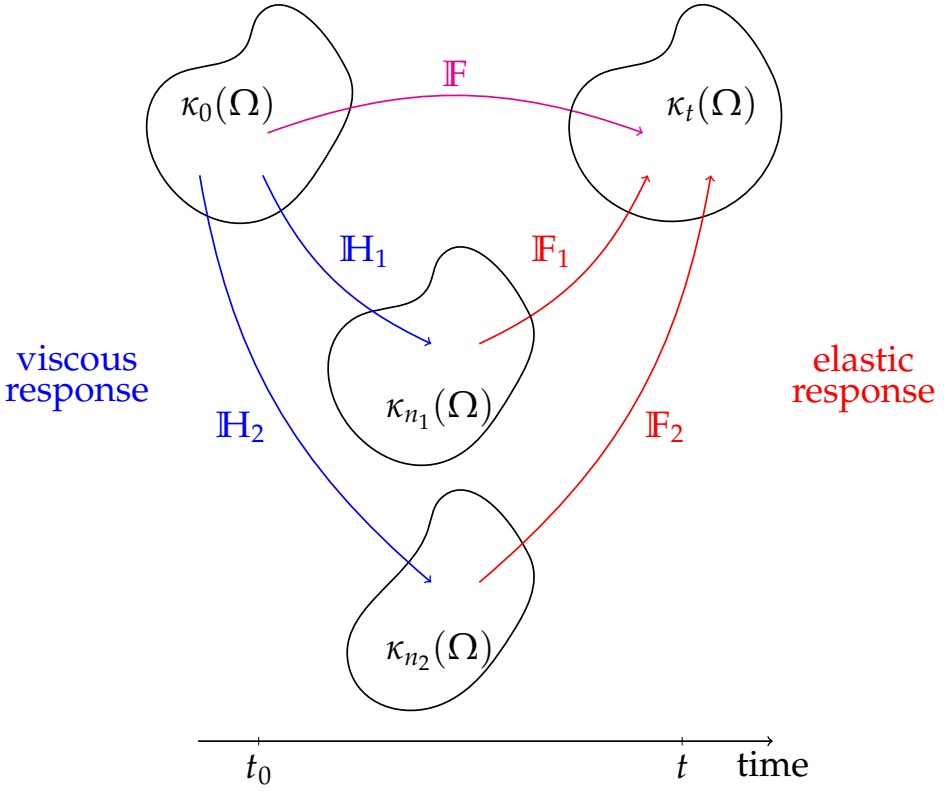

Figure 4.2: Two natural configurations

between the kinematic quantities analog to (2.2) ,

$$(\nabla v)_i := \frac{d\mathbb{H}_i}{dt}\mathbb{H}_i{}^{-1}, \tag{4.13}$$

and its symmetric part

$$\mathbb{D}_i := \frac{1}{2}\left((\nabla v)_i + (\nabla v)_i^T\right).$$

Further, it holds for $i = 1, 2$

$$0 = \frac{d\mathbb{H}_i}{dt}\mathbb{H}_i^{-1} + \mathbb{H}_i\frac{d\mathbb{H}_i^{-1}}{dt}$$

and it yields that

$$\frac{d\mathbb{F}_i}{dt} = (\nabla v)\mathbb{F}_i - \mathbb{F}_i(\nabla v)_i \tag{4.14}$$

which implies

$$\frac{d\mathbb{B}_i}{dt} = (\nabla v)\mathbb{B}_i + \mathbb{B}_i(\nabla v)^T - 2\mathbb{F}_i\mathbb{D}_i\mathbb{F}_i^T. \tag{4.15}$$

This is the sought expression for the time derivative and it is a function of $\mathbb{F}_i$ and $\mathbb{D}_i$, that are associated to the dissipative part of the deformation, and ∇v associated to the total deformation. It means that the viscous responses $\mathbb{H}_i, i = 1,2$ except for $\mathbb{D}_i, i = 1,2$ are not included in the equation (4.15). Our intention the viscous responses to express only as functions of velocity is fulfilled. Similarly, for the elastic part, $\mathbb{B}_i, i = 1,2$ are the key variables.
The definition of the upper convected Oldroyd derivative given by (4.2) implies that

$$\overset{\nabla}{\mathbb{B}}_i = -2\mathbb{F}_i\mathbb{D}_i\mathbb{F}_i^T \tag{4.16}$$

for $i = 1,2$.

Incompressibility condition By assuming the co-existence of two natural configurations we split the total deformation. Therefore, we need to extend the notation of incompressibility introduced in Section 2.2.4.
The material is incompressible if the whole deformation is incompressible, i.e.

$$\det\mathbb{F} = \det\mathbb{F}_i \det\mathbb{H}_i = 1, \quad i = 1,2. \tag{4.17}$$

Differentiation with respect to time of the equation (4.17) gives the known constraint (2.12). But it does not mean that the associated elastic and dissipative parts have to be incompressible, i.e.

$$\det\mathbb{F}_i \neq 1, \quad \det\mathbb{H}_i \neq 1, \quad i = 1,2.$$

There are several possibilities to describe the whole incompressibility of the material. For example, in the case of only one natural configuration the material can be incompressible in two situations: the total deformation is incompressible but the viscous and elastic part are compressible or the material is fully incompressible which means that all, total, elastic and dissipative parts of deformation, are incompressible.
Thus, following the recent study [128] we require the fewest constraints and neither the elastic nor the purely viscous parts of the deformation for both natural configurations are necessarily incompressible. Only the total deformation process has to fulfill the constraint (4.17).

Thermodynamic derivation of the Burgers-type model

We present a full general derived procedure including the possibility of temperature and density dependence, i.e. capable of modeling non-isothermal processes and compressible material behavior and extend the approaches stated in [129, 181]. The concrete properties of the vitreous body in the human

eye follow as a special case. Since the Burgers-type model (4.1) is a generalization of the Navier-Stokes fluid (3.9), we apply the thermodynamical procedure discussed in the Section 3.3.2 in the context of two natural configurations for the description of the viscoelastic vitreous model. In particular, we extend the specific formula for the Helmholtz free energy and edit it by terms measuring the two elastic parts of the deformation.

Helmholtz Free Energy The basic setup is build by the balance equations for mass (2.4), energy (2.7) and entropy (2.8) completed by the formulation of the second law of thermodynamics, $\xi \geq 0$. The fact that the energy storage mechanisms are required to be related to the elastic part of the deformation, see Figure 4.2, suggests that the Helmholtz energy ψ should be enriched by terms measuring the elastic part of the deformation, the two left Cauchy–Green tensors $\mathbb{B}_i, = 1, 2$. For that reason, we assume the following ansatz for the specific Helmholtz free energy:

$$\psi = \tilde{\psi}(\rho, \theta, \mathbb{B}_1, \mathbb{B}_2), \tag{4.18}$$

in contrast to the definition (3.13) for the Navier-Stokes case. Motivated by the discussion of incompressibility it is assumed that the elastic response from each natural to the current configuration is the response of a compressible Neo-Hookean elastic material [129]. Then we postulate the free Helmholtz energy for the sought Burgers-type model to be

$$\psi = \psi_0(\rho) + \psi_1(\theta) + \psi_2(\rho, \mathbb{B}_1) + \psi_3(\rho, \mathbb{B}_2) \tag{4.19}$$

where the viscoelastic parts ψ_2 and ψ_3 are defined by

$$\begin{aligned} \psi_2(\rho, \mathbb{B}_1) &:= \frac{G_1}{2\rho} \left[\operatorname{tr} \mathbb{B}_1 - 3 - \ln(\det \mathbb{B}_1) \right], \\ \psi_3(\rho, \mathbb{B}_2) &:= \frac{G_2}{2\rho} \left[\operatorname{tr} \mathbb{B}_2 - 3 - \ln(\det \mathbb{B}_2) \right]. \end{aligned} \tag{4.20}$$

Further, this approach allows to distinguish between (in)compressibility property $\psi_0(\rho)$, the purely thermal part

$$\psi_{\text{th}} := \psi_1(\theta)$$

and the mechanical parts

$$\psi_{\text{mech}} := \psi_2(\rho, \mathbb{B}_1) + \psi_3(\rho, \mathbb{B}_2)$$

of the free energy. In the simplest case of a fluid with a constant specific heat capacity the thermal part takes the form

$$\psi_1(\theta) = -c_{\mathrm{V,ref}}\theta\left[\ln\left(\frac{\theta}{\theta_{\mathrm{ref}}}\right) - 1\right] \tag{4.21}$$

where θ_{ref} is a reference temperature and $c_V := -\theta\frac{\partial^2\psi}{\partial\theta^2}$ is a positive material parameter (specific heat capacity at constant volume) [38]. For a better overview we continue with the not-specified formula. The knowledge of the balance equations allows one to identify the entropy production mechanisms derived from the given formula for the Helmholtz free energy.
Indeed, taking the material time derivative of (3.12), keep in mind the approach (4.18) and multiply by the density we get

$$\rho\frac{de}{dt} = \rho\theta\frac{d\eta}{dt} + \rho\frac{\partial\psi}{\partial\rho}\frac{d\rho}{dt} + \rho\frac{\partial\psi}{\partial\mathbb{B}_1}\frac{d\mathbb{B}_1}{dt} + \rho\frac{\partial\psi}{\partial\mathbb{B}_2}\frac{d\mathbb{B}_2}{dt}.$$

After substituting the balance equations for energy (2.7) (without external energy sources) and mass (2.4) we obtain

$$\mathbb{T} : \mathbb{D} - \operatorname{div} j_e = \rho\theta\frac{d\eta}{dt} - p_{\mathrm{th}}\operatorname{div} v + \rho\frac{\partial\psi}{\partial\mathbb{B}_1}\frac{d\mathbb{B}_1}{dt} + \rho\frac{\partial\psi}{\partial\mathbb{B}_2}\frac{d\mathbb{B}_2}{dt}$$

where

$$\begin{aligned} p_{\mathrm{th}} :&= \rho^2\frac{\partial\psi}{\partial\rho} = \rho^2\frac{\partial\psi_0}{\partial\rho} + \rho^2\frac{\partial\psi_2}{\partial\rho} + \rho^2\frac{\partial\psi_3}{\partial\rho} \\ &= p_{\mathrm{th}}^{\mathrm{NS}} - \frac{G_1}{2}\left[\operatorname{tr}\mathbb{B}_1 - 3 - \ln(\det\mathbb{B}_1)\right] - \frac{G_2}{2}\left[\operatorname{tr}\mathbb{B}_2 - 3 - \ln(\det\mathbb{B}_2)\right] \end{aligned}$$

denotes the thermodynamic pressure for the Burgers-type model including the thermodynamic pressure $p_{\mathrm{th}}^{\mathrm{NS}}$ for the compressible Navier-Stokes fluid, see (3.14).

Entropy production After rearranging we get a formula for the entropy production ξ defined in (2.8) with entropy flux $j_\eta = \frac{j_e}{\theta}$:

$$\begin{aligned} \theta\xi = \mathbb{T} : \mathbb{D} - \operatorname{div} j_e + p_{\mathrm{th}}\operatorname{div} v \\ - \rho\frac{\partial\psi}{\partial\mathbb{B}_1} : \frac{d\mathbb{B}_1}{dt} - \rho\frac{\partial\psi}{\partial\mathbb{B}_2} : \frac{d\mathbb{B}_2}{dt} + \theta\operatorname{div}\left(\frac{j_e}{\theta}\right). \end{aligned} \tag{4.22}$$

Analog to Section 3.3.2, since the thermodynamic temperature is positive, the right hand side can be further rewritten as

$$\theta\xi = \mathbb{T}_\delta : \mathbb{D}_\delta - j_e \cdot \frac{\nabla\theta}{\theta} + (m + p_{\mathrm{th}})\operatorname{div} v - \rho\frac{\partial\psi}{\partial\mathbb{B}_1}\frac{d\mathbb{B}_1}{dt} - \rho\frac{\partial\psi}{\partial\mathbb{B}_2}\frac{d\mathbb{B}_2}{dt} \tag{4.23}$$

where m denotes the mean normal stress defined in (3.15). The specific postulated Helmholtz free energy (4.19) for the human vitreous yields the following formulas for the partial derivatives of the Helmholtz free energy that appear in equation (4.23):

$$\frac{\partial \psi}{\partial \mathbb{B}_1} = \frac{G_1}{2\rho}\left(\mathbb{I} - \mathbb{B}_1^{-T}\right),$$
$$\frac{\partial \psi}{\partial \mathbb{B}_2} = \frac{G_2}{2\rho}\left(\mathbb{I} - \mathbb{B}_2^{-T}\right),$$

using the Gâteaux derivatives $\frac{\partial \mathrm{tr}\mathbb{A}}{\partial \mathbb{A}} = \mathbb{I}$ and $\frac{\partial \det\mathbb{A}}{\partial \mathbb{A}} = (\det\mathbb{A})\mathbb{A}^{-T}$.
The time derivatives of the left Cauchy-Green tensors associated to each natural configuration can be rewritten as

$$\begin{aligned}\frac{d\mathbb{B}_i}{dt} =& \overset{\nabla}{\mathbb{B}}_i + (\nabla v)\mathbb{B}_i + \mathbb{B}_i(\nabla v)^T \\ =& -2\mathbb{F}_i\mathbb{D}_i\mathbb{F}_i^T + (\nabla v)\mathbb{B}_i + \mathbb{B}_i(\nabla v)^T\end{aligned}$$

using the definition of the upper convected Oldroyd time derivative (4.2) and relation (4.16) for $i = 1, 2$. Inserting these specific forms in (4.23) we obtain

$$\begin{aligned}\theta\xi =& \mathbb{T}_\delta : \mathbb{D}_\delta - j_e \cdot \frac{\nabla\theta}{\theta} + (m + p_{\mathrm{th}})\mathrm{div}\, v \\ &+ 2\rho\frac{\partial\psi}{\partial\mathbb{B}_1} : \mathbb{F}_1\mathbb{D}_1\mathbb{F}_1^T - \rho\frac{\partial\psi}{\partial\mathbb{B}_1}2\mathbb{B}_1 : \mathbb{D} \\ &+ 2\rho\frac{\partial\psi}{\partial\mathbb{B}_2} : \mathbb{F}_2\mathbb{D}_2\mathbb{F}_2^T - \rho\frac{\partial\psi}{\partial\mathbb{B}_2}2\mathbb{B}_2 : \mathbb{D} \\ =& \mathbb{T}_\delta : \mathbb{D}_\delta - j_e \cdot \frac{\nabla\theta}{\theta} + (m + p_{\mathrm{th}})\mathrm{div}\, v \\ &+ G_1\left(\mathbb{C}_1 - \mathbb{I}\right) : \mathbb{D}_1 - G_1\left(\mathbb{B}_1 - \mathbb{I}\right) : \mathbb{D} \\ &+ G_2\left(\mathbb{C}_2 - \mathbb{I}\right) : \mathbb{D}_2 - G_2\left(\mathbb{B}_2 - \mathbb{I}\right) : \mathbb{D}.\end{aligned}$$

Thus the entropy production takes the form

$$\begin{aligned}\theta\xi =& \left(\mathbb{T}_\delta - G_1\left(\mathbb{B}_1\right)_\delta - G_2\left(\mathbb{B}_2\right)_\delta\right) : \mathbb{D}_\delta - j_e \cdot \frac{\nabla\theta}{\theta} \\ &+ \left(m + p_{\mathrm{th}} - \frac{G_1}{3}(\mathrm{tr}\,\mathbb{B}_1) - \frac{G_2}{3}(\mathrm{tr}\,\mathbb{B}_2) + G_1 + G_2\right)\mathrm{div}\, v \\ &+ G_1\left(\mathbb{C}_1 - \mathbb{I}\right) : \mathbb{D}_1 + G_2\left(\mathbb{C}_2 - \mathbb{I}\right) : \mathbb{D}_2\end{aligned} \tag{4.24}$$

since $\mathbb{I}_\delta = 0$.

Constitutive Relations In this setting the constitutive relations for the Cauchy stress tensor $\mathbb{T}$, the heat flux j_e and the other quantities of interest are derived as consequences of the choice of the specific form for the Helmholtz free energy ψ and the entropy production ξ. The main idea is that the behaviour of the material in the processes of interest is determined by two factors, namely its ability to store energy and to produce entropy. It proceeds in the following steps.

The derived entropy production (4.24) can be generally written as

$$\xi = \frac{1}{\theta} \sum_{\alpha=1}^{m} j_\alpha a_\alpha, \quad m > 1 \tag{4.25}$$

where $j_\alpha a_\alpha$ denotes the scalar product of vector or tensor quantities respectively and each summand is supposed to represent an independent entropy producing mechanism [117], as already mentioned in the Section 3.3.2. The quantities j_α are called the thermodynamic fluxes, and the quantities a_α are called the thermodynamic affinities. The affinities are usually the spatial gradients of the involved quantities like $\nabla\theta$ or $\mathbb{D}$, while the fluxes are for example the Cauchy stress tensor $\mathbb{T}$ and energy flux j_e.
This is also the reason for splitting the tensors $\mathbb{T}$ and $\mathbb{D}$ since $\mathbb{D}$ and div v on the right hand side of (4.22) are not independent quantities, due to $\mathrm{tr}\mathbb{D} = \mathrm{div}\, v$. But the fluxes in the form (4.25) should be independent quantities.
The second law of thermodynamics (2.9) states that the entropy production is nonnegative, which means that equation (4.24) must be nonnegative. One way to fulfill this requirement is to postulate the constitutive assumption concerning how the material dissipates the energy. It is called the nonlinear non-equilibrium thermodynamics, a full thermodynamic procedure which is based on the assumption of the maximization of the entropy production [117]. In contrast to the simpler approach of linear thermodynamics used in the setting of deriving the Navier-Stokes equation in Section 3.3.2 where we consider only linear relations between each pair of thermodynamic affinities and fluxes, this approach is capable of describing the behavior of complex materials like the vitreous body. In particular, the procedure allows one to derive nonlinear constitutive relations of the type $j_i = j_i(a_1, ..., a_m), i = 1, \ldots, m$ or vice versa. First we specify the function

$$\zeta := \theta\xi$$

in one of the following forms

$$\zeta = \tilde{\zeta}_{a_1,\ldots,a_m}(j_1, \ldots, j_m) \tag{4.26}$$

or

$$\zeta = \tilde{\zeta}_{j_1,\dots,j_m}(a_1,\dots,a_m).$$

Since the constitutive function ζ is—up to the positive factor θ—tantamount to the entropy production, it must be nonnegative, which guarantees the fulfillment of the second law of thermodynamics. Further, ζ should vanish if the fluxes vanish. Other restrictions concerning the formula for the entropy production can come from classical requirements such as the symmetry and the invariance with respect to the change of the observer.
Moreover, the assumed form of the entropy production (4.26) must be compatible with the already derived form of the entropy production (4.25). Consequently, the following equation must hold

$$\tilde{\zeta}_{a_1,\dots,a_m}(j_1,\dots,j_m) - \sum_{\alpha=1}^{m} j_\alpha a_\alpha = 0$$

and similarly for $\tilde{\zeta}_{j_1,\dots,j_m}(a_1,\dots,a_m)$. Now, the task is to determine the fluxes or affinities that are compatible with above constraints. The choice can be based on the assumption of maximization of the entropy production. The assumption simply requires that the sought constitutive relation is the constitutive relation that leads to the maximal entropy production in the material, and that is compatible with other available information concerning the behavior of the material. Assuming that ζ_A or ζ_J including all fluxes or affinities are smooth and strictly convex with respect to their variables, then the corresponding values of J and A (vectors containing all the affinities and fluxes) are uniquely determined, and can be found by employing the Lagrange multipliers.
In our situation we assume that the constitutive function for ζ is a function of the affinities and is chosen as

$$\begin{aligned}\zeta &= \tilde{\zeta}(\mathbb{D}_\delta, \operatorname{div} v, \mathbb{D}_1, \mathbb{D}_2, \nabla\theta)\\ &= 2\mu_3|\mathbb{D}_\delta|^2 + \frac{2\mu_3+3\lambda}{3}(\operatorname{div} v)^2 + \kappa\frac{|\nabla\theta|^2}{\theta}\\ &\quad + 2\mu_1\mathbb{D}_1\mathbb{C}_1 : \mathbb{D}_1 + 2\mu_2\mathbb{D}_2\mathbb{C}_2 : \mathbb{D}_2.\end{aligned} \tag{4.27}$$

This approach can be found in [181] without considering compressibility and temperature changes. To maximize the entropy production,

$$\max_{\mathbb{D}_\delta, \operatorname{div} v, \mathbb{D}_1, \mathbb{D}_2, \nabla\theta} \tilde{\zeta}(\mathbb{D}_\delta, \operatorname{div} v, \mathbb{D}_1, \mathbb{D}_2, \nabla\theta)$$

among the values of the affinities $A := (\mathbb{D}_\delta, \operatorname{div} v, \mathbb{D}_1, \mathbb{D}_2, \nabla\theta)$, we use the Lagrange formalism and introduce the Lagrange function ϕ under the constraint

that equation (4.24) must hold:

$$\begin{aligned}\phi :=& \tilde{\zeta}(\mathbb{D}_\delta, \operatorname{div} v, \mathbb{D}_1, \mathbb{D}_2, \nabla\theta) + l\Big[\tilde{\zeta}(\mathbb{D}_\delta, \operatorname{div} v, \mathbb{D}_1, \mathbb{D}_2, \nabla\theta) \\ &- (\mathbb{T}_\delta - G_1 (\mathbb{B}_1)_\delta - G_2 (\mathbb{B}_2)_\delta) : \mathbb{D}_\delta + j_e \cdot \frac{\nabla\theta}{\theta} \\ &- \left(m + p_{\text{th}} - \frac{G_1}{3}(\operatorname{tr} \mathbb{B}_1) - \frac{G_2}{3}(\operatorname{tr} \mathbb{B}_2) + G_1 + G_2\right) \operatorname{div} v \\ &- G_1 (\mathbb{C}_1 - \mathbb{I}) : \mathbb{D}_1 - G_2 (\mathbb{C}_2 - \mathbb{I}) : \mathbb{D}_2\Big]\end{aligned}$$

where l is the Lagrange multiplier. Then the maximal entropy production corresponds to the extremes of ϕ where the necessary condition is $\frac{\partial\phi(A)}{\partial A} = 0$. We obtain

$$\begin{aligned}\frac{1+l}{l}\frac{\partial\tilde{\zeta}}{\partial\mathbb{D}_\delta} &= \mathbb{T}_\delta - G_1 (\mathbb{B}_1)_\delta - G_2 (\mathbb{B}_2)_\delta , \\ \frac{1+l}{l}\frac{\partial\tilde{\zeta}}{\partial(\operatorname{div} v)} &= m + p_{\text{th}} - \frac{G_1}{3}(\operatorname{tr} \mathbb{B}_1) - \frac{G_2}{3}(\operatorname{tr} \mathbb{B}_2) + G_1 + G_2, \\ \frac{1+l}{l}\frac{\partial\tilde{\zeta}}{\partial\mathbb{D}_1} &= G_1(\mathbb{C}_1 - \mathbb{I}), \\ \frac{1+l}{l}\frac{\partial\tilde{\zeta}}{\partial\mathbb{D}_2} &= G_2(\mathbb{C}_2 - \mathbb{I}), \\ \frac{1+l}{l}\frac{\partial\tilde{\zeta}}{\partial(\nabla\theta)} &= -\frac{j_e}{\theta}.\end{aligned} \tag{4.28}$$

On the other hand, direct differentiation of (4.27) yields

$$\begin{aligned}\frac{\partial\tilde{\zeta}}{\partial\mathbb{D}_\delta} &= 4\mu_3\mathbb{D}_\delta, \\ \frac{\partial\tilde{\zeta}}{\partial(\operatorname{div} v)} &= \frac{2}{3}(2\mu_3 + 3\lambda)\operatorname{div} v, \\ \frac{\partial\tilde{\zeta}}{\partial\mathbb{D}_1} &= 2\mu_1(\mathbb{D}_1\mathbb{C}_1 + \mathbb{C}_1\mathbb{D}_1), \\ \frac{\partial\tilde{\zeta}}{\partial\mathbb{D}_2} &= 2\mu_2(\mathbb{D}_2\mathbb{C}_2 + \mathbb{C}_2\mathbb{D}_2), \\ \frac{\partial\tilde{\zeta}}{\partial(\nabla\theta)} &= 2\kappa\frac{\nabla\theta}{\theta}.\end{aligned} \tag{4.29}$$

Now it is necessary to find a formula for the Lagrange multiplier l. This can be done as follows. First, each equation in (4.28) is multiplied by the corresponding affinity and then the sum of all equations is taken:

$$\begin{aligned}\frac{1+l}{l}\left[\frac{\partial\tilde{\zeta}}{\partial\mathbb{D}_\delta}:\mathbb{D}_\delta+\frac{\partial\tilde{\zeta}}{\partial(\operatorname{div}v)}\operatorname{div}v+\frac{\partial\tilde{\zeta}}{\partial\mathbb{D}_1}:\mathbb{D}_1+\frac{\partial\tilde{\zeta}}{\partial\mathbb{D}_2}:\mathbb{D}_2+\frac{\partial\tilde{\zeta}}{\partial(\nabla\theta)}\nabla\theta\right]\\ =\left(\mathbb{T}_\delta-G_1\left(\mathbb{B}_1\right)_\delta-G_2\left(\mathbb{B}_2\right)_\delta\right):\mathbb{D}_\delta-j_e\cdot\frac{\nabla\theta}{\theta}\\ +\left(m+p_{\text{th}}-\frac{G_1}{3}(\operatorname{tr}\mathbb{B}_1)-\frac{G_2}{3}(\operatorname{tr}\mathbb{B}_2)+G_1+G_2\right)\operatorname{div}v\\ +G_1\left(\mathbb{C}_1-\mathbb{I}\right):\mathbb{D}_1+G_2\left(\mathbb{C}_2-\mathbb{I}\right):\mathbb{D}_2.\end{aligned}$$

The right hand side is identical to $\tilde{\zeta}=\theta\xi$, see (4.24), while the term on the left hand side reduces, in virtue of (4.27) and (4.29), to $\frac{1+l}{l}\,2\tilde{\zeta}$. Consequently $\frac{1+l}{l}=\frac{\tilde{\zeta}}{2\tilde{\zeta}}$, which fixes the value of the Lagrange multiplier to be

$$\frac{1+l}{l}=\frac{1}{2}. \tag{4.30}$$

Inserting (4.29) and (4.30) into (4.28) one finally concludes that

$$\begin{aligned}\mathbb{T}_\delta-G_1\left(\mathbb{B}_1\right)_\delta-G_2\left(\mathbb{B}_2\right)_\delta&=2\mu_3\mathbb{D}_\delta,\\ m+p_{\text{th}}-\frac{G_1}{3}(\operatorname{tr}\mathbb{B}_1)-\frac{G_2}{3}(\operatorname{tr}\mathbb{B}_2)+G_1+G_2&=\frac{2\mu_3+3\lambda}{3}\operatorname{div}v,\\ G_1(\mathbb{C}_1-\mathbb{I})&=\mu_1(\mathbb{D}_1\mathbb{C}_1+\mathbb{C}_1\mathbb{D}_1),\\ G_2(\mathbb{C}_2-\mathbb{I})&=\mu_2(\mathbb{D}_2\mathbb{C}_2+\mathbb{C}_2\mathbb{D}_2),\\ -\frac{j_e}{\theta}&=\kappa\frac{\nabla\theta}{\theta}.\end{aligned} \tag{4.31}$$

Further, if the third and fourth equations in (4.31) hold, then it can be shown that the symmetric positive definite matrices $\mathbb{C}_i$ and the symmetric matrices $\mathbb{D}_i$ for $i=1,2$ commute. If the matrices commute, then (4.31) in fact reads

$$\begin{aligned}\mathbb{T}_\delta-G_1\left(\mathbb{B}_1\right)_\delta-G_2\left(\mathbb{B}_2\right)_\delta&=2\mu_3\mathbb{D}_\delta,\\ m+p_{\text{th}}-\frac{G_1}{3}(\operatorname{tr}\mathbb{B}_1)-\frac{G_2}{3}(\operatorname{tr}\mathbb{B}_2)+G_1+G_2&=\frac{2\mu_3+3\lambda}{3}\operatorname{div}v,\\ G_1(\mathbb{C}_1-\mathbb{I})&=2\mu_1\mathbb{C}_1\mathbb{D}_1,\\ G_2(\mathbb{C}_2-\mathbb{I})&=2\mu_2\mathbb{C}_2\mathbb{D}_2,\\ j_e&=-\kappa\nabla\theta.\end{aligned} \tag{4.32}$$

Additionally, the third and fourth equations in (4.32) can be rewritten as

$$G_1(\mathbb{C}_1 - \mathbb{I}) = 2\mu_1 \mathbb{C}_1 \mathbb{D}_1 = 2\mu_1 \mathbb{F}_1^T \mathbb{F}_1 \mathbb{D}_1,$$
$$G_2(\mathbb{C}_2 - \mathbb{I}) = 2\mu_2 \mathbb{C}_2 \mathbb{D}_2 = 2\mu_2 \mathbb{F}_2^T \mathbb{F}_2 \mathbb{D}_2$$

which upon multiplication by $\mathbb{F}_i^T$ from the right and by $\mathbb{F}_i^{-T}$ from the left for $i = 1, 2$ yields

$$G_1 \mathbb{F}_1^{-T}(\mathbb{C}_1 - \mathbb{I})\mathbb{F}_1^T = G_1(\mathbb{B}_1 - \mathbb{I}) = 2\mu_1 F_1 \mathbb{D}_1 \mathbb{F}_1^T,$$
$$G_2 \mathbb{F}_2^{-T}(\mathbb{C}_2 - \mathbb{I})\mathbb{F}_2^T = G_2(\mathbb{B}_2 - \mathbb{I}) = 2\mu_2 F_2 \mathbb{D}_2 \mathbb{F}_2^T.$$

These formulas can be substituted into (4.16) that yield the sought evolution equations for the two left Cauchy–Green tensors,

$$\overset{\nabla}{\mathbb{B}}_1 = -\frac{G_1}{\mu_1}(\mathbb{B}_1 - \mathbb{I}),$$
$$\overset{\nabla}{\mathbb{B}}_2 = -\frac{G_2}{\mu_2}(\mathbb{B}_2 - \mathbb{I}).$$

The first two equations in (4.32) allows one to identify the constitutive relation for the full Cauchy stress tensor $\mathbb{T} = m\mathbb{I} + \mathbb{T}_\delta$,

$$\mathbb{T} = -p_{\text{th}}\mathbb{I} + 2\mu_3 \mathbb{D} + G_1(\mathbb{B}_1 - \mathbb{I}) + G_2(\mathbb{B}_2 - \mathbb{I}) + \lambda(\operatorname{div} v)\mathbb{I}.$$

In the setting of continuum mechanics the set of balance equations (2.10) supplemented with the derived constitutive equations

$$\mathbb{T} = -p_{\text{th}}\mathbb{I} + 2\mu_3 \mathbb{D} + G_1(\mathbb{B}_1 - \mathbb{I}) + G_2(\mathbb{B}_2 - \mathbb{I}) + \lambda(\operatorname{div} v)\mathbb{I},$$
$$\overset{\nabla}{\mathbb{B}}_1 = -\frac{G_1}{\mu_1}(\mathbb{B}_1 - \mathbb{I}),$$
$$\overset{\nabla}{\mathbb{B}}_2 = -\frac{G_2}{\mu_2}(\mathbb{B}_2 - \mathbb{I}),$$
$$j_e = -\kappa \nabla\theta, \qquad \left(j_\eta = -\frac{\kappa\nabla\theta}{\theta}\right)$$

forms a closed system of equations.
Using the relation $\eta := -\frac{\partial\psi}{\partial\theta} = -\frac{d\psi_1}{d\theta}$, we can rewrite the evolution equation for entropy (2.8) as

$$\rho\frac{d}{dt}\left(-\frac{d\psi_1}{d\theta}\right) + \operatorname{div} j_\eta = \xi.$$

Consequently, using the special choice of ψ_1 given by (4.21) and the entropy production (4.24) then yields the evolution equation for the temperature in the form

$$\rho c_{\mathrm{V,ref}} \frac{d\theta}{dt} + \theta \mathrm{div} j_\eta = \theta \xi. \tag{4.33}$$

It shows that once the Helmholtz free energy and entropy production are specified, then the corresponding evolution equation for temperature (4.33) is a simple consequence of the choice of ψ and ξ.

Considering the material specific properties of the healthy vitreous containing only isothermal processes and incompressibility which means that

$$\begin{aligned} \nabla\theta &= 0, \\ \mathrm{div}\, v &= 0, \end{aligned}$$

the same procedure as above can be still applied. One starts from (4.27) with the only modification that the terms with div v and $\nabla\theta$ disappear, and one ends up with the same system of equations as those given in (4.32). (With the only exception that the second and last equation are missing.) It reduces to the incompressible viscoelastic Burgers-type model (recall that in virtue of (2.12) one has $\mathbb{D} = \mathbb{D}_\delta$).

$$\begin{aligned} \mathbb{T} &= -p\mathbb{I} + 2\mu_3\mathbb{D} + G_1(\mathbb{B}_1 - \mathbb{I}) + G_2(\mathbb{B}_2 - \mathbb{I}), \\ \overset{\nabla}{\mathbb{B}}_1 &+ \frac{G_1}{\mu_1}(\mathbb{B}_1 - \mathbb{I}) = 0, \\ \overset{\nabla}{\mathbb{B}}_2 &+ \frac{G_2}{\mu_2}(\mathbb{B}_2 - \mathbb{I}) = 0 \end{aligned}$$

by introducing the notation

$$-p := m - \frac{G_1}{3}(\mathrm{tr}\, \mathbb{B}_1) - \frac{G_2}{3}(\mathrm{tr}\, \mathbb{B}_2) + G_1 + G_2$$

where the mean normal stress m is a quantity that can not be specified via a constitutive relation.

4.3 Conversion of Experimental Data

Rheological measurements on the vitreous are very challenging [179]. The vitreous body has a fragile structure that tends to degrade as soon as it is removed from the eyeball. Nickerson et al. [134] and Silva et al. [166] showed

that vitreous properties change significantly after dissection. The shear moduli decrease five-fold from initial to steady-state values in the first hour in [134] but increase after four hours in [166]. Furthermore, as noticed in Section 2.1.5 the vitreous body is heterogeneous and its properties change in space, because of the differences in collagen fibers network density [25, 106, 107]. Also with aging the rheological properties differ [67, 110, 159, 180] and tend towards a more liquid form.
Nevertheless, the vitreous is known to exhibit viscoelastic properties showing two different relaxation times and in the literature this mechanical behavior were measured in experiments on eyes of different species summarized in the Table 4.1.

Parameter	Human [106]	Human [180]	Bovine [107]	Porcine [107]	Porcine [164]	Unit
G_1	4.65	0.19	2.09	1.26	1.66	Pa
G_2	1.66	0.25	1.94	0.82	1.14	Pa
μ_1	2.81	0.89	19.93	8.40	2.4	Pa s
μ_2	0.39	25.01	1.61	0.60	70	Pa s
μ_3	-	9205.31	-	-	1057.0	Pa s

Table 4.1: Parameters for viscoelasticity of the vitreous body of different species in the literature

In [106] the vitreous body was sectioned in three parts and we calculated the average values of the parameters for further manipulation, see Table 4.2.

	Anterior	Central	Posterior	Average	Unit
G_1	3.679	7.263	3.020	4.654	Pa
G_2	2.497	1.270	1.211	1.659	Pa
μ_1	1.398	2.179	4.862	2.813	Pa s
μ_2	0.313	0.352	0.489	0.385	Pa s

Table 4.2: Parameters of the human eye in [106] and their computed average values

Experiments performed by [164, 180] correlate the experimental data to the Burgers-type model with one additional dashpot while other studies like [106, 107] use the original Burgers model. Besides the different approaches of models, the arrangement of the corresponding one-dimensional mechanical

analogs differs from each other. The values of the material parameters reported by [164, 180] were obtained by the following one-dimensional model

$$\begin{aligned}\sigma + \left(\frac{\tilde{\mu}_1+\tilde{\mu}_3}{\tilde{G}_1} + \frac{\tilde{\mu}_2+\tilde{\mu}_3}{\tilde{G}_2}\right)\frac{d\sigma}{dt} + \frac{\tilde{\mu}_1\tilde{\mu}_2+\tilde{\mu}_1\tilde{\mu}_3+\tilde{\mu}_2\tilde{\mu}_3}{\tilde{G}_1\tilde{G}_2}\frac{d^2\sigma}{dt^2} \\ = \tilde{\mu}_3\frac{d\epsilon}{dt} + \left(\frac{\tilde{\mu}_1\tilde{\mu}_3}{\tilde{G}_1} + \frac{\tilde{\mu}_2\tilde{\mu}_3}{\tilde{G}_2}\right)\frac{d^2\epsilon}{dt^2} + \frac{\tilde{\mu}_1\tilde{\mu}_2\tilde{\mu}_3}{\tilde{G}_1\tilde{G}_2}\frac{d^3\epsilon}{dt^3}\end{aligned} \tag{4.34}$$

consisting of two Kelvin-Voigt elements with an additional dashpot in series, see Figure 4.3, where $\tilde{\mu}_i, \tilde{G}_j, i = 1,2,3, j = 1,2$ denote again the viscosities and elastic moduli of the individual springs and dashpots respectively. The

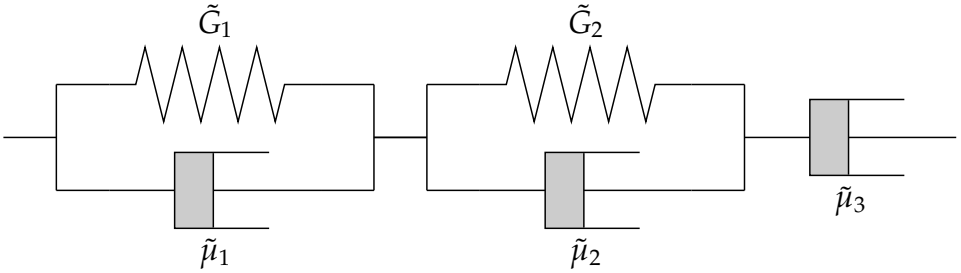

Figure 4.3: One-dimensional mechanical analog used in Sharif-Kashani et al. [164]

corresponding three-dimensional generalization of (4.34) with Cauchy stress $\mathbb{T} = -p\mathbb{I} + \mathbb{S}$ reads,

$$\begin{aligned}\mathbb{S} + \left(\frac{\tilde{\mu}_1+\tilde{\mu}_3}{\tilde{G}_1} + \frac{\tilde{\mu}_2+\tilde{\mu}_3}{\tilde{G}_2}\right)\overset{\nabla}{\mathbb{S}} + \frac{\tilde{\mu}_1\tilde{\mu}_2+\tilde{\mu}_1\tilde{\mu}_3+\tilde{\mu}_2\tilde{\mu}_3}{\tilde{G}_1\tilde{G}_2}\overset{\nabla\nabla}{\mathbb{S}} \\ = 2\tilde{\mu}_3\mathbb{D} + 2\left(\frac{\tilde{\mu}_1\tilde{\mu}_3}{\tilde{G}_1} + \frac{\tilde{\mu}_2\tilde{\mu}_3}{\tilde{G}_2}\right)\overset{\nabla}{\mathbb{D}} + 2\frac{\tilde{\mu}_1\tilde{\mu}_2\tilde{\mu}_3}{\tilde{G}_1\tilde{G}_2}\overset{\nabla\nabla}{\mathbb{D}}\,.\end{aligned} \tag{4.35}$$

Whereas Lee et al. [106, 107] uses only the Burgers model without additional dashpot applying one Maxwell and one Kelvin-Voigt element in series, see Figure 4.4. Consequently, if we want to use the model (4.1) based on the corresponding one-dimensional model (4.6) with two Maxwell elements and one additional dashpot in parallel like in Figure 4.1 (left), we have to convert the set of parameters for the elastic moduli and viscosities [182]. Since the available experimental data do not coincide in their mechanical analog with our preferable model for the human vitreous.

We see that the three-dimensional constitutive equations (4.7) and (4.35) corresponding to the model in this study and the one used in [164] have the same

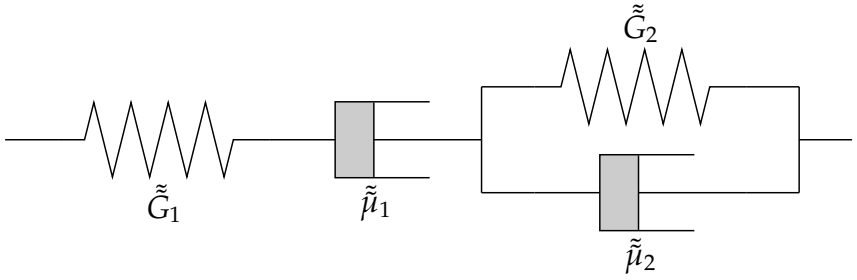

Figure 4.4: One-dimensional mechanical analog used in Lee et al. [106, 107]

formulation

$$\mathbb{S} + c_1 \overset{\nabla}{\mathbb{S}} + c_2 \overset{\nabla\nabla}{\mathbb{S}} = c_3 \mathbb{D} + c_4 \overset{\nabla}{\mathbb{D}} + c_5 \overset{\nabla\nabla}{\mathbb{D}}$$

where $c_i, i = 1, \ldots, 5$ denote the material parameters consisting of the elastic moduli and viscosities depending on the arrangement of springs/dashpots. The procedure is to compare the different sets of material parameters and to express $\mu_i, G_j, i = 1, 2, 3, j = 1, 2$ in terms of $\tilde{\mu}_i, \tilde{G}_j, i = 1, 2, 3, j = 1, 2$ by solving a nonlinear system of equations:

$$\begin{aligned}
\left(\frac{\mu_1}{G_1} + \frac{\mu_2}{G_2}\right) - \left(\frac{\tilde{\mu}_1 + \tilde{\mu}_3}{\tilde{G}_1} + \frac{\tilde{\mu}_2 + \tilde{\mu}_3}{\tilde{G}_2}\right) &= 0, \\
\frac{\mu_1 \mu_2}{G_1 G_2} - \frac{\tilde{\mu}_1\tilde{\mu}_2 + \tilde{\mu}_1\tilde{\mu}_3 + \tilde{\mu}_2\tilde{\mu}_3}{\tilde{G}_1\tilde{G}_2} &= 0, \\
(\mu_1 + \mu_2 + \mu_3) - \tilde{\mu}_3 &= 0, \\
\left(\frac{\mu_1(\mu_2 + \mu_3)}{G_1} + \frac{\mu_2(\mu_1 + \mu_3)}{G_2}\right) - \left(\frac{\tilde{\mu}_1\tilde{\mu}_3}{\tilde{G}_1} + \frac{\tilde{\mu}_2\tilde{\mu}_3}{\tilde{G}_2}\right) &= 0, \\
\frac{\mu_1\mu_2\mu_3}{G_1 G_2} - \frac{\tilde{\mu}_1\tilde{\mu}_2\tilde{\mu}_3}{\tilde{G}_1\tilde{G}_2} &= 0.
\end{aligned}$$

The same procedure can be applied for the models in [106, 107] by reformulating (4.7) into (4.8) by excluding the additional viscous term $2\mu_3\mathbb{D}$ and comparison with the corresponding three-dimensional response of the Burgers model in [106, 107]:

$$\begin{aligned}
\mathbb{T} &= -p\mathbb{I} + \mathbb{S}, \\
\mathbb{S} + \left(\frac{\tilde{\tilde{\mu}}_1}{\tilde{\tilde{G}}_1} + \frac{\tilde{\tilde{\mu}}_2}{\tilde{\tilde{G}}_2} + \frac{\tilde{\tilde{\mu}}_2}{\tilde{\tilde{G}}_1}\right) \overset{\nabla}{\mathbb{S}} + \frac{\tilde{\tilde{\mu}}_1\tilde{\tilde{\mu}}_2}{\tilde{\tilde{G}}_1\tilde{\tilde{G}}_2} \overset{\nabla\nabla}{\mathbb{S}} &= 2\tilde{\tilde{\mu}}_2\mathbb{D} + 2\frac{\tilde{\tilde{\mu}}_1\tilde{\tilde{\mu}}_2}{\tilde{\tilde{G}}_1} \overset{\nabla}{\mathbb{D}}.
\end{aligned}$$

Setting the viscosity $\mu_3 = 0$ allows one to interpret the different sets of parameters listed in the Table 4.3.

Parameter	Human [106]	Human [180]	Porcine [164]	Bovine [107]	Unit
G_1	1.54	0.11	6.45×10^{-1}	1.85	Pa
G_2	0.12	0.07	8.98×10^{-1}	0.01	Pa
μ_1	0.30	9200	1032	1.46	Pa s
μ_2	0.09	4.09	22.5	0.14	Pa s
μ_3	0	0.86	2.37	0	Pa s

Table 4.3: Converted parameter values for the Burgers-type model (4.7)

4.4 Non-Isothermal Processes

Non-isothermal processes are not important in our application. Inside the vitreous humor the temperature in human eyes is 33.9°C or rather 33°C following [103] and [87]. Also a small amount of drug at room temperature injected into the vitreous probably does not change the temperature of the vitreous. But temperature differences play a role in general, for example between the temperature of the the anterior chamber of the eye and the outside temperature. But there are circumstances like fever after an infection in which the temperature can change and plays a role for the fluid flow inside the eye. Additionally, frequently rotations of the liquid inside the vitreous due to head and eye movement during the day allow to rise the kinetic energy and lead to homogeneously distributed temperature.

Thermodynamical frameworks have been developed to deal with temperature changes [172]. If thermal effects are of interest besides mechanical processes, thermodynamic variables such as the temperature or internal energy are additional unknown quantities. Then the temperature can not be considered as a positive constant, but as the solution of its corresponding evolution equation (4.33) describing the thermodynamics, coupled with incompressible Burgers-type model (4.1) characterizing the mechanics. Then the system of governing

equations describing the vitreous body reads

$$\nabla \cdot v = 0, \tag{4.36a}$$

$$\rho \left(\frac{\partial v}{\partial t} + (v \cdot \nabla) v \right) = \nabla \cdot \mathbb{T}, \tag{4.36b}$$

$$-p\mathbb{I} + 2\mu_3 \mathbb{D} + G_1(\mathbb{B}_1 - \mathbb{I}) + G_2(\mathbb{B}_2 - \mathbb{I}) = \mathbb{T}, \tag{4.36c}$$

$$-\frac{G_1}{\mu_1}(\mathbb{B}_1 - \mathbb{I}) = \overset{\nabla}{\mathbb{B}}_1, \tag{4.36d}$$

$$-\frac{G_2}{\mu_2}(\mathbb{B}_2 - \mathbb{I}) = \overset{\nabla}{\mathbb{B}}_2, \tag{4.36e}$$

$$2\mu_3 |\mathbb{D}|^2 + \operatorname{div}(\kappa \nabla \theta) + 2\mu_1 \mathbb{C}_1 \mathbb{D}_1 : \mathbb{D}_1 + 2\mu_2 \mathbb{C}_2 \mathbb{D}_2 : \mathbb{D}_2 = \rho c_{\mathrm{V,ref}} \frac{d\theta}{dt}. \tag{4.36f}$$

(4.36) is a system of equations for the unknown quantities $(v, p, \mathbb{B}_1, \mathbb{B}_2, \theta)$ and it provides a generalization of the incompressible Burgers-type model to the non-isothermal setting. Once boundary and initial conditions are known for the velocity, temperature and left Cauchy-Green tensors, the system provides a complete description of the dynamics of the quantities of interest.

Hron et al. [82] derived viscoelastic rate type fluid models with temperature dependent material coefficients which are of practical importance in non-isothermal engineering applications like the injection molding process. In [172] we examine the stability of the rest state of these models to find the additional restrictions on the energetic/entropic equation of state which are well-known in the case of compressible Navier-Stokes fluid but not in the case of complex viscoelastic fluids. Here the special cases of the incompressible Burgers-type model, namely the Maxwell ($G_2 = \mu_2 = \mu_3 = 0$) and Oldroyd-B model ($G_2 = \mu_2 = 0$), with temperature dependent material parameters are considered for non-isothermal processes. The second law of thermodynamics (2.9) saying that the energy of the system is constant but the entropy strives to the maximum, restricts the material coefficients characterizing the dissipative responses (viscosity and thermal conductivity) to be positive. Whereas the requirement on the stability of the rest state demands the positivity of the material coefficients describing the energy storage mechanisms (heat capacity and shear modulus). Then the rest state of the viscoelastic fluid occupying a completely isolated domain (no mechanically and thermally interaction with its surrounding), modeled by the boundary conditions $v = j_e \cdot n = 0$ on $\partial\Omega$, is stable in the meaning that the entropy attains its maximum at the rest state. This rest state is represented by the quadruple $(v, p, \mathbb{B}_1, \theta) = (0, p_{\mathrm{ref}}, \mathbb{I}, \theta_{\mathrm{ref}})$ where the fluid is at rest, the left Cauchy-Green tensor is undeformed and the

pressure and temperature are fixed to homogeneous reference values.

In the following paragraph we will extend this result to the generalization of Burgers-type model and the weakening of thermally non-isolated condition. The mixed boundary conditions characterizing the biology of the eye would be to complex to analyze the rest state. For simplicity, we consider an isolated domain instead of the vitreous body.

4.4.1 Stability Analysis

In this section the stability of a spatially inhomogeneous non-equilibrium steady state for an incompressible heat conducting viscoelastic Burgers-type fluid occupying a mechanically isolated domain with spatially non-uniform wall temperature is investigated. It is a well-posedness result from the mathematical point of view for modeling by checking the governing equations. It shows that the proposed model behaves like expected, but it has no relevance for the application of drug distribution the human vitreous.
It is the long time behavior of Burgers-type fluid in a domain that is allowed to exchange thermal energy with the surrounding, which is described by an inhomogeneous Dirichlet boundary condition for the temperature. One expects that the fluid comes to the steady state, rest state, as time goes to infinity and it should be independent of the initial state and of the shape of the domain. In this case, the standard methods for thermodynamically isolated systems or systems immersed in a thermal bath can not be used since the steady state is a non-equilibrium (entropy producing) steady state due to the constant spatially nonuniform temperature at the domain's walls.
Dostalik et al. [37] investigated the same stability problem but with a Navier-Stokes-Fourier fluid (incompressible viscous heat conducting fluid) filling the domain. They have shown that the corresponding steady state is spatially inhomogeneous and unconditionally asymptotically stable under specific assumptions. In Dostalik et al. [38] we extend the results from [37] to the case of incompressible viscoelastic rate-type fluids including the Oldroyd-B and Giesekus model. We proved that the steady state is asymptotically stable subject to any finite perturbation.
Following the findings in [37] and [38] one extends the results for the viscoelastic Burgers-type model. It is demonstrated that the norm of velocity perturbation is bounded by an exponentially decaying function. The decay of the temperature perturbations follows then directly.
The needed thermodynamic concept and derivation of the Burgers-type model can be found in Section 4.2.2.

Helmholtz free energy

The specific Helmholtz free energy for the Burgers-type model is given by (4.19) where the thermal part ψ_1 is introduced in (4.21). Directly considering the incompressibility, $\psi_0(\rho)$ vanishes, the density is just a given constant and we have

$$\psi := \psi_1(\theta) + \psi_2(\mathbb{B}_1) + \psi_3(\mathbb{B}_2). \tag{4.37}$$

The following requirements introduced in [38] are satisfied for $i = 1, 2$

$$\psi_{i+1}(\mathbb{B}_i) \geq 0, \qquad \psi_{i+1}(\mathbb{B}_i) = 0 \Leftrightarrow \mathbb{B}_i = \mathbb{I}, \tag{4.38a}$$

$$\frac{\partial \psi_{i+1}}{\partial \mathbb{B}_i}(\mathbb{B}_i) = 0 \Leftrightarrow \mathbb{B}_i = \mathbb{I}, \tag{4.38b}$$

$$\mathbb{B}_i \frac{\partial \psi_{i+1}}{\partial \mathbb{B}_i}(\mathbb{B}_i) = \frac{\partial \psi_{i+1}}{\partial \mathbb{B}_i}(\mathbb{B}_i)\mathbb{B}_i. \tag{4.38c}$$

The viscoelastic parts of the Helmholtz energy ψ_2 and ψ_3 correspond respectively to the Oldroyd-B model for which the structural assumptions (4.38) are shown in Appendix A of [38].
Moreover, it holds for $i = 1, 2$ and the tensorial functions $f_i : \mathbb{R}^{3\times3}_+ \to \mathbb{R}^{3\times3}_+$ that

$$f_i(\mathbb{B}_i) = 0 \Leftrightarrow \mathbb{B}_i = \mathbb{I}, \tag{4.39a}$$

$$\frac{\partial \psi_{i+1}}{\partial \mathbb{B}_i}(\mathbb{B}_i) : f_i(\mathbb{B}_i) \geq 0, \tag{4.39b}$$

$$\psi_{i+1}(\mathbb{B}_i) \leq c_i \frac{\partial \psi_{i+1}}{\partial \mathbb{B}_i}(\mathbb{B}_i) : f_i(\mathbb{B}_i), \tag{4.39c}$$

where c_1 and c_2 are positive constants, $\mathbb{R}^{3\times3}_+$ denotes the space of symmetric positive definite 3×3 matrices and the specific functions for the Burgers-type model are defined by

$$f_i(\mathbb{B}_i) = \mathbb{B}_i - \mathbb{I} \qquad\qquad i = 1, 2.$$

The partial derivatives are given by

$$\frac{\partial \psi_{i+1}}{\partial \mathbb{B}_i}(\mathbb{B}_i) = \frac{G_i}{2\rho}(\mathbb{I} - \mathbb{B}_i^{-1}), \qquad\qquad i = 1, 2.$$

Problem formulation

The system of governing equations describing the behavior of incompressible viscoelastic Burgers-type model with constant density and temperature dependence reads:

Find $W := [p, v, \mathbb{B}_1, \mathbb{B}_2, \theta]$ in the domain Ω representing the closed domain such that

$$\nabla \cdot v = 0, \tag{4.40a}$$

$$\rho\left(\frac{\partial v}{\partial t} + (v \cdot \nabla)v\right) = \nabla \cdot \mathbb{T}, \tag{4.40b}$$

$$-p\mathbb{I} + 2\mu_3(\theta)\mathbb{D} + G_1(\mathbb{B}_1 - \mathbb{I}) + G_2(\mathbb{B}_2 - \mathbb{I}) = \mathbb{T}, \tag{4.40c}$$

$$-\frac{G_i}{\mu_i(\theta)}(\mathbb{B}_i - \mathbb{I}) = \overset{\nabla}{\mathbb{B}}_i, \qquad i = 1, 2, \tag{4.40d}$$

$$\operatorname{div}(\kappa\nabla\theta) + \xi_{\text{mech}} = \rho c_{\text{V,ref}}\frac{d\theta}{dt}, \tag{4.40e}$$

where the material parameters $\rho, G_1, G_2, c_{\text{V,ref}}, \kappa$ are positive constants while the viscosities $\mu_i, i = 1, 2, 3$ are assumed to be positive functions of temperature, since the fluid is affected by the temperature in this scenario. Further, μ_3 is required to be bounded from below and μ_1 and μ_2 to be bounded from above.

The boundary conditions on the domain walls are given by

$$\begin{aligned} v &= 0 && \text{on } \partial\Omega, \\ \theta &= \theta_{\text{bdr}} && \text{on } \partial\Omega \end{aligned}$$

and the initial conditions read

$$\begin{aligned} v &= v_0 && \text{on } \Omega \times \{t = 0\}, \\ \theta &= \theta_0 && \text{on } \Omega \times \{t = 0\} \end{aligned}$$

where θ_{bdr} is a given nontrivial function of position and ξ_{mech} describes the mechanical part of the entropy production $\xi := \frac{1}{\theta}(\xi_{\text{th}} + \xi_{\text{mech}})$ with

$$\xi_{\text{th}} := \kappa\frac{\nabla\theta \cdot \nabla\theta}{\theta}, \tag{4.41}$$

$$\begin{aligned} \xi_{\text{mech}} := 2\mu_3(\theta)\mathbb{D} : \mathbb{D} &+ \frac{G_1^2}{2\mu_1(\theta)}(\mathbb{B}_1 - \mathbb{I}) : (\mathbb{I} - \mathbb{B}_1^{-1}), \\ &+ \frac{G_2^2}{2\mu_2(\theta)}(\mathbb{B}_2 - \mathbb{I}) : (\mathbb{I} - \mathbb{B}_2^{-1}). \end{aligned} \tag{4.42}$$

From the thermodynamic framework and the derived constitutive relations (4.32) we know that

$$\frac{G_i^2}{2\mu_i(\theta)}(\mathbb{B}_i - \mathbb{I}) : (\mathbb{I} - \mathbb{B}_i^{-1}) = 2\mu_i(\theta)\mathbb{C}_i\mathbb{D}_i : \mathbb{D}_i \qquad i = 1, 2.$$

Consequently, the definition of ξ_{mech} matches with the mechanical part of the derived evolution equation (4.36f) for the temperature.

Note that the structure of the temperature evolution equation (4.40e) is the same as for the Navier-Stokes-Fourier fluid in [37] or the viscoelastic models in [38]. Only the specification of the entropy production term ξ_{mech} differs due to the definition of the Helmholtz energy ψ. For the Burgers-type fluid, we assume the co-existence of two natural configurations and therefore two left Cauchy-Green tensors are needed to model the elastic response. Consequently, we deal with two viscoelastic parts $\psi_i, i = 2, 3$ compare to only one in [38] and extend the mechanical entropy production with one additional term.
Since the stability analysis done in [37] required that this term is nonnegative and integrable in time and space, the results obtained in [37] and [38] can be reused to show that this assumption is also fulfilled for the Burgers-type model.

Remark 4.4.1: *The mechanically entropy production can be rewritten into*

$$\xi_{mech} = 2\mu_3(\theta)\mathbb{D} : \mathbb{D} + \rho\frac{G_1}{\mu_1(\theta)}\frac{\partial\psi_2}{\partial\mathbb{B}_1}(\mathbb{B}_1) : f_1(\mathbb{B}_1) + \rho\frac{G_2}{\mu_2(\theta)}\frac{\partial\psi_3}{\partial\mathbb{B}_2}(\mathbb{B}_2) : f_2(\mathbb{B}_2). \tag{4.43}$$

In this notation it is easy to see that regarding the assumptions (4.39) *the mechanically entropy production ξ_{mech} is positive which is a thermodynamically requirement. Since the temperature evolution equation* (4.40e) *is parabolic with a convective term and a positive source, θ is under the given boundary conditions bounded from below uniformly in space and time.*

Steady state

In the steady state $\widehat{W} := [\widehat{p}, \widehat{v}, \widehat{\mathbb{B}_1}, \widehat{\mathbb{B}_2}, \widehat{\theta}]$ the fluid is at rest which means

$$\begin{aligned} \nabla\widehat{p} &= 0, \\ \widehat{v} &= 0, \\ \widehat{\mathbb{B}_1} &= \mathbb{I}, \\ \widehat{\mathbb{B}_2} &= \mathbb{I}, \end{aligned}$$

which follows from the balance equations (4.40). The steady temperature field $\widehat{\theta}$ solves the steady heat equation with Dirichlet boundary condition:

$$\begin{aligned} \operatorname{div}(\kappa\nabla\widehat{\theta}) &= 0 && \text{in } \Omega, \\ \widehat{\theta} &= \theta_{\text{bdr}} && \text{on } \partial\Omega. \end{aligned}$$

Since θ_{bdr} is a nontrivial function of position, $\widehat{\theta}$ is a spatially inhomogeneous bounded function.

Governing equations for perturbations

The aim is to show that the perturbations $\widetilde{W} := [\widetilde{p}, \widetilde{v}, \widetilde{\mathbb{B}_1}, \widetilde{\mathbb{B}_2}, \widetilde{\theta}]$ with respect to the steady state $\widehat{W}$ vanish as time goes to infinity,

$$\lim_{t \to +\infty} \widetilde{W} = 0.$$

Since the solution $W = \widehat{W} + \widetilde{W}$ is described by the balance equations (4.40), the governing equations for the perturbations read

$$\begin{aligned}
\nabla \cdot \widetilde{v} &= 0, \\
-\nabla \widetilde{p} + \nabla \cdot \left[2\mu_3(\widehat{\theta} + \widetilde{\theta})\widetilde{\mathbb{D}} + G_1 \widetilde{\mathbb{B}_1} + G_2 \widetilde{\mathbb{B}_2} \right] &= \rho \left(\frac{\partial \widetilde{v}}{\partial t} + (\widetilde{v} \cdot \nabla)\widetilde{v} \right), \\
\frac{\partial \widetilde{\mathbb{B}_i}}{\partial t} + (\widetilde{v} \cdot \nabla)\widetilde{\mathbb{B}_i} - (\nabla \widetilde{v})\widetilde{\mathbb{B}_i} - \widetilde{\mathbb{B}_i}(\nabla \widetilde{v})^T - 2\widetilde{\mathbb{D}} &= -\frac{G_i}{\mu_i(\widehat{\theta} + \widetilde{\theta})} \widetilde{\mathbb{B}_i}, \quad i = 1, 2, \\
\rho c_{\text{V,ref}} \left(\frac{\partial \widetilde{\theta}}{\partial t} + (\widetilde{v} \cdot \nabla)(\widehat{\theta} + \widetilde{\theta}) \right) - \xi_{\text{mech}}(\widehat{W} + \widetilde{W}) &= \operatorname{div}(\kappa \nabla \widetilde{\theta})
\end{aligned}$$

with the initial and boundary conditions

$$\begin{aligned}
\widetilde{v} &= v_0 && \text{on } \Omega \times \{t = 0\}, \\
\widetilde{\theta} &= \theta_0 - \widehat{\theta} && \text{on } \Omega \times \{t = 0\}, \\
\widetilde{v} &= 0 && \text{on } \partial\Omega, \\
\widetilde{\theta} &= 0 && \text{on } \partial\Omega.
\end{aligned}$$

Following the same argument as in [37, 38] the tool to show the stability analysis is the Lemma on the decay of integrable functions in [37]. The needed quantity satisfying the assumptions of the lemma and that vanishes if and only if the perturbations vanish is constructed using the Lyapunov type functional and introducing a new temperature scale.

Construction of a Lyapunov type functional

The construction of a Lyapunov type functional $\mathcal{V}_{\text{neq}}$ needed to investigate the stability uses the concepts introduced in [37] and [38]. Furthermore, the knowledge of the Lyapunov functional can be helpful to construct a distance

measure that can be used in studying the error between two solutions (regular and weak one, discrete and continuous). We split the Lyapunov type functional $\mathcal{V}_{\text{neq}}$ into two parts

$$\mathcal{V}_{\text{neq}}(\widetilde{W}\|\widehat{W}) = \mathcal{V}_{\text{th}}(\widetilde{W}\|\widehat{W}) + \mathcal{V}_{\text{mech}}(\widetilde{W}\|\widehat{W})$$

where $\mathcal{V}_{\text{th}}$ shall be used to deal with the temperature perturbations $\widetilde{\theta}$ and $\mathcal{V}_{\text{mech}}$ to the mechanical quantities $\widetilde{v}$, $\widetilde{\mathbb{B}_1}$ and $\widetilde{\mathbb{B}_2}$. They are defined as

$$\begin{aligned}
\mathcal{V}_{\text{th}}(\widetilde{W}\|\widehat{W}) &= \int_\Omega \rho c_{\text{V,ref}} \widehat{\theta} \left[\frac{\widetilde{\theta}}{\widehat{\theta}} - \ln\left(1 + \frac{\widetilde{\theta}}{\widehat{\theta}}\right)\right] \,\mathrm{dv}, \\
\mathcal{V}_{\text{mech}}(\widetilde{W}\|\widehat{W}) &= \int_\Omega \rho\psi_2(\mathbb{I} + \widetilde{\mathbb{B}_1}) \,\mathrm{dv} + \int_\Omega \rho\psi_3(\mathbb{I} + \widetilde{\mathbb{B}_2}) \,\mathrm{dv}, \\
&\quad + \int_\Omega \frac{1}{2}\rho|\widetilde{v}|^2 \,\mathrm{dv}
\end{aligned} \tag{4.44}$$

where the Helmholtz energy is chosen as in (4.37) with thermal part (4.21) and mechanical parts (4.20).
The functionals $\mathcal{V}_{\text{neq}}$, $\mathcal{V}_{\text{th}}$ and $\mathcal{V}_{\text{mech}}$ are nonnegative and vanish if and only if the perturbations vanish.

To serve as a genuine Lyapunov functional the time derivative of the constructed functional $\mathcal{V}_{\text{neq}}$ has to be non-positive. It can be shown that the corresponding time derivative has the same structure as in [37, 38] and differs only in the particular choice of the mechanical dissipation $\xi_{\text{mech}}(\widehat{W} + \widetilde{W})$,

$$\begin{aligned}
\frac{d\mathcal{V}_{\text{neq}}}{dt}(\widetilde{W}\|\widehat{W}) = &- \int_\Omega \kappa\widehat{\theta}\nabla \ln\left(1 + \frac{\widetilde{\theta}}{\widehat{\theta}}\right) \cdot \nabla \ln\left(1 + \frac{\widetilde{\theta}}{\widehat{\theta}}\right) \,\mathrm{dv} \\
&+ \int_\Omega \rho c_{\text{V,ref}} \ln\left(1 + \frac{\widetilde{\theta}}{\widehat{\theta}}\right) (\widetilde{v}\cdot\nabla\widehat{\theta}) \,\mathrm{dv} \\
&- \int_\Omega \frac{\widehat{\theta}}{\widehat{\theta} + \widetilde{\theta}} \xi_{\text{mech}}(\widehat{W} + \widetilde{W}) \,\mathrm{dv}.
\end{aligned} \tag{4.45}$$

Estimate on the time derivative of the candidate for a Lyapunov type functional - Decay of perturbations

The first and the last term on the right hand side of (4.45) (without involving their negative sign) are positive. The only term which sign is a priori unknown is

$$\int_\Omega \rho c_{\text{V,ref}} \ln\left(1 + \frac{\widetilde{\theta}}{\widehat{\theta}}\right) (\widetilde{v}\cdot\nabla\widehat{\theta}) \,\mathrm{dv}.$$

If we deal with a spatially homogeneous steady state $\widehat{\theta}$, i.e. the rest state in a thermodynamically isolated domain or in a domain immersed in a thermal bath, then we would have $\nabla\widehat{\theta} = 0$ and the second term would vanish. In this case the stability problem would be solved.

Following [37] and [38] this term is negligible if the velocity perturbation $\widetilde{v}$ decays in time which means that it is bounded by an exponentially decaying function. This property can be obtained by analyzing the mechanical part $\mathcal{V}_{\text{mech}}$ of the functional $\mathcal{V}_{\text{neq}}$, which is more complicated for the viscoelastic models than for the Navier-Stokes-Fourier fluid and especially for the more general viscoelastic Burgers-type model here. After that, one can focus on the temperature perturbation, reuse the results by [37] and show the decay of $\widetilde{\theta}$.

Using the formulas (4.43), (4.44) and following the concept by [38], the time derivative of $\mathcal{V}_{\text{mech}}$,

$$\frac{d\mathcal{V}_{\text{mech}}}{dt}(\widetilde{W}\|\widehat{W}) = -\int_\Omega \xi_{\text{mech}}(\widehat{W}+\widetilde{W})\,\mathrm{dv},$$

can be estimated by

$$\begin{aligned}\frac{d}{dt}\int_\Omega \left(\rho\psi_2(\mathbb{I}+\widetilde{\mathbb{B}_1}) + \rho\psi_3(\mathbb{I}+\widetilde{\mathbb{B}_2}) + \frac{1}{2}\rho|\widetilde{v}|^2\right)\mathrm{dv}\\ \leq -\frac{2\min_{s\in\mathbb{R}_+}\mu_3(s)}{\rho c_p}\int_\Omega \frac{1}{2}\rho|\widetilde{v}|^2\,\mathrm{dv} - \frac{G_1}{c_1\max_{s\in\mathbb{R}_+}\mu_1(s)}\int_\Omega \rho\psi_2(\mathbb{I}+\widetilde{\mathbb{B}_1})\,\mathrm{dv}\\ - \frac{G_2}{c_2\max_{s\in\mathbb{R}_+}\mu_2(s)}\int_\Omega \rho\psi_3(\mathbb{I}+\widetilde{\mathbb{B}_2})\,\mathrm{dv}.\end{aligned}$$

Since the velocity perturbation vanishes on the boundary, $\widetilde{v} = 0$, assumption (4.39c) holds and we have the boundedness of μ_3 and μ_1, μ_2 from below and above respectively. Then it yields that

$$\frac{1}{2}\rho\|\widetilde{v}\|^2_{L^2(\Omega)} \leq \mathcal{V}_{\text{mech}}(\widetilde{W}\|\widehat{W}) \leq \mathcal{V}_{\text{mech}}(\widetilde{W}\|\widehat{W})\big|_{t=0}e^{-C_{\text{mech}}t} \tag{4.46}$$

which implies

$$\int_\Omega \psi_2(\mathbb{I}+\widetilde{\mathbb{B}_1})\,\mathrm{dv} \leq \frac{1}{\rho}\mathcal{V}_{\text{mech}}(\widetilde{W}\|\widehat{W})\big|_{t=0}e^{-C_{\text{mech}}t}, \tag{4.47a}$$

$$\int_\Omega \psi_3(\mathbb{I}+\widetilde{\mathbb{B}_2})\,\mathrm{dv} \leq \frac{1}{\rho}\mathcal{V}_{\text{mech}}(\widetilde{W}\|\widehat{W})\big|_{t=0}e^{-C_{\text{mech}}t} \tag{4.47b}$$

with the positive constant

$$C_{\text{mech}} := \min\left\{\frac{2\min_{s\in\mathbb{R}_+}\mu_3(s)}{\rho c_p}, \frac{G_1}{c_1\max_{s\in\mathbb{R}_+}\mu_1(s)}, \frac{G_2}{c_2\max_{s\in\mathbb{R}_+}\mu_2(s)}\right\}.$$

Estimations (4.46) show that the velocity perturbation is bounded from above by an exponentially decaying function. $\widetilde{v}$ and $\widetilde{\mathbb{B}_1}, \widetilde{\mathbb{B}_2}$ vanish as time goes to infinity. The more general mechanical entropy production $\xi_{\text{mech}}(\widehat{W}+\widetilde{W})$ for the Burgers-type fluid can be bounded in the same way as in [38] for the Oldroyd model and is a non-negative quantity which vanishes at equilibrium.
(4.47) implies only the decay of $\int_\Omega \psi_2(\mathbb{I}+\widetilde{\mathbb{B}_1})\,\mathrm{dv}$ or rather $\int_\Omega \psi_3(\mathbb{I}+\widetilde{\mathbb{B}_2})\,\mathrm{dv}$, no convergence of $\mathbb{B}_1$ and $\mathbb{B}_2$ to zero in a norm. But this can be shown using a specific metric constructed by Bures-Wasserstein distance on the set of positive definite matrices, see [36].

Now, we need the decay of the temperature perturbation and that the spatially inhomogeneous steady temperature field $\widehat{\theta}$ is stable irrespective of the initial temperature field.

Family of functionals Since the sign of the time derivative of the functional (4.45) is a priori not known for a non-constant $\widehat{\theta}$, $\mathcal{V}_{\text{neq}}$ is insufficient to yield asymptotic stability of the steady temperature field $\widehat{\theta}$ via the Lyapunov method. But as it has been shown in [37] and [38] this problem can be dealt by introducing a new temperature scale

$$\frac{\vartheta}{\vartheta_{\text{ref}}} := \left(\frac{\theta}{\theta_{\text{ref}}}\right)^{1-m}$$

with $m\in(0,1)$. The restriction $m<1$ means that the new temperature scale preserves the ordering according hotness which denotes that the heat still flows in the direction of the temperature difference. Repeating the steps from the previous section of construction of a Lyapunov type functional with the new temperature scale, a new family of functionals parametrized by m is obtained:

$$\begin{aligned}\mathcal{V}^m_{\text{neq}}(\widetilde{W}\|\widehat{W}) = &\int_\Omega \rho c_{\text{V,ref}}\widehat{\theta}\left[\frac{\widetilde{\theta}}{\widehat{\theta}} - \frac{1}{m}\left(\left(1+\frac{\widetilde{\theta}}{\widehat{\theta}}\right)^m - 1\right)\right]\,\mathrm{dv}\\ &+\int_\Omega \rho\psi_2(\mathbb{I}+\widetilde{\mathbb{B}_1})\,\mathrm{dv} + \int_\Omega \rho\psi_3(\mathbb{I}+\widetilde{\mathbb{B}_2})\,\mathrm{dv}\\ &+\int_\Omega \frac{1}{2}\rho|\widetilde{v}|^2\,\mathrm{dv},\end{aligned}$$

where the thermal part $\mathcal{V}_{\text{th}}^m$ is defined by

$$\mathcal{V}_{\text{th}}^m(\widetilde{W}\|\widehat{W}) := \int_\Omega \rho c_{\text{V,ref}} \widehat{\theta} \left[\frac{\widetilde{\theta}}{\widehat{\theta}} - \frac{1}{m} \left(\left(1 + \frac{\widetilde{\theta}}{\widehat{\theta}} \right)^m - 1 \right) \right] \, \text{dv}. \tag{4.48}$$

According to [37] the time derivative of $\mathcal{V}_{\text{th}}^m$ reads

$$\begin{aligned} \frac{d\mathcal{V}_{\text{th}}^m}{dt}(\widetilde{W}\|\widehat{W}) = &- \int_\Omega 4 \frac{1-m}{m^2} \kappa \widehat{\theta} \nabla \left[\left(1 + \frac{\widetilde{\theta}}{\widehat{\theta}} \right)^{\frac{m}{2}} - 1 \right] \cdot \nabla \left[\left(1 + \frac{\widetilde{\theta}}{\widehat{\theta}} \right)^{\frac{m}{2}} - 1 \right] \, \text{dv} \\ &- \int_\Omega \frac{1-m}{m} \rho c_{\text{V,ref}} \left[\left(1 + \frac{\widetilde{\theta}}{\widehat{\theta}} \right)^m - 1 \right] (\widetilde{v} \cdot \nabla \widehat{\theta}) \, \text{dv} \\ &+ \int_\Omega \left(1 - \frac{1}{\left(1 + \frac{\widetilde{\theta}}{\widehat{\theta}} \right)^{1-m}} \right) \xi_{\text{mech}}(\widehat{W} + \widetilde{W}) \, \text{dv}. \end{aligned} \tag{4.49}$$

Note that [37] has shown equation (4.49) for the entropy production term $\xi_{\text{mech}} = 2\mu_3 \mathbb{D} : \mathbb{D}$. However, (4.49) holds for the more general entropy production (4.42) as well since the specific form is inconsequential in the analysis.

Nevertheless, all the algebraic manipulations for the case of the standard Navier-Stokes-Fourier fluid occupying a mechanically isolated domain with spatially non-uniform wall temperature in [37] can be adopted and lead to the same result that $\mathcal{V}_{\text{neq}}^m$ remains nonnegative and vanishes if and only if the perturbation $\widetilde{W}$ vanishes for any fixed $m \in (0,1)$.

The assumptions are the boundedness of $\|\widetilde{v}\|_{L^2(\Omega)}$ from above by an exponentially decaying function and the non-negativity of the mechanical entropy production $\xi_{\text{mech}}(\widehat{W} + \widetilde{W})$ that vanishes at equilibrium. Over all, these properties hold in the case of Burgers-type fluid, (4.46) and (4.47), and we can generalize the results of [38].

In particular, for $n, m \in (0,1), n > m > \frac{n}{2}$ and

$$\mathcal{Y}_{\text{th}}^{m,n}(\widetilde{W}\|\widehat{W}) := \mathcal{V}_{\text{th}}^m(\widetilde{W}\|\widehat{W}) - \mathcal{V}_{\text{th}}^n(\widetilde{W}\|\widehat{W})$$

it holds that

$$\mathcal{Y}_{\text{th}}^{m,n}(\widetilde{W}\|\widehat{W}) \to 0, \qquad t \to +\infty.$$

Regarding the equation (4.48) this leads to

$$\int_\Omega \rho c_{\mathrm{V,ref}} \widehat{\theta} \left[\frac{1}{n} \left(1 + \frac{\widetilde{\theta}}{\widehat{\theta}} \right)^n - \frac{1}{m} \left(1 + \frac{\widetilde{\theta}}{\widehat{\theta}} \right)^m + \frac{n-m}{mn} \right] \mathrm{dv} \to 0, \qquad t \to +\infty \tag{4.50}$$

and involves the decay of the relative entropy in any Lebesgue space $L^p(\Omega)$, $p \in [1, +\infty)$ using the results in [37].
To obtain (4.50), the necessary condition requires all terms on the right side of equation (4.49) to be finite under integration over time from zero to infinity, which follows from estimation (4.46). Then a lemma on the decay of integrable functions, see [37], applied to the functional $\mathcal{Y}_{\mathrm{th}}^{m,n}$ provides the convergence (4.50).

It is shown that the spatially inhomogeneous non-equilibrium steady state for an incompressible viscoelastic Burgers-type fluid in a thermodynamically open system is asymptotically stable irrespective of the initial conditions and of the shape of the domain. It is a generalization of the results by [38] where we investigated the same stability problem but only for simpler viscoelastic models.
Nevertheless, the vitreous is no isolated system and the outlined methodology can not be applied to the complex biology in the eye. For that reason and the fact that the temperature is usually constant inside the vitreous we do not include the temperature in the governing equations of our models in this study.

4.5 Mechanical Behavior of Healthy and Liquefied Vitreous in a Deforming Eye (Fluid-Structure-Interaction)

4.5.1 Experiment Description

The vitreous humour acts as a mechanical damper and transmits stresses protecting the eye and holding the retina in contact with the retinal pigment epithelium [159]. During vitreous motion vitreoretinal tractions are created and this might potentially lead to vitreous and retinal detachment. But despite this link the mechanical properties of the vitreous body and its motion are not well understood.
In our publication Tůma et al. [182] we analyze its mechanical behavior in a setting that resembles recent experimental work on the same [163] and improve the understanding of the physiology and pathophysiology of the eye.

The motion of the vitreous is induced by the deformation of the eyeball leading to an interaction between the deforming nonlinear hyperelastic sclera/ lens (solid) and (non-) Newtonian vitreous (fluid), a fluid-structure-interaction problem described by a system of partial differential equations and solved numerically. Since the sclera and lens have a measurable positive thickness and elastic parameters which are known from the literature, see Table 4.4, the simpler shell problem without full-description of the elastic structures is not reasonable.
In contrast to other studies focusing on the saccadic eye movement (rapid oscillations of the eyeball as the whole) [24, 153] the geometry of the vitreous is not fixed and does not take the spherical shape but a realistic geometrical setting in which the deformation of the sclera induces the flowing of the vitreous. Additionally, we take into account the various rheological properties of the vitreous including the viscoelasticity and compare their influence in the deforming eye.

In the experiments in Shah et al. [163] the bovine eyes were cut in an anterior-posterior direction to create samples with an optically clear window to analyze the changes during the experiment. They were put into a loading machine and glued on the sides. Then the eyes were uniaxially stretched in 3 mm increments up to 12 mm with 2 min of equilibration time between each displacement step. Imaging these samples we construct the three-dimensional geometry like in Figure 4.5. For mathematical simplicity, we set the height to be constant and decompose the eye in three tissues: the vitreous, lens and sclera.

4.5.2 Full System of Governing Equations

The vitreous is modeled as an incompressible fluid in the Eulerian framework where we distinguish between the pathological/ liquefied vitreous using the incompressible Navier-Stokes model (3.9) and the healthy viscoelastic vitreous using the incompressible Burgers-type model (4.1).
The sclera and the lens are modeled as hyperelastic solids in the Lagrangian framework, see the Section 2.2.2, in which one is interested in the reference configuration, the single particles and their deformation. Here our domain, the vitreous body, is denoted by $\Omega_R \subset \mathbb{R}^d, d = 2, 3$ and represents the vitreous before it is deformed. It corresponds to the reference configuration $\kappa_0(\Omega)$ in Section 2.2.2. In this setting, the so-called hyperelastic material, a subclass of an elastic material, postulates the existence of a Helmholtz free-energy function $\psi = \psi(\mathbb{F})$ which is solely a function of $\mathbb{F}$ and referred to as the strain-energy function or stored-energy function [81]. It is assumed to be continuous and

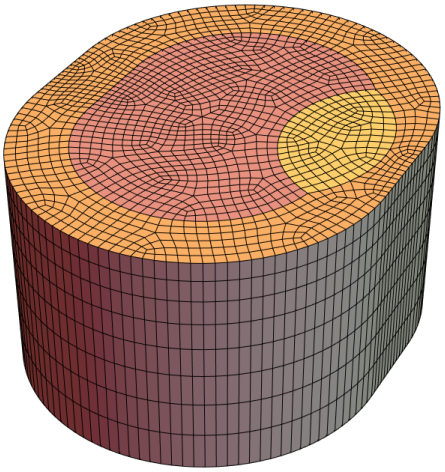

Figure 4.5: Discretization of the reference configuration [Reprinted by permission from Elsevier, [182]]

homogeneous (ψ depends only upon the deformation gradient $\mathbb{F}$ and not upon the position of a point in the material X). The balance of mass and linear momentum take the following form in the Lagrangian description:

$$\rho_R = (\det \mathbb{F})\rho \qquad \text{in } \Omega_R \times (0, T], \tag{4.51a}$$

$$\rho_R \frac{\partial^2 u}{\partial t^2} = \mathrm{DIV}\ \mathbb{T}_R \qquad \text{in } \Omega_R \times (0, T], \tag{4.51b}$$

where ρ_R and ρ denote the density in the reference configuration and in the current configuration. $u := \chi(X, t) - X$ is the displacement being in relation with the deformation gradient tensor by $\mathbb{F} = \mathbb{I} + \nabla u$ where χ was introduced in Section 2.2.2, DIV denotes the divergence operator in the reference configuration and $\mathbb{T}_R$ describes the first Piola-Kirchhoff stress tensor which is related to Cauchy stress tensor $\mathbb{T}$ in the current configuration through the formulas

$$\mathbb{T}_R := \det\mathbb{F}\ \mathbb{T}\ \mathbb{F}^{-T}$$

and

$$\mathrm{DIV}\mathbb{T}_R := \det\mathbb{F}\ \mathrm{div}\mathbb{T}.$$

Following [71, 182] the strain-energy function $\psi : \Omega_R \times \mathbb{R}^{d\times d}_{+} \to \mathbb{R}$ such that $\mathbb{T}_R = \frac{\partial \psi(x,\mathbb{F})}{\partial \mathbb{F}}$ for the sclera and lens takes the d-dimensional form:

$$\psi(\mathbb{F}) = \frac{1}{2} G \left(J^{-2/d} \mathrm{tr}\, \mathbb{C} - d \right) + \frac{1}{2} \kappa (\ln J)^2. \tag{4.52}$$

$\mathbb{C}$ defines the right Cauchy-Green tensor introduced in (2.3), $J := \det \mathbb{F}$ and the material parameters G and κ are referred to the elastic shear modulus and the elastic bulk modulus. Therefore, it follows that the first Piola-Kirchhoff stress reads

$$\mathbb{T}_R = GJ^{-2/d}\left(\mathbb{F} - \frac{1}{d}(\operatorname{tr}\mathbb{C})\mathbb{F}^{-T}\right) + \kappa(\ln J)\mathbb{F}^{-T}.$$

Since both sclera and lens are almost incompressible, we assume $\kappa := 1000G$ which consequently means that $\det \mathbb{F} = 1$ and hence $\rho = \rho_R = \text{const}$. Parameter values for human sclera and lens used in the numerical simulations are shown in Table 4.4.

4.5.3 Modeling of Sclera and Lens as Hyperelastic Solids

The sclera and the lens are nearly incompressible (or slightly compressible) modeled as compressible hyperelastic solids. Within them the dilational changes require a much higher exterior work than volume-preserving changes and the compressibility effects are small. Therefore, it is useful to split the deformation gradient into a volume-changing (volumetric) and volume-preserving (isochoric) part, see [81, 167]. Further, the multiplicative decomposition of $\mathbb{F}$ is supported by the field of computational mechanics because it is often advantageous to separate numerical treatments of the volumetric and isochoric parts to avoid numerical complications in the finite element analysis [81].
In particular, we write

$$\mathbb{F} = \widehat{\mathbb{F}}\overline{\mathbb{F}}$$

where $\overline{\mathbb{F}} = J^{-1/\mathrm{d}}\mathbb{F}$ is associated with the volume-preserving deformation, i.e. $\det \overline{\mathbb{F}} = 1$. The tensor $\widehat{\mathbb{F}} = J^{1/\mathrm{d}}\mathbb{I}$ describes the volume-changing part with $\det \widehat{\mathbb{F}} = \det \mathbb{F}$.
This concept can be carried on to other kinematic tensors:

$$\overline{\mathbb{C}} = \overline{\mathbb{F}}^T\overline{\mathbb{F}}, \qquad \overline{\mathbb{B}} = \overline{\mathbb{F}}\overline{\mathbb{F}}^T$$

with $\det \overline{\mathbb{C}} = \det \overline{\mathbb{B}} = 1$, which can be expressed by the original Cauchy–Green tensors $\mathbb{C} = \mathbb{F}^T\mathbb{F}$ and $\mathbb{B} = \mathbb{F}\mathbb{F}^T$ via

$$\overline{\mathbb{C}} = J^{-2/\mathrm{d}}\mathbb{C}, \qquad \overline{\mathbb{B}} = J^{-2/\mathrm{d}}\mathbb{B}.$$

$\overline{\mathbb{F}}$ and $\overline{\mathbb{C}}$ are called the modified deformation gradient and the modified right Cauchy-Green tensor. In addition the strain energy function $\psi = \psi(\mathbb{F})$ defined in (4.52) is decoupled:

$$\psi(\mathbb{F}) = \psi_{\mathrm{iso}}(\overline{\mathbb{C}}) + \psi_{\mathrm{vol}}(J)$$

where

$$\psi_{\text{iso}}(\overline{\mathbb{C}}) = \frac{1}{2}G\left(\operatorname{tr}\overline{\mathbb{C}} - \operatorname{tr}\mathbb{I}\right) \tag{4.53}$$

and

$$\psi_{\text{vol}}(J) = \frac{1}{2}\kappa(\ln J)^2 \tag{4.54}$$

describe the isochoric (incompressible) and volumetric (compressible) elastic response of the tissue, respectively. Additionally, the volumetric component is a strictly convex scalar-valued function of J with its unique minimum at $J = 1$, the state of full incompressibility.
This model (4.52) for ψ is motivated by a compressible neo-Hookean solid which is a simple hyperelastic model similar to Hooke's law and can be used for predicting the nonlinear stress-strain behavior of materials undergoing large deformations. In contrast to linear elastic materials, the stress-strain curve of a neo-Hookean material is not linear (initially linear, but at a certain point the stress-strain curve will plateau).
The hyperelastic model emphasizes the reversibility of deformations and the idea that energy can be stored in the material and used afterwards to do work.

Existence and Uniqueness

The existence theory for elastic problems is based on the direct methods of variation, i.e. to find a minimizing deformation of the elastic strain energy $\psi(\mathbb{F})$ subject to the specific boundary conditions. In order to ensure the existence of minimizers, the energy function has to be polyconvex (first introduced by Ball in [16]) and coercive. Details concerning existence in finite elasticity can be found in the literature in [119].
In this section the existence of the solution to the non-homogeneous boundary-value problem,

$$-DIV\frac{\partial\psi(\mathbb{F})}{\partial\mathbb{F}} = 0 \qquad \text{in } \Omega_R, \tag{4.55a}$$

$$\chi(X) = \chi_0(X) \qquad \text{on } \Gamma_R. \tag{4.55b}$$

considering the specific $\psi(\mathbb{F})$ modeling the mechanical behavior of the sclera and the lens will be shown, in contrast to the more complex setting (4.51) for the fluid-structure interaction problem.

Theorem 4.5.1 (Existence)**:**
Let the reference configuration $\Omega_R \subset \mathbb{R}^3$ be a bounded Lipschitz domain and $\psi : \mathbb{R}^{3\times3}_+ \to \mathbb{R}$ a stored energy function with the following properties:

- *ψ is polyconvex*

- ψ *is p-coercive.*

Let Γ_R *be a part of the boundary,* $\Gamma_R \subset \partial\Omega_R$*, with non-vanishing Lebesgue measure and let* $\chi_0 \in W^{1,p}(\Omega_R)$ *be given with* $I(\chi_0) < +\infty$*. Let*

$$\phi := \{\chi \in W^{1,p}(\Omega_R), \chi(X) = \chi_0(X) \text{ for } X \in \Gamma_R, \det\mathbb{F} > 0 \text{ a.e.}\}$$

be non-empty.
Then there exists a minimum of

$$I(\chi) = \int_{\Omega_R} \psi(\mathbb{F}) dX$$

on ϕ *with* $\nabla_X \chi := \frac{\partial \chi(X,t)}{\partial X} = \mathbb{F}$ *corresponding to problem* (4.55)*.*

Proof. See [76] for details. □

But first, the strain-energy function $\psi(\mathbb{F})$ is assumed to satisfy physically plausible conditions [81]:

$$\psi(\mathbb{I}) = 0, \tag{4.56}$$
$$\psi(\mathbb{F}) \geq 0, \tag{4.57}$$
$$\psi(\mathbb{F}) \to +\infty, \qquad \det\mathbb{F} \to +0, \tag{4.58}$$
$$\psi(\mathbb{F}) \to +\infty, \qquad \det\mathbb{F} \to +\infty. \tag{4.59}$$

$\psi(\mathbb{F})$ must vanish in the reference configuration where $\mathbb{F} = \mathbb{I}$ and increases monotonically with the deformation and attains its global minimum at the thermodynamic equilibrium $\mathbb{F} = \mathbb{I}$. Relations (4.56) and (4.57) ensure that the stress in the reference configuration (called residual stress) is zero. Therefore, the reference configuration is called stress-free.
Moreover, we require for the behavior at finite strains that ψ must fulfill growth conditions. Physically, an infinite amount of energy is necessary to expand a body infinitely and to compress it to zero volume, where the determinant of the deformation gradient is assumed to be positive, $\det\mathbb{F} > 0$.

We will show that the material specific strain energy density modeling the mechanical behavior of the sclera and the lens given by (4.52) guarantees the existence of at least one minimizer for non-homogeneous boundary-value problem (4.55) under certain circumstances. At the beginning we will check the physical conditions and then we will proof the polyconvexity and coercivity condition of the strain energy density function ψ in the case of three-dimensions. These results can be adopted to other dimensions.

The polyconvexity condition is based on expressions defined on the deformation gradient $\mathbb{F}$. Therefore, we reformulate (4.52) in terms of $\mathbb{F}$ and $\det \mathbb{F}$:

$$\psi(\mathbb{F}, \det \mathbb{F}) = \frac{1}{2} G \left((\det \mathbb{F})^{-2/3} |\mathbb{F}|^2 - 3 \right) + \frac{1}{2} \kappa \left(\ln(\det \mathbb{F}) \right)^2 \tag{4.60}$$

where $|\mathbb{F}|^2 = \operatorname{tr} \mathbb{C}$ defines the scalar product of the deformation gradient.
After calculation it is easy to see that the physical plausible assumptions (4.56) and (4.57) are fulfilled since we know that $(\det \mathbb{F})^{-2/3} |\mathbb{F}|^2 - 3 \geq 0$ shown in [76]. (4.58) is guaranteed due to the property of the natural logarithm, $\left(\ln(\det \mathbb{F}) \right)^2 \to +\infty$ for $\det \mathbb{F} \to +0$. Only for the last constraint (4.59) the model shows non-physical behaviour.
Further, ψ given by equation (4.60) with $G, \kappa \geq 0$ is polyconvex due to the additivity of polyconvex functions, but only for $0 < \det \mathbb{F} \leq e$, restricted from above by the Euler number e. In particular, the isochoric part of the strain energy function ψ_{iso} introduced in (4.53) is polyconvex according to the Lemma 2.2 in [76]. The volumetric part of the strain energy function ψ_{vol} defined in (4.54) is a model of the literature from [167] and has merely to be convex in the variable $J = \det \mathbb{F}$. The convexity requirement implies

$$\frac{d^2 \psi_{\text{vol}}}{dJ^2}(J) = \frac{\kappa}{J^2}(1 - \ln J) \geq 0$$

which is fulfilled except for $\det \mathbb{F} > e$.
At last, we need the coercivity property which states that the elastic stored energy functional $I(\chi)$ is p-coercive whenever

$$I(\chi) \leq K, \quad \Rightarrow \quad \|\chi\|_{W^{1,p}(\Omega_R)} \leq \tilde{K}$$

with constants $K, \tilde{K} > 0$, see [76] for the definition and further information.

Theorem 4.5.2 (Coercivity)**:**
Let the elastic strain energy density be given by equation (4.60) *with* $G, \kappa \geq 0$*. Then* $I(\chi)$ *is coercive for* $p = 4$ *in the range of validity of polyconvexity for* $0 < \det \mathbb{F} \leq e$*.*

Proof.

$$
\begin{aligned}
\|\mathbb{F}\|^p_{L^p(\Omega_R)} &= \left\| \frac{\mathbb{F}}{(\det \mathbb{F})^{1/3}} (\det \mathbb{F})^{1/3} \right\|^p_{L^p(\Omega_R)} \\
&= \int_{\Omega_R} \left| \frac{\mathbb{F}}{(\det \mathbb{F})^{1/3}} \right|^p (\det \mathbb{F})^{p/3} dX \\
&\qquad\qquad \text{(apply Young's inequality with } \tfrac{1}{a} + \tfrac{1}{b} = 1) \\
&\leq \int_{\Omega_R} \left(2 \left| \frac{\mathbb{F}}{(\det \mathbb{F})^{1/3}} \right|^{p/2} + 2(\det \mathbb{F})^{p/6} \right) dX \qquad (a = b = \tfrac{1}{2}) \\
&= \int_{\Omega_R} \left(2 \frac{|\mathbb{F}|^2}{(\det \mathbb{F})^{2/3}} + 2(\det \mathbb{F})^{2/3} \right) dX \qquad (p = 4) \\
&\leq \frac{4}{G} I(\chi) + 6 + \int_{\Omega_R} 2(\det \mathbb{F})^{2/3} dX \\
&\leq \frac{4}{G} I(\chi) + 6 + \int_{\Omega_R} 2e^{2/3} dX \\
&\leq \frac{4}{G} I(\chi) + 6 + 2e^{2/3} |\Omega_R|
\end{aligned}
$$

Applying Poincaré's inequality will complete the proof if Dirichlet boundary conditions are applied. □

Now, having the above results about polyconvexity and 4-coercivity of the chosen stored energy function (4.52) for sclera and lens there exists a minimizer of (4.55) according to the Theorem 4.5.1.

Parameter

An elastic solid material, like the sclera, lens or cornea, undergoes a reversible deformation (the material returns to its original shape after the load is removed) when an external force is applied to it. The several quantities measuring the stiffness of these materials (resistance to being deformed elastically) are reported in Table 4.4 and are called (elastic) moduli. They all arise in the generalized Hooke's law describing the stress-strain behavior of elastic materials undergoing deformations.

All moduli describe the material's response (strain) to the stress where stress is the force causing the deformation divided by the area to which the force is applied and strain is the ratio of the change in some parameter caused by the

deformation to the original value of the parameter. A stiffer material will have a higher elastic modulus.
There are many types of elastic moduli since stress and strain can be measured in many ways including directions, but all are defined as the ratio of stress and strain. Examples are:

1. Young's modulus E:
   It describes the strain to linear stress (uniaxial deformation), i.e. the tendency to deform along an axis when opposing forces are applied along that axis.

2. The shear modulus G:
   It describes the material's response to shear stress (the deformation of shape at constant volume).

3. The bulk modulus κ:
   It describes the material's response to (uniform) hydrostatic pressure. It is a measure of how resistant to compression that material is and an extension of Young's modulus to three dimensions.

4. Poisson's ratio ν:
   It describes the response in the directions orthogonal to uniaxial stress (a measure of compressibility).

Parameter	Unit	Bovine	Human	Porcine
			Lens	
Density ρ	kg/m^3	$1.104 - 1.14 \times 10^3$ [176]	1.059×10^3 [27]	1.125×10^3 [176]
Poisson's ration ν	-		0.5 [79], 0.495 [27]	
Young's modulus E	Pa	$1.6 - 25.9 \times 10^3$ [194]		$1.2 - 5.7 \times 10^3$ [194]
Shear modulus G	Pa		$0.19 - 59.6 \times 10^3$ [189] 0.47×10^3 [27]	
Elastic bulk modulus κ	Pa		$100 \times G$ [27, 189]	
			Sclera	
Density ρ	kg/m^3	1.076×10^3 [176]	1.049×10^3 [176]	0.987×10^3[176]
thickness	m		0.6×10^3 [127]	
Poisson's ration ν	-		0.47 [183]	
Young's modulus E	Pa	$1 - 7 \times 10^6$ [114]	17×10^3 [43]	
Shear modulus G	Pa		330×10^3 [71]	
Elastic bulk modulus κ	Pa		$1000 \times G$ [71]	
			Cornea	
Density ρ	kg/m^3	$1.061 - 1.107 \times 10^3$ [176]	$1.024 - 1.087 \times 10^3$ [176]	1.062×10^3[176]
Poisson's ration ν	-		0.42 [183]	
Young's modulus E	Pa	$40 - 185 \times 10^3$ [114]	19×10^3 [43]	

Table 4.4: Material parameter values characterizing the elasticity

Homogeneous and isotropic (similar in all directions) solid materials have their (linear) elastic properties fully described by two elastic moduli and all other elastic moduli can be calculated via the following formulas [79]:

$$E = 3\kappa(1 - 2\nu),$$
$$E = 2G(1 + \nu).$$

The moduli are not independent and simple relations exist between them for homogeneous isotropic materials.

4.5.4 Numerical Simulations

The corresponding fluid-structure interaction problem was solved numerically by the finite element method. For more details of the numerical solution of the problem with the corresponding initial and boundary conditions and the numerical implementation we refer to our publication [182].
We compared the two rheological models for the vitreous in order to identify their impact on the response of the eye. The numerical results showed that the magnitude of the Cauchy stress tensor can be as much as two times higher for the pathological vitreous predicted by the Navier–Stokes model than for the healthy one predicted by the Burgers-type model in a deforming eye, see Figure 4.6. Higher stresses in the healthy vitreous damp the external mechanical load due to the elastic collagen network compared to the pathological vitreous. For visualization purposes one can see the magnitude of the Cauchy stress in the sliced vitreous in Figure 4.7. The choice of the material specific equations of the vitreous which describes its properties influences the generated stress inside the vitreous and has significant impact on the magnitude of the eigenvalues of $\mathbb{T}$ and their spatial distribution. But it has a negligible influence on the overall flow pattern in the vitreous. From the practical point of view it is of interest that the stress distribution at the fluid/solid interface is very sensitive to the choice of the rheological model of the vitreous humor since some eye pathologies such as posterior vitreous (PVD) or retinal detachment are thought to be closely linked to mechanical processes with high stresses. Incomplete PVD and the resultant vitreoretinal traction can lead to further diseases including macular holes, macular edema, vitreous hemorrhage and retinal tears. The only treatment currently available is surgical removal of the vitreous (vitrectomy) and hence it is necessary to investigate the mechanical stress distribution in the eye in realistic loading scenarios.

The presented model in [182] can be used to predict key mechanical quantities such as the complete characterization of the mechanical stress acting at

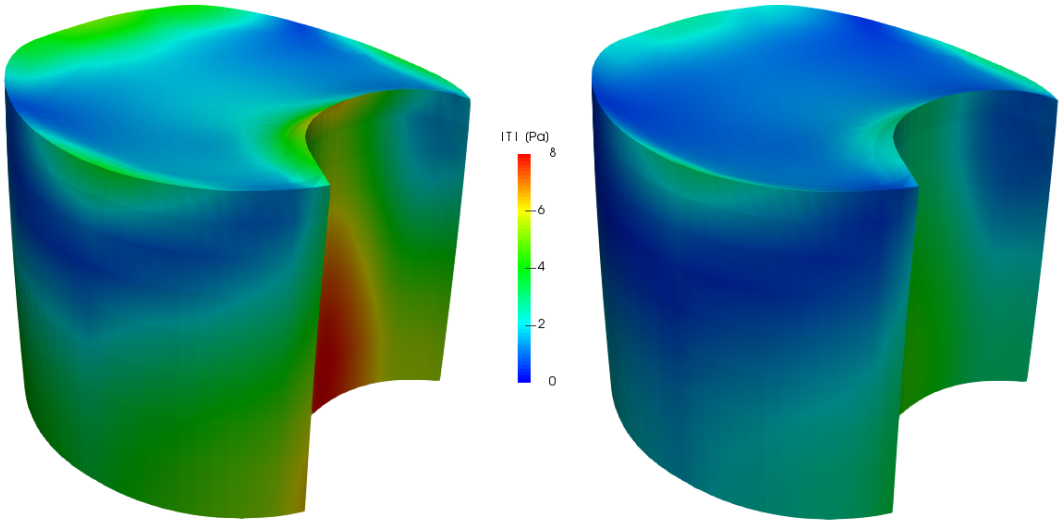

Figure 4.6: Magnitude of the Cauchy stress tensor inside the vitreous after the deformation, current configuration. Vitreous is modelled using the Burgers-type model (left) and the Navier–Stokes model (right). [Reprinted by permission from Elsevier, [182]]

the interface between the vitreous and the retina. The focus on the interplay between the rheology of the vitreous and the stress field in it is of interest in the study of retinal pathologies and can answer clinically relevant questions. Compared to cost and time intensive experiments the numerical simulations of the flow of the vitreous can be repeated as often as desired and can test different parameters in different scenarios. Additionally, the virtual experiments can reproduce the in vivo anisotropic collagen structure density where high strains corresponds with locations of lower collagen content.

4.6 Drug Distribution in Homogeneous Vitreous

To our knowledge, regarding the application of an intravitreal injection for the treatment of retinal diseases, firstly we consider the non-Newtonian nature of the vitreous body. We model the drug distribution in the healthy viscoelastic vitreous body taking into account the elastic collagen fiber network and gel-like consistency which slow down the drug diffusion compare to the completely liquefied case. As a result, the vitreous acts as a drug depot due to the lower diffusion coefficient [14]. The structure of the vitreous itself and its consistency influence the drug distribution to the posterior segment of the eye [184]. The

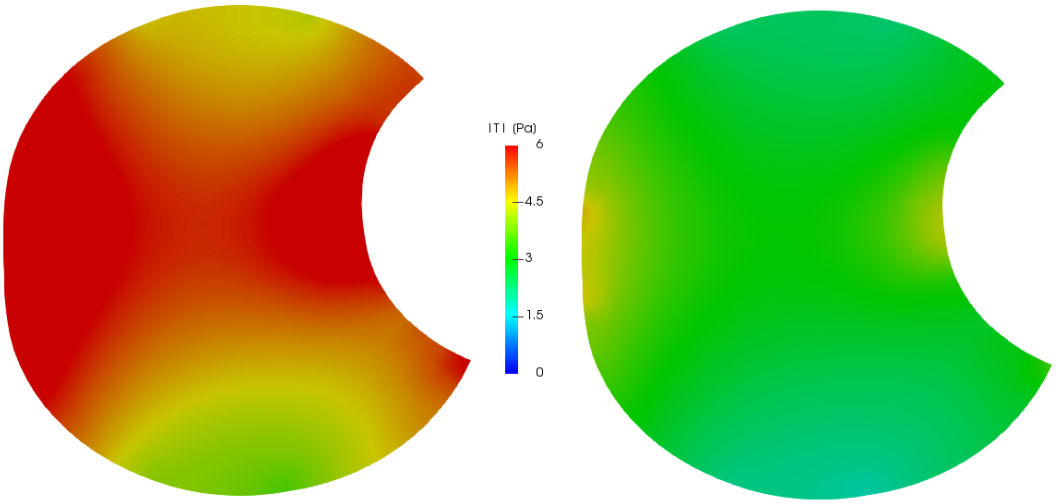

Figure 4.7: Magnitude of the Cauchy stress tensor of the cross section at the middle of the domain after the deformation, current configuration. Vitreous is modelled using the Burgers-type model (left) and the Navier–Stokes model (right). [Reprinted by permission from Elsevier,[182]]

high viscosity values for the viscoelastic vitreous affect the diffusion of intravitreal injected drugs [78].
In this Section, we demonstrate the more realistic models of drug distribution within the healthy vitreous. Afterwards, we consider different couplings of the drug diffusion equation with the induced flow field of the viscoelastic vitreous.

4.6.1 Coupling Through Convection

First, we start with the simple coupling through convection. For future works including numerical simulations, we provide the weak formulation of the system coupling the drug diffusion equation (3.17) with the Burgers-type model (4.1). The governing equations completed with the corresponding initial and boundary conditions take the following form.

We search for $(v,p) \in L^2(0,T;\{v_{\text{in}} + H_0^1(\Omega;\Gamma_{\text{D}})^d\}) \times L^2(\Omega)$ plus the unknown left Cauchy-Green tensors $\mathbb{B}_1, \mathbb{B}_2 \in L^2\left(0,T;\{\mathbb{B}_i^{\text{D}} + H_0^{1,\text{sym}}(\Omega;\Gamma_{\text{D}})^{d\times d}\}\right)$ and drug concentration $C \in L^2(0,T;H_0^1(\Omega;\Gamma_{\text{h}}))$ such that the initial conditions $v(x,0) = v_0(x), \mathbb{B}_i(x,0) = \mathbb{I}, C(x,0) = C_0(x)$ are satisfied, $v_{\text{in}} \in H^1(\Omega)^d$, $\mathbb{B}_i^{\text{D}} \in H^{1,\text{sym}}(\Omega)^{d\times d}$ for $i = 1,2$ and for almost all time steps $t \in (0,T]$ with

$T \in (0, \infty)$ it holds that

$$(\nabla \cdot v, \xi) = 0, \tag{4.61a}$$

$$\rho(\partial_t v, \phi) + \rho((v \cdot \nabla)v, \phi) + (\mathbb{T}, \nabla\phi) - (k_{\text{perm}}(v \cdot n)n, \phi)_{\Gamma_r} = 0, \tag{4.61b}$$

$$\overset{\nabla}{(\mathbb{B}_1}, \omega_1) + \frac{\mu_1}{G_1}(\mathbb{B}_1 - \mathbb{I}, \omega_1) = 0, \tag{4.61c}$$

$$\overset{\nabla}{(\mathbb{B}_2}, \omega_2) + \frac{\mu_2}{G_2}(\mathbb{B}_2 - \mathbb{I}, \omega_2) = 0, \tag{4.61d}$$

$$\left(\frac{dC}{dt}, \varphi\right) + (D\nabla C, \nabla\varphi) + (PC + (n \cdot v)(k_{vr} - 1)C, \varphi)_{\Gamma_r} = 0, \tag{4.61e}$$

for all test functions $(\phi, \xi) \in \{v_{\text{in}} + H_0^1(\Omega; \Gamma_D)^d\} \times L^2(\Omega)$ and $(\omega_i, \varphi) \in \{\mathbb{B}_i^D + H_0^{1,\text{sym}}(\Omega; \Gamma_D)^{d\times d}\} \times H_0^1(\Omega; \Gamma_h)$ with $i = 1, 2$.
The function space $H_0^{1,\text{sym}}(\Omega; \Gamma_D)^{d\times d}$ is defined as

$$H_0^{1,\text{sym}}(\Omega; \Gamma_D)^{d\times d} := \{\mathbb{B} \in H_0^1(\Omega; \Gamma_D)^{d\times d} : \mathbb{B} = \mathbb{B}^T\},$$

and $\mathbb{B}_i^D$ defined on the Dirichlet boundary $\Gamma_D := \Gamma_l \cup \Gamma_h$ is an extension to the whole domain Ω,

$$\mathbb{B}_i^D := \begin{cases} \mathbb{I} & \text{on } \Gamma_l \times (0, T] \\ \mathbb{B}_i^{\text{in}} & \text{on } \Gamma_h \times (0, T] \end{cases}, \qquad i = 1, 2.$$

By using integration by parts we get the boundary terms in the second and last equation in (4.61). According to the construction, the velocity is equal to zero at the transition of the boundaries denoting the lens Γ_l and hyaloid membrane Γ_h, hence we have a continuous transition for $\mathbb{B}_i^D$.
In the system (4.61) the flow and drug concentration can be decoupled from each other for an easier numerical implementation. If we just couple through convection, the viscoelastic structure of the vitreous has no influence on the drug distribution and vice versa. Therefore, the coupling only through convection does not seem to be appropriate since we know that the viscoelastic behavior of the healthy vitreous acts as a barrier in drug delivery [6].

4.6.2 Back Coupling Through Surface Tension

In the literature [75, 153] only the convective flow from the anterior to the posterior segment of the eye influences the drug distribution and other impacts are not included. We propose a fully coupled system extended by the Korteweg stress in which the drug diffusion and flow inside the vitreous can effect each

other. As mentioned in the Section 3.4.5 of the liquefied vitreous, surface tension can also occur in the drug distribution in the healthy viscoelastic vitreous after the intravitreal injection. The change of concentration gradients at the interface of two miscible fluids, i.e. vitreous and drug injection, causes a distributed stress during mixing. Here, the effect could be even greater compared to the Navier-Stokes model (3.28) since the diffusion is slower due to the smaller diffusion coefficient in the healthy viscoelastic vitreous. In [131, 165] they investigated the surface tension in processes involving diffusion across interfaces between miscible fluids in which one of them is a non-Newtonian fluid, a viscoelastic fluid described by the Maxwell model. So we take into account some additional terms in the equation of motion due to the concentration inhomogeneities called Korteweg stress which is associated with surface tension.

Under the same assumptions as for the liquefied case, the problem reads:

$$\nabla \cdot v = 0, \tag{4.62a}$$

$$\rho \left(\frac{\partial v}{\partial t} + (v \cdot \nabla) v \right) = \nabla \cdot \mathbb{T}, \tag{4.62b}$$

$$-p\mathbb{I} + 2\mu_3 \mathbb{D} + G_1(\mathbb{B}_1 - \mathbb{I}) + G_2(\mathbb{B}_2 - \mathbb{I}) + T(C) = \mathbb{T}, \tag{4.62c}$$

$$-\frac{G_1}{\mu_1}(\mathbb{B}_1 - \mathbb{I}) = \overset{\nabla}{\mathbb{B}}_1, \tag{4.62d}$$

$$-\frac{G_2}{\mu_2}(\mathbb{B}_2 - \mathbb{I}) = \overset{\nabla}{\mathbb{B}}_2, \tag{4.62e}$$

$$\frac{\partial C}{\partial t} + (v \cdot \nabla) C - \nabla \cdot (D \nabla C) = 0, \tag{4.62f}$$

with the Korteweg stress $T(C)$ defined in (3.29) and the parameter $k_{\text{kor}} > 0$. The system (4.62) is completed by the appropriate initial and boundary conditions defined in the previous sections for the diffusion (3.17) and Burgers-type model (4.1). An example for the coupling of the Korteweg stress with a viscoleastic rate-type model is mentioned in [90], where the author describes the relaxation of stresses due to gradients of composition (concentration) to the Korteweg stresses using the viscoelastic Maxwell model. In the fluid dynamics of mixtures of incompressible miscible liquids motions can be driven by additional stresses associated with gradients of composition, which are modeled by the theory of Korteweg.

In this thesis, we do not work on the mathematical theory for the developed

model (4.62). It is not analyzed in the literature and known results about existence and uniqueness are proved only for the case of the Navier-Stokes equation (3.28) by Kostin et al. [98], as presented in Section 3.4.5 for the interested reader. Yet theoretically, the same trick that the Korteweg stress tensor and terms from the convection-diffusion equation cancel each other out could be applied for the healthy viscoelastic vitreous modeled by the Burgers-type model, since the same needed terms from (3.28) are present in (4.62). Then assuming the existence of the flow in 2D and considering the same boundary conditions, the a priori estimation could be shown [98].

4.6.3 Back Coupling Through Stress Driven Diffusion

Another aspect in the drug distribution in the healthy viscoelastic vitreous and third way to couple the diffusion equation with the induced flow field of the viscoelastic vitreous is the so-called stress driven diffusion, compared to the previous Section 4.6.1 of coupling only through the convection. The human vitreous can be seen as a natural polymer [159] and synthetic polymers are used as current available vitreous substitutes [96]. From experimental and theoretical studies in the literature [45, 46, 186] it is known that the diffusion of a penetrant liquid through polymer does not follow the standard Fickian diffusion model and is described by stress driven diffusion. Therefore, the diffusion through the viscoelastic vitreous does not obey Fick's law and we have to consider the influence of the mechanical property of the vitreous on the distribution rate of the drug by adding one term to the diffusion equation (3.17). Due to the elastic collagen network within the vitreous it acts as a barrier to the diffusion [6, 184]. As the medicine strains the vitreous by the Brownian motion of diffusion, the viscoelastic vitreous reacts with a stress of opposite sign [51, 72].
Several authors have studied mathematical models to describe transport of drugs in biodegradable implants/polymers [11, 52, 69, 54]. The viscoelastic behavior of the implant/polymer is defined by the Maxwell model. But the diffusion of drug through the viscoelastic vitreous, modeled by the Burgers-type fluid, including non-Fickian contribution has not yet been addressed in the literature. We use the more complicated viscoelastic Burgers-type model which characterizes adequate properties of the vitreous, compare to the simpler Maxwell model. As a result, we extend the existing approach of drug transport in implants with new boundary conditions capable of modeling the drug exchange with the surrounding tissues of the vitreous. Further, we introduce a possible generalization to three space dimensions including the Cauchy stress tensor and a three-dimensional assumption for the relation be-

tween deformation and stress. Using the balance equations for mass (2.4) and linear momentum (2.5) containing the Cauchy stress, the governing equations for the description of the velocity are given and we are also able to add the convection part to the drug diffusion. In this section, we will propose a system of coupled partial differential equations which considers passive, stress driven diffusion and the viscoelastic vitreous' properties to simulate the evolution of drug distribution injected into the posterior part of the eye.

We start with the simpler one-dimensional viscoelastic model. The transport phenomena by diffusion are classically described by Fick's law but it does not take into consideration the viscoelastic nature of the vitreous. As the diffusing drug enters the vitreous, it causes a deformation which induces a stress driven diffusion that act as a barrier to the drug penetration. Thus Azdhari et al. [10, 11, 12] have proposed diffusion models based on a modified flux, where diffusive and mechanical properties are coupled.
Let us recall from the Section 3.4 that the Fickian diffusion of the penetrating drug injection is described by the conservation law:

$$\partial_t C = -\nabla \cdot J,$$

with the difference that $J = J_F + J_{NF}$ is the modified flux resulting from the sum of the Fickian flux $J_F := -D\nabla C$ and non-Fickian flux $J_{NF} := -D_v \nabla \sigma$ denoting the viscoelastic influence in the drug transport. $D_v > 0$ stands for the so-called viscoelastic diffusion coefficient and σ represents the one-space-dimensional stress. σ is related with the strain ϵ by the spring/dashpot analogue of viscoelastic Burgers-type model (4.6) illustrated in Figure 4.1, describing the mechanistic behavior of the vitreous. For further manipulation it is preferable to rewrite the stress-strain relation (4.6) considering the Burgers-type model as a combination of one dashpot and two Maxwell elements in parallel:

$$\sigma = \mu_3 \frac{d\epsilon}{dt} + \sigma_1 + \sigma_2, \tag{4.63a}$$

$$\sigma_1 + \frac{\mu_1}{G_1}\frac{d\sigma_1}{dt} = \mu_1 \frac{d\epsilon}{dt}, \tag{4.63b}$$

$$\sigma_2 + \frac{\mu_2}{G_2}\frac{d\sigma_2}{dt} = \mu_2 \frac{d\epsilon}{dt}, \tag{4.63c}$$

where the total stress is a sum of the stress in the dashpot, i.e. $\mu_3 \frac{d\epsilon}{dt}$, and the two Maxwell elements σ_1, σ_2. The Parameters are the same as before. For more information about the spring/dashpot analogue of viscoelastic Maxwell element see [181].

Summarized, the drug diffusion through the viscoelastic vitreous Ω during the time $t \in (0, T]$ is described by the following model:

$$\sigma = \mu_3 \frac{d\epsilon}{dt} + \sigma_1 + \sigma_2, \tag{4.64a}$$

$$\sigma_1 + \frac{\mu_1}{G_1}\frac{d\sigma_1}{dt} = \mu_1 \frac{d\epsilon}{dt}, \tag{4.64b}$$

$$\sigma_2 + \frac{\mu_2}{G_2}\frac{d\sigma_2}{dt} = \mu_2 \frac{d\epsilon}{dt}, \tag{4.64c}$$

$$\frac{\partial C}{\partial t} - \nabla \cdot (D\nabla C + D_v \nabla \sigma) = 0 \tag{4.64d}$$

in $\Omega \times (0, T]$ where C represents the unknown concentration of drug inside the vitreous and σ is the unknown stress. Since we have no description for the velocity here, we use the diffusion equation (3.17) without the convection term. System (4.64) is completed with the initial conditions

$$\begin{aligned} C &= C_0 && \text{on } \Omega \times \{t = 0\}, \\ \sigma &= \sigma_0 && \text{on } \Omega \times \{t = 0\} \end{aligned}$$

and boundary conditions

$$\begin{aligned} (D\nabla C) \cdot n &= 0 && \text{on } \Gamma_l \times (0, T], \\ C &= 0 && \text{on } \Gamma_h \times (0, T], \\ -(D\nabla C) \cdot n - PC + (n \cdot v)(1 - k_{vr})C &= 0 && \text{on } \Gamma_r \times (0, T], \\ \mu_3 \delta_0 \frac{1}{G_1 + G_2}\sigma_0 + \frac{1}{G_1 + G_2}\sigma_0 \left(c_1 e^{\lambda_1 t} + c_2 e^{\lambda_2 t}\right) &= \sigma && \text{on } \partial\Omega \times (0, T], \end{aligned}$$

where δ_0 stands for the Dirac distribution and the coefficients are defined as

$$\begin{aligned} \lambda_1 &:= \frac{-\tau_1 - \tau_2 + \sqrt{(\tau_1 + \tau_2)^2 - 4\tau_1\tau_2}}{2}, \\ \lambda_2 &:= \frac{-\tau_1 - \tau_2 - \sqrt{(\tau_1 + \tau_2)^2 - 4\tau_1\tau_2}}{2}, \\ c_1 &:= \frac{\mu_2\tau_1 + \mu_1\tau_2}{\tau_1\tau_2} - c_2, \\ c_2 &:= \frac{(\mu_1 + \mu_2)\tau_1\tau_2 - (\tau_1 + \tau_2)(\mu_2\tau_1 + \mu_1\tau_2) - \lambda_1(\mu_2\tau_1 + \mu_1\tau_2)\tau_1\tau_2}{\tau_1^2\tau_2^2(\lambda_2 - \lambda_1)}. \end{aligned}$$

The boundary condition for σ has been obtained by extending the solution of (4.63) analog to [12] using the Maxwell model, see [181] for details to the Burgers model. The stress decreases going to zero as the time increases, since $\lambda_2 \leq \lambda_1 < 0$. The stress driven diffusion (4.64d) is valid for small deformations and used in the literature [11, 54]. But the thermodynamic derivation of the model and its stability of the rest state are not proven.

In the following paragraphs, we investigate in more detail the viscoelastic diffusion coefficient D_v and present the relation between deformation and concentration. Furthermore, we give an overview about the restrictions on the parameters D, D_v etc., which are needed to guarantee the uniqueness of the solution and its stability in bounded time intervals. At the end, we generalize the introduced approach to a possible three-dimensional description.

Viscoelastic Diffusion Coefficient

The physical meaning of the diffusion coefficient D in (3.17) and (4.64d) is well known and its behavior can be described by many different functional relations as explained in Section 3.4.1. The viscoelastic diffusion coefficient D_v has not been clearly studied. Even its sign is not certain throughout the literature. The authors of [115, 57] consider D_v to be constant and negative while in [45, 69] it is assumed to be a positive parameter. Ferreira et al. [12, 13] set the coefficient to be $D_v = 1 \times 10^{-11}$ mol m^{-1} Pa^{-1} s^{-1} in the context of a diffusing drug through the viscoelastic implant which is used in the vitreous body to release drug to the retina. The corresponding diffusion coefficient of the drug in the implant is defined by $D_1 = 1 \times 10^{-11}$ m^2 s^{-1}, whereas the diffusion coefficient in the vitreous is defined by $D_2 = 1 \times 10^{-8}$ m^2 s^{-1}. The considered drug is not specified. The findings in [12] show that the viscoelastic properties of the polymeric implant are an effective control mechanism to delay or to speed up the release of drug. Further, analog to D the viscoelastic diffusion coefficient D_v can either be seen as a constant or a tensor by multiplying the constant value with the identity matrix [12, 13].
In [51] a concentration dependent expression for $D_v(C)$ based on Darcy's law is established. Assuming the existence of a stress gradient and interpreting the non-Fickian flux as a convective field induced by the stress where the velocity follows Darcy's law they conclude that

$$D_v(C) = \frac{K}{\mu} C \tag{4.65}$$

where $\frac{K}{\mu}$ is the hydraulic conductivity. In virtue of (4.65) they conclude that the parameter D_v is positive and thus the non-Fickian flux represents a contribution

to the mass flux which develops from high to low stress [45, 51, 69]. Applying the assumption (4.65) to our problem considering the parameters defined in the Table 5.1, we see that $D_v(C) \leq 7.86 \times 10^{-9}$ kg m^{-1} Pa^{-1} s^{-1}, with our specific initial concentration C_0 introduced in (3.19) and the relation $C \leq C_0 \leq 93.56$ kg m^{-3}. For comparison, the diffusion coefficient for the drug through the healthy vitreous is of order 10^{-11}.

Relation Between Deformation and Concentration

Following [51] the strain ϵ must be eliminated as a variable in (4.63) for a plausible back-coupling. Therefore one considers a nonlinear functional relation between strain and concentration,

$$\epsilon = f(C)$$

where f is assumed regular enough for the mathematical analysis and is based on physical arguments, briefly described below. We refer the interested reader to [51].
For a sake of simplicity, we consider a cylindrical dry vitreous sample (no drug absorbed) with cross section S and volume V_0. We assume that the deformation ϵ occurs only in a orthogonal direction to S as shown in Figure 4.8. As the

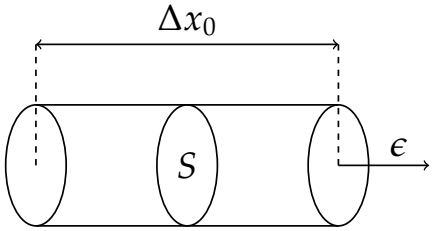

Figure 4.8: Cylindrical vitreous sample

deformation occurs orthogonally to S, it leads to the following expression

$$\epsilon = \frac{\frac{V_0+V_d}{S} - \frac{V_0}{S}}{\frac{V_0}{S}} = \frac{V_d}{V_0}$$

where V_d is the volume of drug absorbed by the vitreous up to time t. Using the fact that $V_d = \frac{m}{\rho_p}$ and $C = \frac{m}{V_0+V_d}$ with m and ρ_p representing the drug mass and density [51], it follows that

$$\epsilon = f(C) = \frac{C}{\rho_p - C} \tag{4.66}$$

under the reasonable hypothesis that the mixing of the vitreous and the injected drug occurs in an ideal manner. Then the final volume is $V_0 + V_d$ which means that when in contact with the penetrate drug an instantaneous swelling occurs. Some authors [10] use the linear approximation $f(C) = kC$ of the approach above, where $k > 0$ stands for a dimensional positive constant. Figure 4.9 with $\rho_p = k = 1.5$ shows that $f(C)$ in (4.66) and kC are increasing positive functions of the concentration where ρ_p or respectively k influence the slope. Thus, in the context of physically meaningful values of $C \geq 0$ the function f is smooth. In

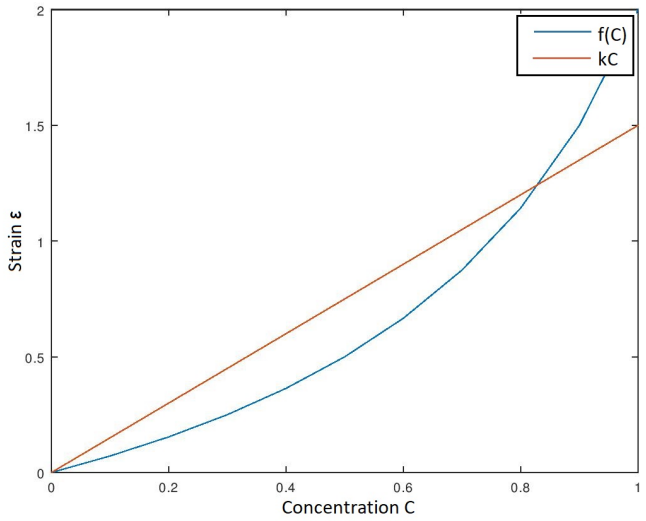

Figure 4.9: Behavior of the function describing the strain

[11, 12, 45] they assume that the strain and the concentration are proportional such that

$$\epsilon = k \int_0^t C(x, s) \mathrm{d}s. \tag{4.67}$$

This relation (4.67) is another linear approximation of $\epsilon = f(C)$ in (4.66). σ and ϵ have opposite sign, since the vitreous acts as a barrier to the distribution of the drug. Replacing (4.67) in (4.64) and considering the minus sign in the right

hand side, we obtain:

$$\sigma = -\mu_3 kC + \sigma_1 + \sigma_2, \tag{4.68a}$$

$$\sigma_1 + \frac{\mu_1}{G_1}\frac{d\sigma_1}{dt} = -\mu_1 kC, \tag{4.68b}$$

$$\sigma_2 + \frac{\mu_2}{G_2}\frac{d\sigma_2}{dt} = -\mu_2 kC, \tag{4.68c}$$

$$\frac{\partial C}{\partial t} - \nabla \cdot (D\nabla C + D_v \nabla \sigma) = 0. \tag{4.68d}$$

Restrictions on the Parameters

Reviewing the literature, in [12] they analyzed the stability behavior of the following initial value problem:

$$\sigma + \frac{\mu_1}{G_1}\frac{d\sigma}{dt} = -\mu_1 kC \qquad \text{in } \Omega \times (0,T], \tag{4.69a}$$

$$\frac{\partial C}{\partial t} - \nabla \cdot (D(M)\nabla C + D_v \nabla \sigma) = -k_1 C \qquad \text{in } \Omega \times (0,T], \tag{4.69b}$$

$$\frac{\partial M}{\partial t} + \beta_1 M = \beta_2 C \qquad \text{in } \Omega \times (0,T], \tag{4.69c}$$

$$C = C_0 \qquad \text{on } \Omega \times \{t = 0\}, \tag{4.69d}$$

$$\sigma = \sigma_0 \qquad \text{on } \Omega \times \{t = 0\}, \tag{4.69e}$$

$$M = M_0 \qquad \text{on } \Omega \times \{t = 0\}, \tag{4.69f}$$

$$C = 0 \qquad \text{on } \partial\Omega \times (0,T], \tag{4.69g}$$

$$\sigma = \sigma_0 e^{-\frac{G_1}{\mu_1}t} \qquad \text{on } \partial\Omega \times (0,T], \tag{4.69h}$$

$$M = M_0 e^{-\frac{G_1}{\beta_1}t} \qquad \text{on } \partial\Omega \times (0,T], \tag{4.69i}$$

with diffusion D and viscoelastic diffusion D_v, which are 2×2 tensors. M is the unknown molecular weight of the considered material in [12], β_1 and β_2 are positive constants and k_1 represents the degradation rate. They used the Maxwell model instead of Burgers-type model for characterizing the viscoelastic properties ($G_2 = \mu_2 = \mu_3 = 0$) and completed the governing equations with homogeneous Dirichlet boundary conditions for the concentration.
By imposing strong conditions on the parameters the energy estimates lead to the uniqueness of the solution of the corresponding variational problem and its stability in bounded time intervals, provided that the initial data are smooth enough.
As the model in [12] is nonlinear, their study is based on a local linearization

in the neighborhood of the steady state solutions for short and large times. The results were established under the assumption that D, D_v are non-zero diagonal matrices where the entries of the diffusion tensor has to be positive

$$D_{ii} \geq \overline{D} > 0, \qquad i = 1, 2$$

and the entries of the viscoelastic diffusion tensor are bounded from above

$$|(D_v)_{ii}| \leq \overline{D}_v, \qquad i = 1, 2.$$

The restrictions on the parameters D, D_v, k and the material parameters G_1, μ_1 denoting the viscoelasticity such that

$$\overline{D} - \overline{D}_v^2 G_1 k - \frac{\mu_1^2 k}{4G_1} > 0$$

are a reasonable assumption. Indeed, from the physical point of view it means that the Fickian contribution in diffusion (4.64d) dominates the non-Fickian one, because otherwise it would lead to a negative total flux. This is a physically sound restriction due to the interpretation of vitreous' viscoelasticity, which represents a barrier to the penetration of drug.

Possible extension to 3D

In all the works in the literature [12, 10, 11, 51, 72] the authors only use the simplified one-dimensional viscoelastic model. In this section we generalize their approach to a possible three-dimensional description and apply the viscoelastic Burgers-type model to characterize the behavior of the vitreous, where we replace the 1D stress σ and its components σ_1 and σ_2 by the extra part of the 3D Cauchy stress tensor $\mathbb{S} := \mathbb{T} + p\mathbb{I}$ and its components $\mathbb{S}_1$ and $\mathbb{S}_2$. First, we look at the model without back-coupling between deformation and concentration. We consider the three-dimensional generalization of (4.64). In $\Omega \times (0, T]$ it holds that

$$\nabla \cdot v = 0, \tag{4.70a}$$

$$\rho \left(\frac{\partial v}{\partial t} + (v \cdot \nabla) v \right) = \nabla \cdot \mathbb{T}, \tag{4.70b}$$

$$-p\mathbb{I} + 2\mu_3 \mathbb{D} + \mathbb{S}_1 + \mathbb{S}_2 = \mathbb{T}, \tag{4.70c}$$

$$\mathbb{S}_1 + \frac{\mu_1}{G_1} \overset{\nabla}{\mathbb{S}}_1 = 2\mu_1 \mathbb{D}, \tag{4.70d}$$

$$\mathbb{S}_2 + \frac{\mu_2}{G_2} \overset{\nabla}{\mathbb{S}}_2 = 2\mu_2 \mathbb{D}, \tag{4.70e}$$

$$\frac{\partial C}{\partial t} + (v \cdot \nabla) C = \nabla \cdot (D \nabla C + D_v \nabla \cdot \mathbb{S}). \tag{4.70f}$$

Since the Newtonian Navier-Stokes fluid with $\mathbb{S} = 2\mu_0\mathbb{D}$ has no elastic properties and therefore should show no stress driven diffusion effect in the drug distribution,

$$\nabla \cdot (D_v \nabla \cdot \mathbb{S}) = 0,$$

the three-dimensional space generalization of $\nabla\sigma$ should be interpreted as the divergence of the traceless extra part of the Cauchy stress, namely $\nabla \cdot \mathbb{S}$. Due to the full description of the velocity we can add the convection term to the last equation in (4.70) and therefore insert the balance equations for mass and linear momentum.
Second, we transfer the 1D assumption (4.67) of Ferreira [11] into a possible 3D extension. By taking the time derivative of (4.67) it can be rewritten into

$$\frac{d\epsilon}{dt} = kC. \tag{4.71}$$

The common generalization of $\frac{d\epsilon}{dt}$ is $2\mathbb{D}$ as introduced in Section 4.2.1, motivated by the simple shear flow. Then we can set

$$2\mathbb{D} = kC\mathbb{M} \tag{4.72}$$

with the tensor $\mathbb{M} \in \mathbb{R}^{d\times d}$ defined by (4.72) which describes a dimensionless quantity. Finally, a possible generalization of the drug diffusion through the viscoelastic vitreous into 3D of the full coupled system (4.68) is described by the following system of partial differential equations:

$$\nabla \cdot v = 0, \tag{4.73a}$$

$$\rho\left(\frac{\partial v}{\partial t} + (v \cdot \nabla)v\right) = \nabla \cdot \mathbb{T}, \tag{4.73b}$$

$$-p\mathbb{I} - \mu_3 kC\mathbb{M} + \mathbb{S}_1 + \mathbb{S}_2 = \mathbb{T}, \tag{4.73c}$$

$$\mathbb{S}_1 + \frac{\mu_1}{G_1}\overset{\nabla}{\mathbb{S}}_1 = -\mu_1 kC\mathbb{M}, \tag{4.73d}$$

$$\mathbb{S}_2 + \frac{\mu_2}{G_2}\overset{\nabla}{\mathbb{S}}_2 = -\mu_2 kC\mathbb{M}, \tag{4.73e}$$

$$\frac{\partial C}{\partial t} + (v \cdot \nabla)C = \nabla \cdot (D\nabla C + D_v \nabla \cdot \mathbb{S}). \tag{4.73f}$$

Now, we see the reason for the further manipulation of the one-dimensional Burgers-type model (4.6) into (4.63) and its three-dimensional generalization in (4.70). It was necessary to use a viscoelastic model which includes only the first time derivative of the strain in 1D or rather no time derivative of the symmetric part of the velocity gradient $\mathbb{D}$ in 3D to implement the assumption

(4.67) respectively (4.72) in a straight forward way.

If we consider a simplified flow model problem in a channel geometry with Poiseuille velocity profile $v = (\tilde{v}(y,z), 0, 0)$, then the symmetric part of the velocity gradient $\mathbb{D}$ has the following specific form,

$$2\mathbb{D} = \begin{pmatrix} 2\partial_x v_x & \partial_x v_y + \partial_y v_x & \partial_x v_z + \partial_z v_x \\ \partial_x v_y + \partial_y v_x & 2\partial_y v_y & \partial_y v_z + \partial_z v_y \\ \partial_x v_z + \partial_z v_x & \partial_y v_z + \partial_z v_y & 2\partial_z v_z \end{pmatrix} = \begin{pmatrix} 0 & \partial_y v_x & \partial_z v_x \\ \partial_y v_x & 0 & 0 \\ \partial_z v_x & 0 & 0 \end{pmatrix},$$

and we can define the tensor $\mathbb{M}$ in (4.72), i.e.

$$\mathbb{M} := \begin{pmatrix} 0 & 1 & 1 \\ 1 & 0 & 0 \\ 1 & 0 & 0 \end{pmatrix},$$

such that $2\mathbb{D}_{ij} = kC$ for all $i, j = \{1, 2, 3\}$ with $\mathbb{D}_{ij} \neq 0$ according to the 1D assumption (4.71). Since we have $\operatorname{tr} \mathbb{M} = 0$ it holds that

$$2(\operatorname{tr} \mathbb{D}) = kC(\operatorname{tr} \mathbb{M}) = 0$$

and the incompressibility constraint (2.12) is fullfilled.

Since we have the second-order space derivatives of $\mathbb{S}$ in the stress driven diffusion equation (4.70f), the system (4.70) needs additional boundary conditions for the extra stress tensor. Several issues like the specific definition of these boundary conditions and the thermodynamic derivation of (4.70f) and for the one-dimensional case (4.64d) must be addressed in the future.

Existence and Uniqueness

Looking at the modeling of the drug transport coupled with the viscoelastic Burgers-type flow including stress driven diffusion (4.68) there are no theoretical results known in the literature, due to the issues about the flow mentioned before and our complex boundary conditions. But as mentioned in the section about the restrictions on the parameters, for simpler models like the Maxwell model describing the viscoelasticity, the uniqueness of the solution of the corresponding variational problem (4.69) and its stability in bounded time intervals, provided that the initial data are smooth enough, are shown in [12]. In contrast to the Burgers-type model the 1D mechanical analog for the Maxwell model consists of only one spring and one dashpot in series, consequently

$G_2 = \mu_2 = \mu_3 = 0$ in the Figure 4.1.
Concerning the existence of the one-dimensional stress driven diffusion there is one result in [72] using the generalized Maxwell-Wiechert model with homogeneous Dirichlet boundary conditions,

$$\begin{aligned}
-\int_0^t G_1(t-s)\frac{\partial \epsilon}{\partial s}(s)ds &= \sigma(t) && \text{in } \Omega \times (0,T],\\
\epsilon &= f(C) && \text{in } \Omega \times (0,T],\\
\frac{\partial C}{\partial t} - \nabla \cdot (D\nabla C + D_v \nabla \sigma) &= 0 && \text{in } \Omega \times (0,T],\\
C &= C_0 && \text{on } \Omega \times \{t=0\},\\
C &= 0 && \text{on } \partial\Omega \times (0,T],
\end{aligned}$$

where f is assumed regular enough for the mathematical analysis [72]. They used the outcomes in [68] for the nonlinear Cauchy problem to show the existence and uniqueness of the weak solution under several conditions.

4.7 Heterogeneous Vitreous

As addressed in the biological background 2.1.5 the healthy vitreous body can be considered as an anisotropic fluid due to the network of collagen fibers.
In this Section, we extend the stress driven diffusion to an anisotropic ansatz taking into account the heterogeneous structure of collagen fibers which have a certain orientation in the vitreous body. Depending on the size of the drug the structure of the vitreous can influence drug diffusion and reflect an anisotropic diffusion. Then we further improve the viscoelastic constitutive equation (4.1) for the vitreous which is isotropic with regard to its viscous as well as its elastic response. Indeed, we extend it to an anisotropic viscoelastic fluid model considering the preferred direction of the elastic collagen fibers.

4.7.1 Anisotropic Drug Distribution Along Collagen Fibers

All existing diffusion models of previous investigations [10, 11, 12] assumed that the diffusion is homogeneous and therefore the 1D stress driven diffusion (4.68d) is isotropic, i.e. dealing with a constant stress driven diffusion coefficient D_v. We extend it to an anisotropic ansatz taking into account the heterogeneous collagen structure of the vitreous which is observed in experiments on autopsy eyes [159]. By using the space-dependent anisotropic tensor $\tilde{D}_v(x)$ instead of the constant coefficient D_v in the stress driven diffusion equation

(4.68d) and (4.73f) we obtain the following anisotropic diffusion equations

$$\frac{\partial C}{\partial t} - \nabla \cdot \left(D \nabla C + \tilde{D}_v(x) \nabla \sigma \right) = 0 \qquad \text{in 1D,} \qquad (4.74a)$$

$$\frac{\partial C}{\partial t} + (v \cdot \nabla) C - \nabla \cdot \left(D \nabla C + \tilde{D}_v(x) \nabla \cdot (\mathbb{T} + p\mathbb{I}) \right) = 0 \qquad \text{in 3D.} \qquad (4.74b)$$

It includes the certain orientation of the collagen fibers and reflects the tendency that the vitreous opposes a resistance to the diffusion of drug molecules. Along the preferential direction of the fibers there is the stress response to the strain induced by the drug molecules, as opposed to isotropic diffusion, which means homogeneity in all directions. Therefore, it presents a more accurate model for the drug distribution in the healthy vitreous than any in the literature.
The anisotropic tensor $\tilde{D}_v(x)$ has privileged orientations along the collagen fibers and the resulting stress driven diffusion develops from high to low stress. Inspired by Dal et al. [31] modeling the application of electrical stimulation of cardiac tissues with curving fibers by anisotropic diffusion-reaction equations, the space-dependent anisotropic tensor takes the form,

$$\tilde{D}_v(x) := D_v \left[d_{\parallel} (f \otimes f) + d_{\perp} (\mathbb{I} - f \otimes f) \right]. \qquad (4.75)$$

$D_v > 0$ denotes the stress driven diffusion coefficient and $d_{\parallel} \geq d_{\perp} > 0$ are the extra two parameters, which describe the stress driven diffusion along the fiber direction and orthogonal plane to it, respectively. $f = (cos(\theta), sin(\theta), 0)^T$ stands for the fiber direction vector and $\theta(x)$ denotes the fiber orientation angle, i.e. the angle between fiber direction and x-axis. The tensor product of two vectors a and b is denoted by $a \otimes b := ab^T$.
Further, $\tilde{D}_v(x)$ can be decomposed into an isotropic and anisotropic component:

$$\tilde{D}_v(x) = D_v d_{\perp} \mathbb{I} + D_v (d_{\parallel} - d_{\perp})(f \otimes f).$$

For the special case of perfect isotropic diffusion the off-diagonal elements are all zero. The diagonal elements are all the same and equal the single stress driven diffusion coefficient, D_v, which means

$$\tilde{D}_v(x) = D_v \mathbb{I}$$

with $d_{\perp} = d_{\parallel}$. Now, the task is to prescribe the fiber direction f closely to the observed structure of the bundles of collagen fibers inside the human vitreous, which is generally coursed in an anterior-posterior direction. Anteriorly, these fibers arise from the basal vitreous and insert posteriorly into the retina. Step by step we construct the appropriate f to mimic the known course. Figure 4.13 shows the resulted structure of the orientation of the fibers, which is in

agreement with results from the literature [67]. The construction is based on the structure of the angle θ which has the following form

$$\theta = -sin(p_x(x))sin(p_y(y))$$

with

$$p_x(x) = 0.5\frac{\pi(2x - x_{max} - x_{min})}{x_{max} - x_{min}} \quad \text{and} \quad p_y(y) = 0.5\frac{\pi y}{y_{max}}$$

where

$p_x(x_{min}) = -0.5\pi, \quad p_x(x_{max}) = 0.5\pi, \quad p_y(y_{min}) = -0.5\pi, \quad p_y(y_{max}) = 0.5\pi,$
$x_{min} \leq x \leq x_{max}$ and $y_{min} \leq y \leq y_{max}$

for all $(x, y) \in \Omega$. The resulting two-dimensional fiber directions $f = (\cos\theta, \sin\theta)^T$ are shown in Figure 4.10 where the red line denotes the two-dimensional vitreous domain. In the next step, we split the domain in two subdomains along

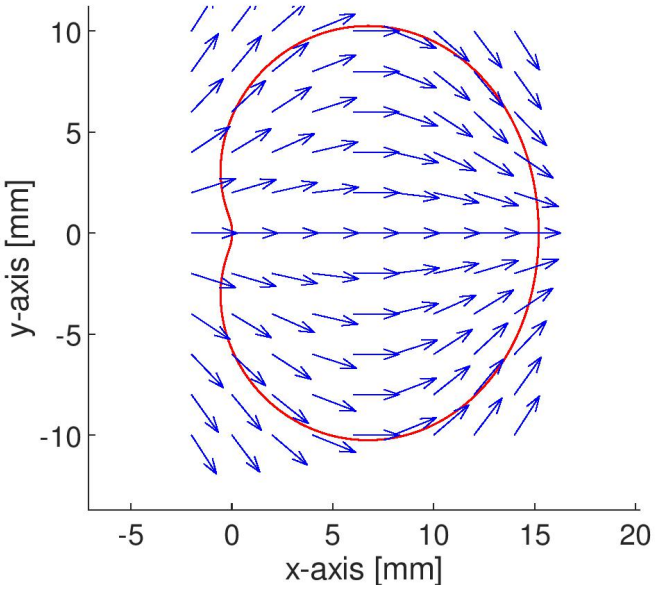

Figure 4.10: 2D structure of the collagen fibers direction

the x-axis,

$$\Omega_{\text{up}} := \{w \in \Omega : \, y > 0\}, \qquad \Omega_{\text{down}} := \Omega \setminus \Omega_{\text{up}},$$

and rotate the fiber direction f about $+15^\circ$ for coordinates inside the subdomain Ω_{down} and about -15° for Ω_{up}, which is illustrated in Figure 4.11. By

splitting and rotating we mimic the theoretical structure of the collagen fiber network in the human vitreous shown in [67].

Finally, we rotate the constructed 2D-surface in the xy-plane to get a 3D-

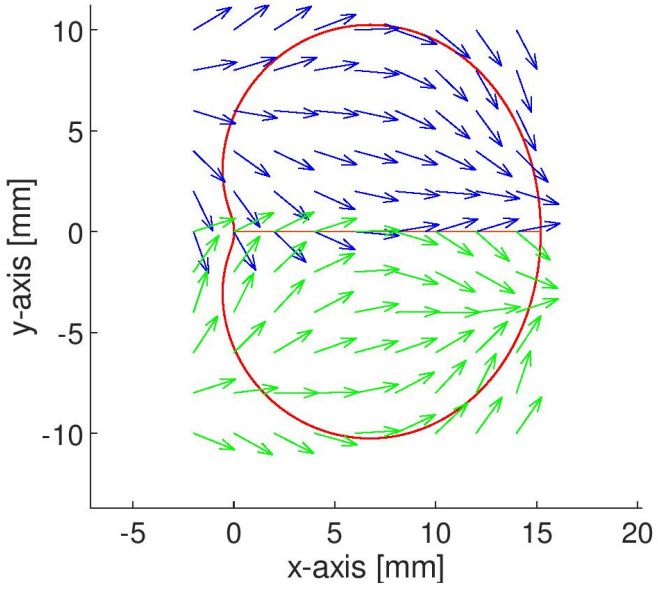

Figure 4.11: 2D structure of the collagen fibers direction in splitted domain

volume with the rotation matrix

$$R_\varphi := \begin{pmatrix} 1 & 0 & 0 \\ 0 & \cos\varphi & -\sin\varphi \\ 0 & \sin\varphi & \cos\varphi \end{pmatrix}$$

around the x-axis with the angle $\varphi = acos\left(\frac{(x^2+y^2)^{\frac{1}{2}}}{(x^2+y^2+z^2)^{\frac{1}{2}}}\right)$ and interpret the fiber direction as $f := (\cos\theta, \sin\theta, 0)^T$.

The Figure 2 in [67] presents a theoretical diagram showing the orientation of collagen fibrils within the vitreous. For an even more realistic structure according to this diagram one can split the 2D domain in Figure 4.10 not along the x-axis but along the line between the center of the boundary of the lens and the optic nerve, see Figure 4.12.

The resulting collagen bundle orientation in the numerical simulation is shown in Figure 4.13. It shows a qualitative good accordance to the theoretical diagram in [67] demonstrating a collagen bundle orientation in the vitreous. Further,

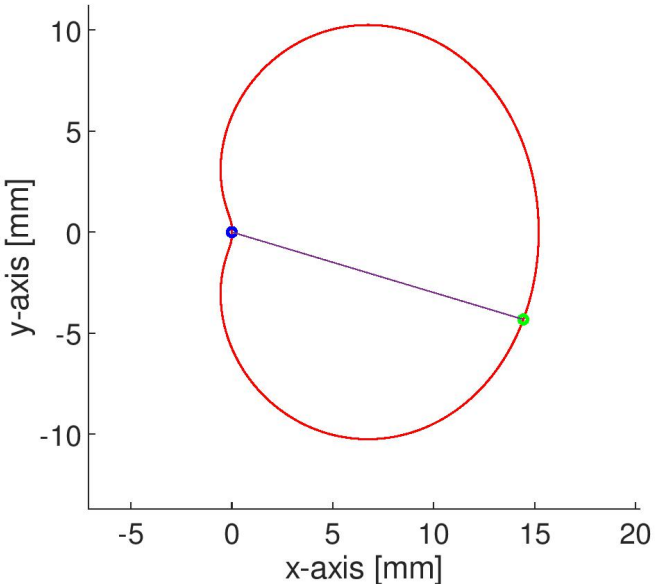

Figure 4.12: 2D vitreous domain (red), location of the center of the boundary of the lens (blue) and optic nerve (green)

the diagram is only a schematic drawing and not an exact illustration of reality, since the vitreous and its structure are not visible without any coloring and microscopic visualization. This approach of the anisotropic diffusion tensor (4.75) can be mainly used for large drug molecules and nanoparticles, since the average pore diameter in the collagen network is 95 nm for human vitreous bodies [162]. But the pore size in the central vitreous can vary from 500 nm to over 1 μm according to experiments in [193]. Besides anti-VEGF drugs for the treatment of aged-related macular degeneration, the equations (4.74) can be adopted to other large drug molecules.

Properties of the Anisotropic Tensor

The constructed anisotropic stress driven diffusion tensor $\tilde{D}_v(x)$ defined in (4.75) is symmetric and positive definite. For this purpose, we need to show that the eigenvalues are real and positive by constructing the characteristic polynom to each eigenvalue and compute the roots. Then, we get that the eigenvalues for $\tilde{D}_v(x)$ are

$$\lambda_1 = D_v d_{\parallel} > 0, \quad \lambda_2 = D_v d_{\perp} > 0, \quad \lambda_3 = D_v > 0$$

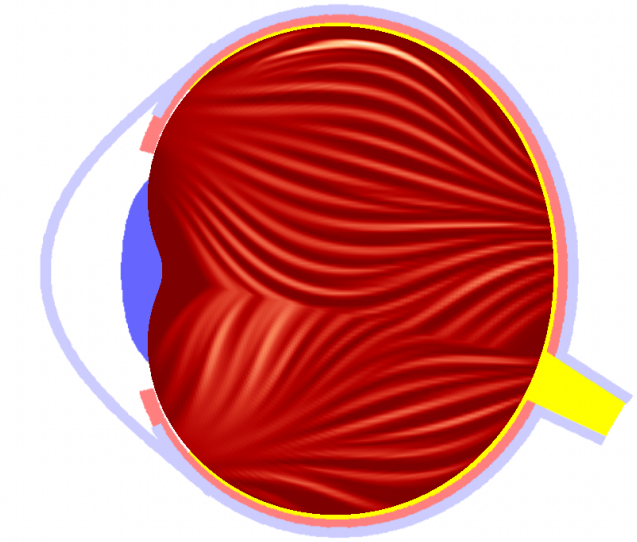

Figure 4.13: Structure of the collagen fiber bundles in the human vitreous [numerical simulation by Simon Dörsam]

and for the isotropic case with $\tilde{D}_v(x) = D_v \mathbb{I}$ we obtain

$$\lambda_1 = \lambda_2 = \lambda_3 = D_v > 0.$$

The symmetry propperty can be seen in the following rewritten defintion,

$$\tilde{D}_v(x) = \begin{pmatrix} d_\parallel \cos^2(\theta) + d_\perp \sin^2(\theta) & \cos(\theta)\sin(\theta)(d_\parallel - d_\perp) & 0 \\ \cos(\theta)\sin(\theta)(d_\parallel - d_\perp) & d_\parallel \sin^2(\theta) d_\perp \cos^2(\theta) & 0 \\ 0 & 0 & 1 \end{pmatrix},$$

consequently we have $\tilde{D}_v(x) = \tilde{D}_v(x)^T$.

4.7.2 Anisotropic Viscoelastic Model

At first in this section we will give a short introduction to the modeling of the vitreous as a collagen fiber suspension immersed in a viscous fluid by predicting the fiber orientation evolution equation. Secondly, we derive a thermodynamically consistent model for the vitreous as a viscoelastic fluid whose elastic reaction is anisotropic taking into account the preferred direction of the elastic collagen fibers. Here, we further improve the viscoelastic constitutive equation (4.1) for the vitreous which is isotropic with regard to its viscous as well as its elastic response to the modeling of anisotropic viscoelastic vitreous.

Anisotropy of Fiber Suspension in Viscous Newtonian fluids

One way to model the network of collagen fibers suspended in hyaluronic acid is to propose a mathematical model of fiber suspension rheology, where the fibers (rods) are rigid cylinders uniform in length and diameter and immersed in a viscous Newtonian fluid.
Then the vitreous' response is anisotropic due to the dissipative nature of the liquid part in virtue of the motion of the fibers inside. The resulted rate of dissipation depends on the motion along different directions. It considers the anisotropic fiber diffusion/motion and fiber-fiber interaction from a microscopic viewpoint. The resulted flow is modified by the presence of fibers and vice versa, i.e. during flow fibers change their direction and the final orientation influences the mechanical properties of the material (e.g. vitreous is stiffer in the direction in which the most fibers are oriented) [59]. For example in [141], they simulate the injection molding of fiber reinforced composite products, an industrial process for producing large quantities of complex plastic parts. They deal with the flow of incompressible, non-isothermal non-Newtonian fluid containing suspensions of short-fibers.
In 1922 Jeffrey studied the flow of fiber suspensions, i.e. the motion of a single rotating fiber immersed in a viscous Newtonian liquid [88]. In his model, Jeffery assumed that the fibers are neutrally buoyant, axisymmetric, and sufficiently large so that Brownian motion (motion arising from collision of molecules in the fluid medium with the suspended particles) can be neglected. His fiber orientation evolution equation describing the distribution function of the orientation angle of the particle is valid only for dilute suspensions. Folgar and Tucker [59] have modified the Jeffery's equation by adding an isotropic rotary diffusion term, $2c_I\gamma(\mathbb{I} - 3\mathbb{A})$, with a diffusivity proportional to the scalar rate of deformation to take into account the fiber-fiber interactions for concentrated fiber suspensions:

$$\nabla \cdot v = 0, \tag{4.76a}$$

$$\rho\left(\frac{\partial v}{\partial t} + (v \cdot \nabla)v\right) = \nabla \cdot \mathbb{T}, \tag{4.76b}$$

$$-p\mathbb{I} + 2\mu\mathbb{D} + 2\mu\phi_V N_p \mathbb{D} : \mathbb{A}_4 = \mathbb{T}, \tag{4.76c}$$

$$\mathbb{W}\mathbb{A} - \mathbb{A}\mathbb{W} + \xi\left(\mathbb{D}\mathbb{A} + \mathbb{A}\mathbb{D} - 2\mathbb{D} : \mathbb{A}_4\right) + 2c_I\gamma(\mathbb{I} - 3\mathbb{A}) = \frac{d\mathbb{A}}{dt}, \tag{4.76d}$$

where μ is the viscosity, ϕ_V describes the fiber volume fraction and N_p is the particle number, $\gamma = \sqrt{2\mathbb{D} : \mathbb{D}}$ denotes the scalar magnitude of strain rate and c_I is the interaction coefficient modeling the fiber-fiber interactions which is an empirical dimensionless parameter whose value is determined by fitting

experimental data. $\xi := (a_r^2 - 1)/(a_r^2 + 1)$ is the particle shape factor which depends on the fiber aspect ratio a_r, i.e. the quotient of length and diameter of a single fiber. The second-order orientation tensor $\mathbb{A}$ is a symmetric tensor whose diagonal components describe the degree of orientation in flow direction, cross-flow direction and thickness direction. The fourth-order orientation tensor $\mathbb{A}_4$ added to the stress in (4.76c) models the probability of a fiber lying with the specific orientation at this point and is determined by using a higher order polynomial closure approximation in terms of $\mathbb{A}$, e.g. the quadratic approximation in d space-dimensions,

$$(\mathbb{A}_4)_{ijkl} := \mathbb{A}_{ij}\mathbb{A}_{kl}, \qquad i,j,k,l = 1,\dots,d.$$

The strain reduction factor (SRF) by Huynh [86] and the reduced strain closure (RSC) [187] models were developed as empirical modifications to the Folgar–Tucker model (4.76d) to improve the fiber orientation prediction, especially slower development of fiber orientation as observed experimentally.

These models predict the mechanical properties of a suspension once the fiber orientation is known and imply that the development of fiber orientation depends on the flow itself. The fiber suspension rheology adds considerable complexities to the flow study of the vitreous and the orientation evolution equation is highly dependent on the initial fiber orientation which is not known in reality [141, 29].

Anisotropy in Viscoelastic Fluids

Viscoelastic materials that are modeled within the framework of natural configurations like the introduced Burgers-type model for the vitreous can exhibit anisotropy with regard to mechanical response in two ways. On one side you can consider that the viscous response described by the rate of dissipation function or on the other side that the elastic response described by the Helmholtz potential behaves anisotropic. We look at the case where the elastic behavior is anisotropic since it is known that one important reason for the anisotropy of the vitreous comes from the collagen fibers which show elastic properties.
The presented approach is an extension of the framework of multiple natural configurations to the development of the constitutive equations for anisotropic viscoelastic fluids. It does not require specifying any additional boundary conditions, since the theory does not involve higher gradients compared to the directory theory approach usually applied for viscous flows [92, 140]. In the directory theory approach the usual balance laws are generalized by postulating a director balance law employing gradients of the director fileds as one of the constitutive unknowns along with notions of a director body force

and director (or cosserat) stress, which requires boundary conditions for the directors. Our ansatz is based on the thermodynamical framework and the resulted evolution equations being determined by the maximization of the entropy production satisfying the second law of thermodynamics introduced in Section 4.2.2. The aim is a complete system of governing equations by choosing the specific constitutive relation for the Helmholtz potential depending on the preferred direction of the elastic collagen fibers inside the vitreous instead of directly prescribing the anisotropic constitutive equations. Then we derive the constitutive equation for the Cauchy stress tensor $\mathbb{T}$ and the required evolution equation for the preferred direction of anisotropy.

The (fixed) direction of the unit vector A denotes the preferred direction of the elastic collagen fibers inside the vitreous in its reference. a describes the corresponding vector in the current configuration. In simpler cases of anisotropic elastic solids and only viscous fluids the formulas are known from the literature [70, 81]. Here, we do not have the splitting of the deformation into viscous and elastic response. For solids, the desired quantity is the left Cauchy-Green tensor $\mathbb{B}$ defined in (2.3) which will be used in the ansatz of the Helmholtz potential, $\psi = \tilde{\psi}(\mathbb{B}, a \cdot \mathbb{B}a)$, following the thermodynamic framework. We can easily see that the sought evolution equation for the direction of anisotropy reads,

$$\frac{da}{dt} = \frac{d\mathbb{F}}{dt}A = (\nabla v)\mathbb{F}A = (\nabla v)a \tag{4.77}$$

since we have $a = \mathbb{F}A$. Further, we have the simplification

$$\frac{d\mathbb{B}}{dt} = (\nabla v)\mathbb{B} + \mathbb{B}(\nabla v)^T \tag{4.78}$$

which follows from the relation (2.2) or rather

$$\overset{\nabla}{\mathbb{B}} = 0$$

by using the definition (4.2) of the upper convected Oldroyd derivative. For an anisotropic viscous fluid, the desired quantity is the symmetric part of the velocity gradient. The corresponding evolution equation for a coincides with (4.77) modified by an additional term depending on $\mathbb{D}$ and a according to Green [70],

$$\frac{da}{dt} = (\nabla v)a + \lambda\left[\mathbb{D}a - \mathrm{tr}\left(\mathbb{D}(a \otimes a)\right)a\right] - \mathbb{D}a.$$

But the modeling of constitutive theory for anisotropic viscoelastic fluids like vitreous is much more complicated since the complexity increases due to the splitting of the deformation and taking into account the natural configurations.

The viscoelastic fluids exhibit elastic and viscous properties characterized by the corresponding quantities $\mathbb{B}_1, \mathbb{B}_2$ of (4.12) and the velocity or rather $\mathbb{D}$. The difficulty is to find an expression for $\mathbb{T}$ and $\frac{da}{dt}$ such that

$$\begin{aligned}\frac{da}{dt} &= (\nabla v)a + f_1(\mathbb{B}_1, \mathbb{B}_2, a),\\ \mathbb{T} &= -p\mathbb{I} + 2\mu\mathbb{D} + f_2(\mathbb{B}_1, \mathbb{B}_2, a)\end{aligned}$$

with appropriate functions f_1 and f_2.
For simplicity, we model the vitreous as a transversely isotropic viscoelastic fluid whose elastic response is anisotropic following the idea in [148]. There is only one direction and perpendicular to it the material properties are independent of the considered direction. Further, we assume viscoelastic behavior which can be described by the co-existence of two natural configurations according to the splitting of the deformation in (4.11), motivated by the experimental observation of two different relaxation times capable by the Burgers-type model. In this setting, A denotes the preferred direction of the

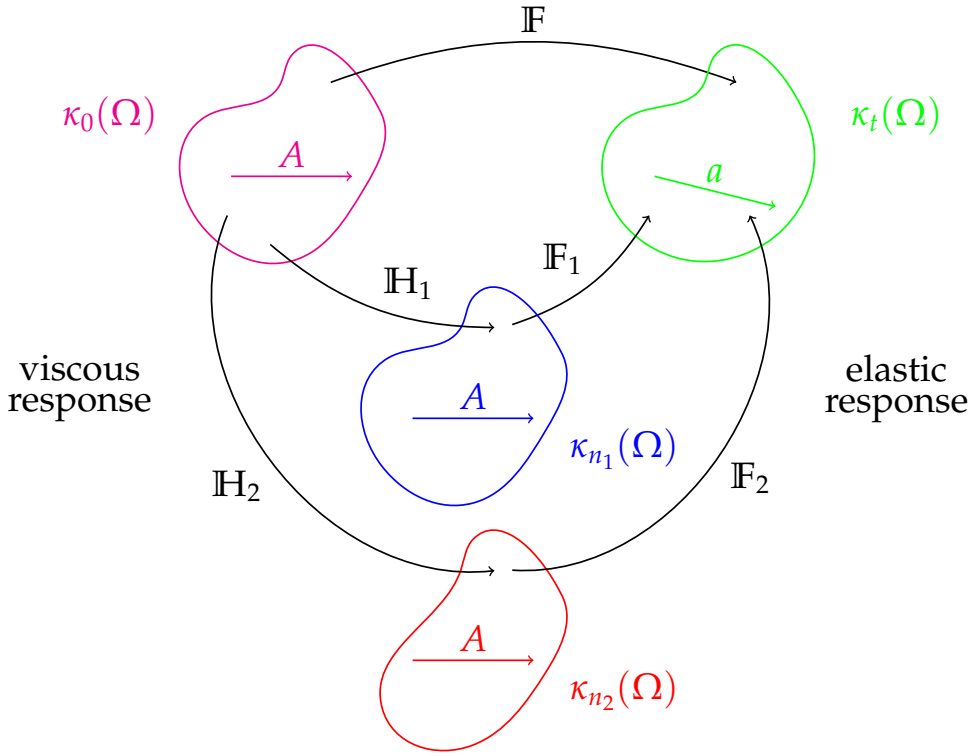

Figure 4.14: Direction of the axis of anisotropy in the framework of two natural configurations

elastic collagen fibers inside the vitreous in its reference and natural configuration, i.e. the direction of the axis of anisotropy shown in Figure 4.14. Then the corresponding vector a in the current configuration at time t takes the form

$$a = \mathbb{F}_1 A$$

or

$$a = \mathbb{F}_2 A.$$

For better understanding we recapitulate the important definitions in the setting of two natural configurations as in the Subsection 4.2.2 for $i = 1, 2$:

$$\mathbb{B}_i := \mathbb{F}_i \mathbb{F}_i^T, \qquad (\nabla v)_i := \frac{d\mathbb{H}_i}{dt} \mathbb{H}_i^{-1},$$

see (4.12) and (4.13). Since we know the time derivative

$$\frac{d\mathbb{F}_i}{dt} = (\nabla v)\mathbb{F}_i - \mathbb{F}_i(\nabla v)_i$$

from the relation (4.14) we can compute the sought evolution equation for a:

$$\frac{da}{dt} = \frac{d\mathbb{F}_i}{dt} A = (\nabla v)a - \mathbb{F}_i(\nabla v)_i \mathbb{F}_i^{-1} a \tag{4.79}$$

but $\mathbb{F}_i$ and $(\nabla v)_i$ are not desired quantities.
Since we are interested in modeling the incompressible anisotropic viscoelastic vitreous considering isothermal processes, the Helmholtz potential should be related to the elastic parts of the deformation $\mathbb{B}_i, i = 1, 2$, and fiber direction a. Therefore, we postulate that:

$$\begin{aligned}\psi &= \psi(\mathbb{B}_1, \mathbb{B}_2, a) \\ &:= \frac{G_1}{2\rho}\left(\operatorname{tr}\mathbb{B}_1 - 3 - \ln(\det\mathbb{B}_1)\right) + \frac{G_2}{2\rho}\left(\operatorname{tr}\mathbb{B}_2 - 3 - \ln(\det\mathbb{B}_2)\right) \\ &\quad + \frac{G_1}{\rho} a \cdot \mathbb{B}_1 a + \frac{G_2}{\rho} a \cdot \mathbb{B}_2 a.\end{aligned}$$

Note that this specific choice is motivated by the theory of isotropic viscoelastic Burgers-type model with ψ defined in (4.19) and the material parameters are the same. However, the Helmholtz potential depends additionally on a compared to the previous introduced ansatz (4.18) and since the elastic reaction is anisotropic a is directly coupled to the left Cauchy-Green tensors expressed in the terms, $a \cdot \mathbb{B}_i a$ for $i = 1, 2$. Then the material time derivative of the

potential $\frac{d\psi}{dt}$ is the starting point for the derivation of the constitutive equations. Following the thermodynamic framework for the entropy production by using the energy-dissipation relation (3.12) and substituting the balance equations for incompressible flows we get

$$\theta\xi = \mathbb{T}_\delta : \mathbb{D} - \rho\frac{\partial\psi}{\partial\mathbb{B}_1}\frac{d\mathbb{B}_1}{dt} - \rho\frac{\partial\psi}{\partial\mathbb{B}_2}\frac{d\mathbb{B}_2}{dt} - \rho\frac{\partial\psi}{\partial a}\frac{da}{dt}. \tag{4.80}$$

Now, we see that the derived expression (4.79) for $\frac{da}{dt}$ is needed for further analysis of (4.80). From the definition of the upper convected Oldroyd derivative (4.2), we know that for $i = 1, 2$ it holds

$$\frac{d\mathbb{B}_i}{dt} = \overset{\nabla}{\mathbb{B}}_i + (\nabla v)\mathbb{B}_i + \mathbb{B}_i(\nabla v)^T$$

in comparison to (4.78) for solids. Further, the partial derivatives of the prescribed potential ψ are

$$\begin{aligned}
\frac{\partial\psi}{\partial a}\otimes a &= (a\otimes a)\left(\frac{G_1}{\rho}\mathbb{B}_1 + \frac{G_2}{\rho}\mathbb{B}_2\right) + \left(\frac{G_1}{\rho}\mathbb{B}_1 + \frac{G_2}{\rho}\mathbb{B}_2\right)(a\otimes a),\\
\frac{\partial\psi}{\partial\mathbb{B}_i} &= \frac{G_i}{2\rho}\left(\mathbb{I} - \mathbb{B}_i^{-1}\right) + \frac{G_i}{\rho}(a\otimes a), \qquad i = 1, 2.
\end{aligned}$$

Consequently, we see that $\frac{\partial\psi}{\partial\mathbb{B}_i}$ for $i = 1, 2$ and $\frac{\partial\psi}{\partial a}\otimes a$ are symmetric and we can use,

$$\mathbb{A} : \nabla v = \mathbb{A} : (\nabla v)^T = \mathbb{A} : \mathbb{D}$$

for any symmetric tensor $\mathbb{A} \in \mathbb{R}^{3\times 3}$. Nevertheless, we can not use any longer the simplification

$$\frac{\partial\psi}{\partial\mathbb{B}_i}\mathbb{B}_i + \mathbb{B}_i\frac{\partial\psi}{\partial\mathbb{B}_i} = 2\frac{\partial\psi}{\partial\mathbb{B}_i}\mathbb{B}_i, \qquad i = 1, 2$$

since the matrix multiplication does not commute. Then further manipulation of (4.80) leads to

$$\begin{aligned}
\theta\xi &= \mathbb{T}_\delta : \mathbb{D} - \rho\frac{\partial\psi}{\partial\mathbb{B}_1} :\overset{\nabla}{\mathbb{B}}_1 - \rho\frac{\partial\psi}{\partial\mathbb{B}_1} : (\nabla v\mathbb{B}_1 + \mathbb{B}_1(\nabla v)^T) \\
&\quad - \rho\frac{\partial\psi}{\partial\mathbb{B}_2} :\overset{\nabla}{\mathbb{B}}_2 - \rho\frac{\partial\psi}{\partial\mathbb{B}_2} : (\nabla v\mathbb{B}_2 + \mathbb{B}_2(\nabla v)^T) - \rho\frac{\partial\psi}{\partial a}\cdot\frac{da}{dt} \\
&= \mathbb{T}_\delta : \mathbb{D} - \rho\frac{\partial\psi}{\partial\mathbb{B}_1} :\overset{\nabla}{\mathbb{B}}_1 - \rho\left(\mathbb{B}_1\frac{\partial\psi}{\partial\mathbb{B}_1} + \frac{\partial\psi}{\partial\mathbb{B}_1}\mathbb{B}_1\right) : \mathbb{D} \\
&\quad - \rho\frac{\partial\psi}{\partial\mathbb{B}_2} :\overset{\nabla}{\mathbb{B}}_2 - \rho\left(\mathbb{B}_2\frac{\partial\psi}{\partial\mathbb{B}_2} + \frac{\partial\psi}{\partial\mathbb{B}_2}\mathbb{B}_2\right) : \mathbb{D} \\
&\quad - \rho\frac{\partial\psi}{\partial a}\cdot(\nabla v)a + \rho\frac{\partial\psi}{\partial a}\cdot\mathbb{F}_i(\nabla v)_i\mathbb{F}_i^{-1}a \\
&= \left(\mathbb{T}_\delta - \rho\left(\mathbb{B}_1\frac{\partial\psi}{\partial\mathbb{B}_1} + \frac{\partial\psi}{\partial\mathbb{B}_1}\mathbb{B}_1 + \mathbb{B}_2\frac{\partial\psi}{\partial\mathbb{B}_2} + \frac{\partial\psi}{\partial\mathbb{B}_2}\mathbb{B}_2\right) - \rho\frac{\partial\psi}{\partial a}\otimes a\right) : \mathbb{D} \\
&\quad - \rho\frac{\partial\psi}{\partial\mathbb{B}_1} :\overset{\nabla}{\mathbb{B}}_1 - \rho\frac{\partial\psi}{\partial\mathbb{B}_2} :\overset{\nabla}{\mathbb{B}}_2 + \rho\frac{\partial\psi}{\partial a}\otimes a : \mathbb{F}_i(\nabla v)_i\mathbb{F}_i^{-1}.
\end{aligned}$$

To fulfill the requirement of the second law of thermodynamics (2.9), we make the simpler approach of linear non-equilibrium thermodynamics in contrast to the nonlinear non-equilibrium thermodynamics in (4.26), see [117] for more details. As for the Navier-Stokes fluid in Section 3.3.2 we consider linear relations between each pair of thermodynamic affinities and fluxes,

$$j_\alpha = c_\alpha a_\alpha$$

where $c_\alpha, \alpha = 1,\dots 4$, are positive constants and the entropy production is represented by the sum of each flux times affinity as in (4.25). Then the entropy production, $\theta\xi = \sum_\alpha c_\alpha|a_\alpha|^2$, is a positive quantity, if the constitutive relations are chosen as follows for $i = 1, 2$,

$$\begin{aligned}
\mathbb{T}_\delta &= 2\mu_3\mathbb{D} + G_1(\mathbb{B}_1 - \mathbb{I}) + G_2(\mathbb{B}_2 - \mathbb{I}) \\
&\quad + G_1\mathbb{B}_1(a\otimes a) + G_1(a\otimes a)\mathbb{B}_1 \\
&\quad + G_2\mathbb{B}_2(a\otimes a) + G_2(a\otimes a)\mathbb{B}_2 \\
&\quad + (a\otimes a)\,(G_1\mathbb{B}_1 + G_2\mathbb{B}_2) + (G_1\mathbb{B}_1 + G_2\mathbb{B}_2)\,(a\otimes a), \\
\overset{\nabla}{\mathbb{B}}_i &= -c_i\frac{G_i}{2}\left(\mathbb{I} - \mathbb{B}_i^{-1}\right) - c_iG_i(a\otimes a), \\
\mathbb{F}_i(\nabla v)_i\mathbb{F}_i^{-1} &= c_3\rho\frac{\partial\psi}{\partial a}\otimes a
\end{aligned}$$

with positive constants c_1, c_2, c_3 and μ_3. For the sought time derivative of the anisotropic direction it follows that

$$\begin{aligned}\frac{da}{dt} &= (\nabla v)a - c_3(a\otimes a)\left(G_1\mathbb{B}_1 + G_2\mathbb{B}_2\right)a \\ &\quad - c_3\left(G_1\mathbb{B}_1 + G_2\mathbb{B}_2\right)(a\otimes a)a.\end{aligned}$$

Then the complete system of governing equations describing the anisotropic viscoelastic vitreous arising from the balance laws and the derived constitutive relations reads:

$$\nabla\cdot v = 0, \tag{4.81a}$$

$$\nabla\cdot\mathbb{T} = \rho\left(\frac{\partial v}{\partial t} + (v\cdot\nabla)v\right), \tag{4.81b}$$

$$\begin{aligned}\mathbb{T} = &-p\mathbb{I} + 2\mu_3\mathbb{D} + G_1(\mathbb{B}_1 - \mathbb{I}) + G_2(\mathbb{B}_2 - \mathbb{I}) \\ &+ G_1\mathbb{B}_1(a\otimes a) + G_1(a\otimes a)\mathbb{B}_1 \\ &+ G_2\mathbb{B}_2(a\otimes a) + G_2(a\otimes a)\mathbb{B}_2 \\ &+ (a\otimes a)\left(G_1\mathbb{B}_1 + G_2\mathbb{B}_2\right) + \left(G_1\mathbb{B}_1 + G_2\mathbb{B}_2\right)(a\otimes a),\end{aligned} \tag{4.81c}$$

$$\overset{\nabla}{\mathbb{B}}_1 = -c_1\frac{G_1}{2}\left(\mathbb{I} - \mathbb{B}_1^{-1}\right) - c_1G_1(a\otimes a), \tag{4.81d}$$

$$\overset{\nabla}{\mathbb{B}}_2 = -c_2\frac{G_2}{2}\left(\mathbb{I} - \mathbb{B}_2^{-1}\right) - c_2G_2(a\otimes a), \tag{4.81e}$$

$$\frac{da}{dt} = (\nabla v)a - c_3(a\otimes a)\left(G_1\mathbb{B}_1 + G_2\mathbb{B}_2\right)a \tag{4.81f}$$

$$- c_3\left(G_1\mathbb{B}_1 + G_2\mathbb{B}_2\right)(a\otimes a)a. \tag{4.81g}$$

Note that the Cauchy stress tensor $\mathbb{T}$ keeps its symmetric property.

The system (4.81) in $\Omega\times(0,T]$ is completed with the initial and boundary conditions (4.5) and (4.4) for the healthy viscoelastic vitreous plus the initial fiber orientation,

$$a = a_0 \qquad\qquad \text{on } \Omega\times\{t=0\}.$$

The developed framework can be applied to general flows by choosing different definitions for the Helmholtz free energy ψ (allowing numerous natural configurations) and can be extended to more than one preferred direction and moreover considering non-isothermal processes.
It is a novel description for the healthy human vitreous which was not considered in the literature before. It is capable to model the complex mechanical behavior of the vitreous including the heterogeneous structure of collagen

fibers.

Moreover, the term $a \otimes a$ characterizing the orientation of the collagen fibers can also be added to the evolution equation (3.17) for the concentration assuming a fixed direction a. Instead of the diffusion matrix D one can consider the modified diffusion matrix $D + a \otimes a$ resulting in

$$\frac{\partial C}{\partial t} + (v \cdot \nabla)C - \nabla \cdot ((D + a \otimes a)\nabla C) = 0 \qquad \text{in } \Omega \times (0, T].$$

This approach of the anisotropic diffusion includes the certain orientation of the collagen fibers and reflects the tendency for diffusion to follow the preferential direction along the collagen fiber bundles.

4.8 Numerical Simulations for Drug Distribution

In this section we compare the different rheological models of the vitreous body introduced in the previous chapters and their impact on the drug distribution by numerical simulations performed with the finite element method [26]. The data-based realistic three-dimensional geometry is constructed after own in-vivo measurements performed in the Department of Ophthalmology [35]. The numerical simulations and pictures were implemented by the working group members Simon Dörsam and Alexander Drobny using Finite Element library deal.ii [17].

We consider the three introduced approaches for the description of the drug distribution coupled through convection with the different models of the vitreous: the healthy vitreous modeled by the porous medium approach (3.26) and the viscoelastic approach (4.61) and the liquefied vitreous in age modeled by the Navier-Stokes equation (3.27). All are completed by the corresponding boundary and initial conditions.
In our application of the human eye with equal in- and outflow and no external forces it is enough to study the steady case. In this specific situation we know that the time-dependent elastic properties of the Burgers-type model have negligible influence on the overall flow pattern which converges to the Naviers-Stokes velocity profile. Nevertheless, the resulting drug concentration profiles differ due to the different parameter values. The computed velocity profiles and more details concerning the numerical implementation and discretization can be seen in [39, 40, 41, 60].
The drug distribution after 15 minutes, 1 day and 6 days (from left to right) in the sliced vitreous for visualization purposes is illustrated in Figure 4.15. It is

more convection dominated in the liquefied vitreous with faster diffusion process due to the higher diffusion coefficient than in the healthy cases described by Darcy's law and the viscoelastic Burgers-type model. But at the beginning, 15 minutes after injection, the whole drug concentration stays near the injection position for all three approaches for the vitreous. The aim of the therapy for the treatment of retinal diseases is the drug stays as long as possible in the vitreous. To measure this mathematically, we introduce the following functional: With $J_1(C,t) : L^2(0,T;H_0^1(\Omega;\Gamma_h)) \times (0,T] \to \mathbb{R}_+$ we denote the relative amount of the drug in the vitreous at the current time point,

$$J_1(C,t) := \frac{\int_\Omega C(x,t)\,\mathrm{d}x}{\int_\Omega C(x,0)\,\mathrm{d}x},$$

for more information see [41, 60]. The comparison of the results of J_1 over time for the three approaches is shown in Figure 4.16. For a better overview the half-life times of the drug concentration in the vitreous are summarized in the Table 4.5. After one month there is no drug in the vitreous independent of the

	Healthy viscoelastic vitreous (Burgers-type)	Healthy vitreous (Darcy)	Liquefied vitreous (Navier-Stokes)
Intravitreal half-life of drug concentration [d]	5.2	4.75	2.7

Table 4.5: Comparison of the half-life times of Aflibercept concentration in the vitreous

rheological model of the vitreous. The liquefaction of the vitreous, the degeneration process of the vitreous humor associated with aging, causes the fastest drug distribution and an increase in the convection flow due to the disruption of the fibers' mesh composing the vitreous humor modeled by the highest diffusion coefficient. This finding is also concluded in the literature [177, 14]. In [174] a simulated liquefaction caused a 12-fold faster distribution of fluorescein sodium compared to the simulated young vitreous model without liquefaction. Especially, for drugs with low diffusion coefficients and in low viscosity vitreous fluids, like the diffusion of Aflibercept in the liquefied vitreous, high convection can lead to high drug concentrations on the retina, which can be potentially toxic [93]. In our simulations, the half-life time for average Aflibercept concentration in the vitreous for the viscoelastic case is about 1.1 times

longer than for the Darcy flow and about 1.9 times longer than in the liquefied scenario with Navier-Stokes flow. The measured half-life time of Aflibercept in human eyes according to experiments from Stewart et al. [175] is 7.13 days which is higher than our calculated values. This difference comes from the lack of the values of some parameters in the literature which are used to model the drug distribution within the vitreous. In these cases we use values from other species than humans or other drugs like Ranibizumab which half-life time is 4.75 d [175] corresponding exactly to our value for the healthy vitreous modeled by Darcy's law. For this reason, the present results of the numerical simulations are only of the same order as the measurements from experiments, but they make physical sense and are in agreement with the reality. Most animal models in the literature indicate that intravitreal drugs have reduced half-lives and increased clearance in vitrectomized eyes [44]. For example, Niwa et al. [136] measured the pharmacokinetic parameters in vitrectomized and non-vitrectomized monkey eyes. Here, the half-life of ranibizumab and aflibercept was shorter in vitrectomized eyes than in non-vitrectomized eyes. Drug half-life time differences around 52 % requires more frequently injections for liquefied vitreouses, whereas we have more effective drug interaction for a healthy (viscoelastic) vitreous which should be considered in personalized therapies. In [93] they also conclude that the drug concentration distribution depends on the properties of the vitreous, beside the diffusion coefficient of the drug and the permeability of the retinal surface.

The numerical simulations validate the developed mathematical models, corroborate their solubility with plausible results and show the necessity to distinguish between the rheological models for the vitreous body and their impact on the drug distribution. By considering patient individual differences we can improve the therapeutic approaches for retinal diseases. Our models and their simulation allow fast and cost effective tests in comparison to in vivo experiments, speed up drug development by analyzing different conditions and parameters like the influence of a specific drug or the injection protocols (position, frequency) and many more.

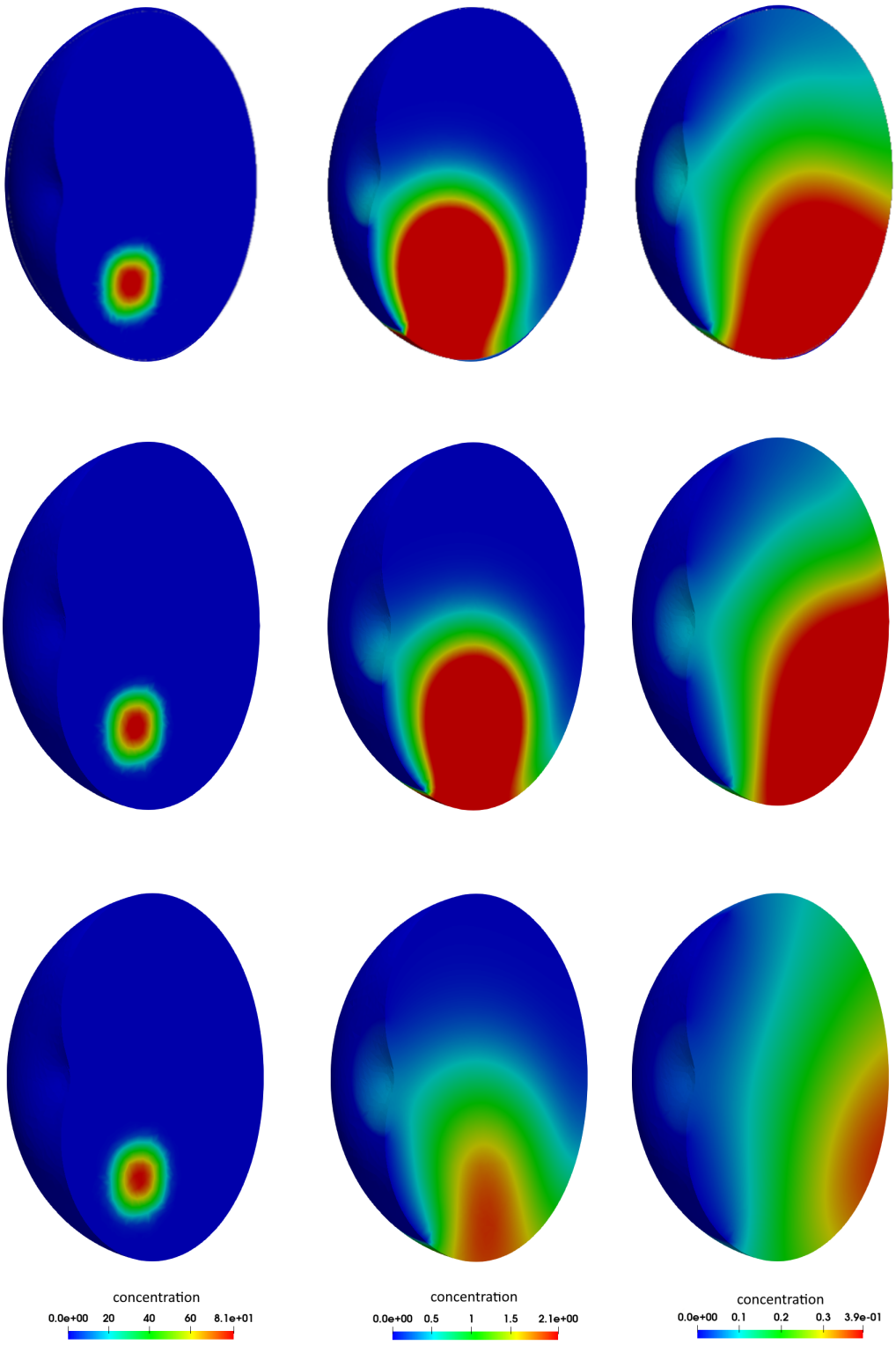

Figure 4.15: Concentration [kg/m^3] in the sliced vitreous modeled by Darcy's law (top row), Burgers-type model (middle) and Navier-Stokes equation (bottom) after 15 min, 1 day and 6d (left to right) [simulation by Alexander Drobny and Simon Dörsam]

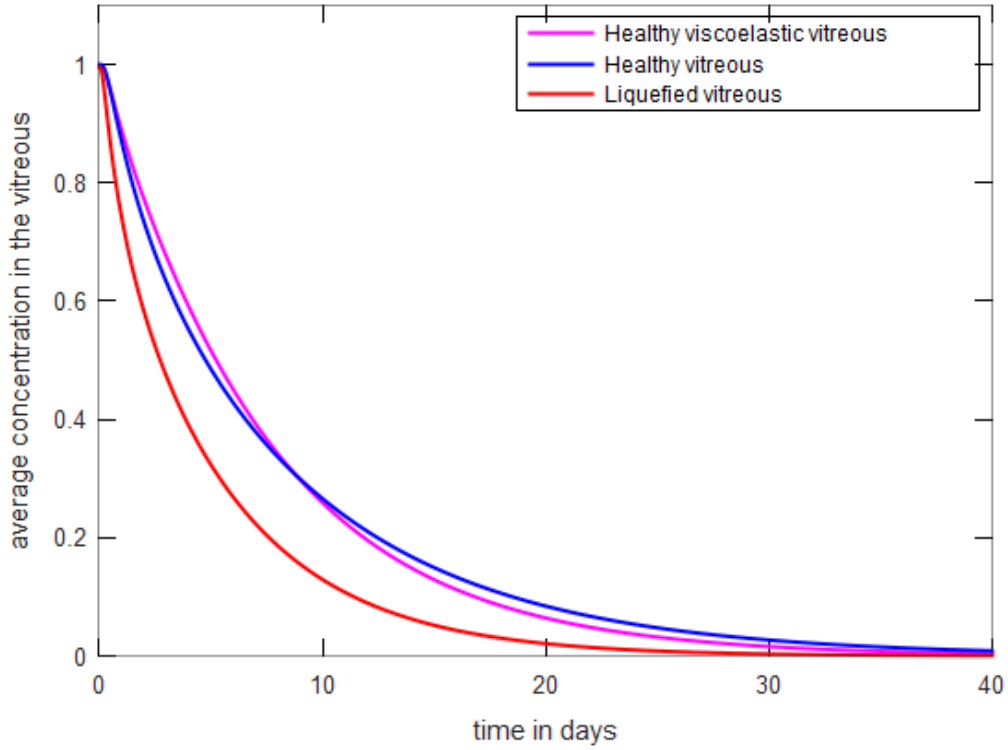

Figure 4.16: Relative average drug concentration in the vitreous over time for the healthy (Darcy), healthy viscoelastic (Burgers-type) and liquefied (Navier-Stokes) vitreous [simulation by Alexander Drobny and Simon Dörsam]

5 Conclusion and Outlook

For the treatment of retinal diseases by drug distribution in the human vitreous, we have developed the mathematical model of the vitreous. Compare to previous works we focused on the vitreous as a viscoelastic fluid including its heterogeneous property due to the orientation of collagen fibers.
All of the previous studies [62, 75, 10, 170] model the vitreous humor as an incompressible Newtonian fluid ignoring its non-Newtonian nature. But it is a gel that has both viscous and elastic properties caused from the interaction between hyaluronic acid, aqueous humor and collagen fibers. This mechanical behavior of the healthy vitreous is modeled by the incompressible viscoelastic Burgers-type model based on experimental data in the literature. The model is thermodynamically derived and capable of describing two different relaxation times observed by these measurements. Especially, looking at applications where the stress is the significant quantity, it is the more appropriate one. We achieved the following results, that the healthy vitreous predicted by the Burgers-type model shows twice as high stress as the pathological one predicted by the Navier–Stokes model, while the overall flow patterns are rather insensitive to the chosen rheology in a deforming eye ball. The focus on the interplay between the rheology of the vitreous and the stress field in it is of interest in the study of eye pathologies such as posterior vitreous or retinal detachment. These eye pathologies are thought to be closely linked to mechanical processes with high stresses. The collagen fibers inside the vitreous responsible for the elastic properties are directionally oriented. This finding emphasize the need to use the anisotropic viscoelastic model and improve the evolutionary equation for the stress. Then the vitreous as a viscoelastic fluid whose elastic reaction is anisotropic takes into account the preferred direction of the collagen fibers.
Finally for the treatment of retinal diseases, the coupling of the viscoelastic Burgers-type model with the stress driven diffusion provides an accurate description for the drug transport in the human vitreous. In contrast to the literature we propose a fully coupled system in which the drug diffusion and flow inside the vitreous can effect each other. The drug diffusion depends on the viscoelastic properties of the vitreous which act as a barrier. The extension to an anisotropic stress driven diffusion reflects the tendency to follow the preferential direction along the collagen fibers depending on the molecule

size. The difficulty of this research is to set the correct parameters $(D_v, k, d_{\parallel}, d_{\perp})$ for the stress driven diffusion and its anisotropic approach due to the lack of experimental data and the phenomenological ansatz for the description of the collagen fibers.
The development of mathematical models for the vitreous body in the human eye is a very challenging task. The vitreous is the medium and transport pathway of nutritions and substances that pass the blood aqueous and blood retina barrier. It changes continuously during life ending as a very liquefied inhomogeneous body. In the aging eye diseases such as macular degeneration or diabetes retinopathy or vascular diseases reach a very high incidence and are the leading cause for blindness in western countries. The treatment of these diseases involves injection of drugs into the vitreous targeting the retinal pathology. How these drugs interact with the vitreous, how they distribute and reach the target tissue is essential for the treatment of these pathologies. Our developed models for the drug distribution in the human vitreous after the injection are important for the development and optimization of new treatment modalities, but also to understand how current treatments work or why they sometimes fail. The impact of the viscoelastic modeling for the vitreous compared to the standard Darcy or Navier-Stokes equation is even more pronounced in applications with external force. This work provides a better understanding about the mechanical behavior of the vitreous and how the medical treatment is influenced by the changing properties of the vitreous. It will influence the treatment schemes and can speed up the drug development to improve the administered ophthalmic therapy. The need for animal studies or extended human trials can be minimized or even avoided based on the developed models in this dissertation.

Outlook The development of mathematical models for drug transport in the human eye is a promising field for future research. Further extensions of the proposed models of this complex real-world application are possible in various directions. For future work we propose the following points.
First, one could consider other physiologies describing the state of the vitreous and combine the viscoelastic approach with the liquefied description by the Navier-Stokes equation. For example, the situation of early liquefaction could give a deep insight into the aging of the vitreous. Here, the structure of the gel is dissolved and replaced with aqueous lacunaea (pockets of liquid vitreous), which melt together over time. Also, the modeling of the posterior vitreous detachment requires the coupling of the properties of the vitreous and aqueous humor flow separated by a permeable interface. The challenge is the modeling of the (moving) interface problem with realistic interface conditions including

the unknown permeability of the drugs.
Second, the viscoelastic Burgers-type model could depend on the collagen fiber concentration. The human vitreous is heterogeneous and the collagen fiber concentration varies between different regions [6]. The corresponding parameters like the relaxation times could be modeled as space-dependent functions of the concentration of the collagen fibers, i.e. $\tau_i = \tilde{\tau}_i(C_{\text{col}}(x))$ for $i = 1, 2$.
Finally, one could focus on the poroelastic description of the vitreous motivated by the elastic collagen network. Poroelasticity studies the macroscopic interaction between fluid flow and solid deformation within a linear porous medium. The theory developed by Biot [22] states that the deformation of the medium influences the flow of the fluid and vice versa.

Appendix: Parameter

Intravitreal drug distribution depends on many parameters related to the specific drug used for the treatment and to the physiology of the eye. The used parameter values to solve the above mentioned mathematical models by numerical simulations are listed in the following Table 5.1 supported by their literature sources.

Parameter	Meaning	Value	Unit	Source
	General Values for Human Vitreous			
ρ	Density of vitreous	1005.3-1008.9	kg m^{-3}	[23]
	Weight	3.9×10^{-3}	kg	[23]
	Diameter cavity	22.55	mm	[127]
	Volume	4.7; 5	ml	[127]
θ	Temperature	307.05	K	[103]
	Porous Medium Approach for Healthy Vitreous			
D	Diffusion coefficient (Bevacizumab, rabbit)	4×10^{-11}	m^2 s^{-1}	[143]
	Diffusion coefficient (Fluorescein)	6×10^{-10}	m^2 s^{-1}	[8, 75, 122]
μ	Dyn. viscosity of aq. humor	6.9×10^{-4}	Pa s	[75, 122]
$\frac{K}{\mu}$	Hydraulic conductivity	8.4×10^{-11}	m^2 Pa^{-1} s^{-1}	[54, 75, 118]
	Liquefied vitreous			
μ_0	Dyn. viscosity	7.36×10^{-4}	Pa s	[152]
D	Diffusion coefficient (Aflibercept)	8.3×10^{-11}	m^2 s^{-1}	[12]

G_1	First elastic shear modulus	0.11	Pa	[180]
G_2	Second elastic shear modulus	0.07	Pa	[180]
μ_1	First dynamic viscosity	9200	Pa s	[180]
μ_2	Second dynamic viscosity	4.09	Pa s	[180]
μ_3	Third dynamic viscosity	0.86	Pa s	[180]
D	Diffusion coefficient (Bevacizumab, rabbit)	4×10^{-11}	$m^2\ s^{-1}$	[143]
	Drug			
ρ_p	Density (Aflibercept)	1370	$kg\ m^{-3}$	[4]
	Density (Ranibizumab)	1370	$kg\ m^{-3}$	[4]
	Density (Bevacizumab)	1370	$kg\ m^{-3}$	[4]
m	Mass (Aflibercept particle)	1.9×10^{-22}	kg	[4]
	Mass (Fluorescein particle)	5.5×10^{-25}	kg	[4]
	Mass (Ranibizumab particle)	7.968×10^{-23}	kg	[4]
	Mass (Bevacizumab particle)	2.4734×10^{-22}	kg	[4]
MW	Molecular weight (Aflibercept with glycosylation)	115	kDa	[4]
	Molecular weight (Aflibercept)	97	kDa	[4]
	Molecular weight (Ranibizumab)	48	kDa	[4]

	Molecular weight (Bevacizumab)	149	kDa	[4]
	Molecular weight (Fluorescein)	332	kDa	[6, 127]
r	Hydrodynamic radius (Aflibercept)	3.70×10^{-9}	m	[4]
	Hydrodynamic radius (Ranibizumab)	2.76×10^{-9}	m	[4]
	Hydrodynamic radius (Bevacizumab)	4.58×10^{-9}	m	[4]
d	Diameter (Aflibercept)	5.2×10^{-9}	m	[6]
	Diameter (Ranibizumab)	2.8×10^{-9}	m	[6]
	Diameter (Bevacizumab)	5.2×10^{-9}	m	[6]
	Intravitreal half-life (Aflibercept, human)	7.13	d	[175]
	Intravitreal half-life (Ranibizumab, human)	4.75	d	[175]
	Intravitreal half-life (Bevacizumab, human)	8.25	d	[175]
	Other Tissues (Retina,...)			
k_{vr}	Partition coefficient (vitreous/retina) (FITC-Dextran)	0.4	—	[42, 75]
	Partition coefficient (vitreous/retina) (Fluorescein)	0.9	—	[42, 75]
	Partition coefficient (vitreous/retina)	10	—	[99]
P	Retinal Permeability (Bevacizumab)	1.84×10^{-9}	$\mathrm{m\,s^{-1}}$	[85]

	Retinal Permeability (Fluorescein)	2.6×10^{-7}	$\mathrm{m\ s^{-1}}$	[75, 122]
	Retinal Permeability (Ranibizumab)	2.6×10^{-9}	$\mathrm{m\ s^{-1}}$	[85]
K_{RCS}	Hydraulic conductivity of RCS for aq. humor (bovine)	1.5×10^{-15}	$\mathrm{m^2\ Pa^{-1}\ s^{-1}}$	[75, 144]
P_v	Episcleral venous pressure (human)	1200	Pa	[75, 168]
	RCS thickness (rabbit)	0.3	mm	[49]
L	RCS thickness (human)	1.15	mm	calculated
	Retinal thickness	0.21-0.25	mm	[127]
	Choriodal thickness	0.32	mm	[127]
	Scleral thickness	0.6	mm	[127]
IOP	Intraocular pressure (healthy human eye)	2000	Pa	[94]
	Scleral density (human)	1.076	$\mathrm{g\ cm^{-3}}$	[176]
	Sclera shear modulus (human)	330×10^3	Pa	[71]
	Lens density (bovine)	1.104	$\mathrm{g\ cm^{-3}}$	[176]
	Anterior Chamber Depth (human)	3.28	mm	[127]
	Axial Length (Optical, human)	23	mm	[127]
k_{perm}	Retinal permeability	-1.9×10^{12}	$\mathrm{Pa\ s\ m^{-1}}$	calculated
	Aq. hum. production	2.5	μl/min	[55, 127]
$v_{\max}$	inflow b.c. at hyaloid membrane	1.2×10^{-3}	m/s	[55]
G	lens shear modulus (human)	$0.19 - 59.6 \times 10^3$	Pa	[189]

G	sclera shear modulus (human)	330×10^3	Pa	[71]
κ	lens elastic bulk modulus (human)	$100 \times G$	Pa	[189]
κ	sclera elastic bulk modulus (human)	$1000 \times G$	Pa	[71]
g_{const}	Gravitational acceleration	9.81	m s^{-2}	[58]
ρ_a	Aq. Hum. density	1.0×10^3	kg m^{-3}	[58]

Table 5.1: Model parameters

Acknowledgements

First of all, I would like to thank my first supervisor Prof. Dr. Elfriede Friedmann for the opportunity to work on such an interesting topic, the funding, her encouragement and support. I am grateful for all the fruitful discussions and her guidance throughout my doctoral research project.
I thank my second supervisor, Assistant Prof. Vít Průša from the Mathematical Institute at the Charles University in Prague for his helpful advice and answered questions even from abroad.

I would like to thank Prof. Rolf Rannacher and the Mathematical Modeling Group of Josef Málek, especially Karel Tůma for the calculations.
I thank Prof. Dr. med. Auffarth from the Department of Ophthalmology in the Heidelberg University Hospital and Dr. Patrick Merz from the David J. Apple International Laboratory for Ocular Pathology for their medical and biological informations about the human eye, explanation of the treatment of retinal diseases and for the opportunity to watch vitrectomy surgery and experiments on autopsy eyes.
In addition, I would like to express my special thanks to my colleagues. I am thankful for the pleasant working atmosphere and friendly support over the years. I enjoyed all our activities and trips. Many thanks to Simon Dörsam, Alexander Drobny, Dr. Vladislav Olkhovskiy and Dr. Mania Sabouri for scientific discussions.

Furthermore, I would like to thank the Klaus Tschira foundation gGmbH for their financial support within the Project No.00.265.2015.
As a member of the Heidelberg Graduate School of Mathematical and Computational Methods for the Sciences (HGS MathComp) founded by DFG grant GSC 220 in the German Universities Excellence Initiative, I gratefully acknowledge the financial support for traveling to conferences, many interesting workshops and exchange with other PhD students.

Finally, I am also deeply grateful to my family and friends for their support and encouragement in all situations.

Bibliography

[1] Global, regional, and national incidence, prevalence, and years lived with disability for 310 diseases and injuries, 1990–2015: a systematic analysis for the Global Burden of Disease Study 2015. In: *The Lancet* 388 (2016), Nr. 10053, S. 1545 – 1602

[2] ABOUALI, O. ; MODARESZADEH, A. ; GHAFFARIYEH, A. ; TU, J. : Numerical simulation of the fluid dynamics in vitreous cavity due to saccadic eye movement. In: *Medical Engineering & Physics* 34 (2012), Nr. 6, S. 681 – 692

[3] AGANOVIĆ, I. ; MIKELIĆ, A. : Homogenization of nonstationary flow of a two-constituant mixture through a porous medium. In: *Asymptotic Analysis* 6 (1992), S. 173–189

[4] AL., L. M. H.: Hydrodynamic Radii of Ranibizumab, Aflibercept and Bevacizumab Measured by Time-Resolved Phosphorescence Anisotropy. In: *Pharmaceutical Research* 33 (2016), S. 2025–2032

[5] ALEXANDER, C. M. ; DABROWIAK, J. C. ; GOODISMAN, J. : Gravitational sedimentation of gold nanoparticles. In: *Journal of Colloid and Interface Science* 396 (2013), S. 53 – 62

[6] AMO, E. M. ; RIMPELÄ, A.-K. ; HEIKKINEN, E. ; KARI, O. K. ; RAMSAY, E. ; LAJUNEN, T. ; SCHMITT, M. ; PELKONEN, L. ; BHATTACHARYA, M. ; RICHARDSON, D. ; SUBRIZI, A. ; TURUNEN, T. ; REINISALO, M. ; ITKONEN, J. ; TOROPAINEN, E. ; CASTELEIJN, M. ; KIDRON, H. ; ANTOPOLSKY, M. ; VELLONEN, K.-S. ; RUPONEN, M. ; URTTI, A. : Pharmacokinetic aspects of retinal drug delivery. In: *Progress in Retinal and Eye Research* 57 (2017), S. 134 – 185

[7] ANDERSON, D. M. ; MCFADDEN, G. B. ; WHEELER, A. A.: Diffuse-interface methods in fluid mechanics. In: *Annual review of fluid mechanics* 30 (1998), Nr. 1, S. 139–165

[8] ARAIE, M. ; MAURICE, D. M.: The loss of fluorescein, fluorescein glucuronide and fluorescein isothiocyanate dextran from the vitreous by the

anterior and retinal pathways. In: *Experimental Eye Research* 52 (1991), Nr. 1, S. 27–39

[9] AZARBAYJANI, A. F. ; JOUYBAN, A. ; CHAN, S. Y.: Impact of surface tension in pharmaceutical sciences. In: *Journal of pharmacy & pharmaceutical sciences* 12 (2009), Nr. 2, S. 218–228

[10] AZHDARI, E. ; FERREIRA, J. A. ; OLIVEIRA, P. de ; SILVA, P. M.: Numerical and analytical study of drug release from a biodegradable viscoelastic platform. In: *Mathematical Methods in the Applied Sciences* 39 (2016), Nr. 16, 4688–4699. http://dx.doi.org/10.1002/mma.3375. – DOI 10.1002/mma.3375. – ISSN 1099–1476

[11] AZHDARI, E. ; FERREIRA, J. ; OLIVEIRA, P. de ; SILVA, P. : Analytical and numerical study of diffusion through biodegradable viscoelastic materials. In: *Proceedings of the 13th International Conference on Computational and Mathematical Methods in Science and Engineering* (2013), 06, S. 185–195

[12] AZHDARI, E. ; FERREIRA, J. A. ; OLIVEIRA, P. de ; SILVA, P. M.: Diffusion, viscoelasticity and erosion: Analytical study and medical applications. In: *Journal of Computational and Applied Mathematics* 275 (2015), Nr. Supplement C, S. 489 – 501

[13] AZHDARI, E. ; FERREIRA, J. A. ; OLIVEIRA, P. d. ; SILVA, P. : Drug delivery from an ocular implant into the vitreous chamber of the eye. In: *Proceedings of the 13th International Conference on Computational and Mathematical Methods in Science and Engineering-CMMSE 203* Bd. 1 CMMSE, 2013, S. 174–184

[14] BALACHANDRAN, R. K. ; BAROCAS, V. H.: Contribution of saccadic motion to intravitreal drug transport: theoretical analysis. In: *Pharmaceutical research* 28 (2011), Nr. 5, S. 1049–1064

[15] BALARATNASINGAM, C. ; DHRAMI-GAVAZI, E. ; MCCANN, J. T. ; GHADIALI, Q. ; FREUND, K. B.: Aflibercept: a review of its use in the treatment of choroidal neovascularization due to age-related macular degeneration. In: *Clinical ophthalmology (Auckland, NZ)* 9 (2015), S. 2355

[16] BALL, J. M.: Convexity conditions and existence theorems in nonlinear elasticity. In: *Archive for Rational Mechanics and Analysis* 63 (1976), Dec, Nr. 4, S. 337–403

[17] BANGERTH, W. ; HARTMANN, R. ; KANSCHAT, G. : deal. II—a general-purpose object-oriented finite element library. In: *ACM Transactions on Mathematical Software (TOMS)* 33 (2007), Nr. 4, S. 24–es

[18] BARTON, K. ; SHUI, Y.-B. ; PETRASH, M. ; BEEBE, D. : Comment on: The Stokes-Einstein equation and the physiological effects of vitreous surgery. In: *Acta ophthalmologica Scandinavica* 85 (2007), 06, S. 339–40. http://dx.doi.org/10.1111/j.1600-0420.2007.00902.x. – DOI 10.1111/j.1600–0420.2007.00902.x

[19] BEAR, J. ; BACHMAT, Y. : Introduction to modeling of transport phenomena in porous media, Springer Netherlands, 1990 (Theory and Applications of Transport in Porous Media)

[20] BEAVERS, G. S. ; JOSEPH, D. D.: Boundary conditions at a naturally permeable wall. In: *Journal of Fluid Mechanics* 30 (1967), Nr. 1, S. 197–207. http://dx.doi.org/10.1017/S0022112067001375. – DOI 10.1017/S0022112067001375

[21] BEJAOUI, O. ; MAJDOUB, M. : Global weak solutions for some Oldroyd models. In: *Journal of Differential Equations* 254 (2013), jan, Nr. 2, S. 660–685

[22] BIOT, M. A.: Theory of elasticity and consolidation for a porous anisotropic solid. In: *Journal of applied physics* 26 (1955), Nr. 2, S. 182–185

[23] BLACK, J. ; HASTINGS, G. : *Handbook of Biomaterial Properties*. Springer US, 2013

[24] BONFIGLIO, A. ; REPETTO, R. ; SIGGERS, J. H. ; STOCCHINO, A. : Investigation of the motion of a viscous fluid in the vitreous cavity induced by eye rotations and implications for drug delivery. In: *Physics in Medicine and Biology* 58 (2013), mar, Nr. 6, S. 1969–1982

[25] BOS, K. ; HOLMES, D. ; MEADOWS, R. ; KADLER, K. ; MCLEOD, D. ; BISHOP, P. : Collagen fibril organisation in mammalian vitreous by freeze etch/rotary shadowing electron microscopy. In: *Micron* 32 (2001), Nr. 3, S. 301 – 306

[26] BRENNER, S. C. ; SCOTT, L. R. ; SCOTT, L. R.: *The mathematical theory of finite element methods*. Bd. 3. Springer, 2008

[27] BURD, H. ; WILDE, G. ; JUDGE, S. : An improved spinning lens test to determine the stiffness of the human lens. In: *Experimental eye research* 92 (2011), Nr. 1, S. 28–39

[28] CASTRO, Á. ; CÓRDOBA, D. ; GANCEDO, F. ; ORIVE, R. : Incompressible flow in porous media with fractional diffusion. In: *Nonlinearity* 22 (2009), Nr. 8, S. 1791

[29] CHANG, R.-Y. ; YANG, W.-H. : Numerical simulation of mold filling in injection molding using a three-dimensional finite volume approach. In: *International Journal for Numerical Methods in Fluids* 37 (2001), S. 125–148

[30] CRANK, J. : *Mathematics of Diffusion*. Oxford & Clarendon Press, 1975

[31] DAL, H. ; GÖKTEPE, S. ; KALISKE, M. ; KUHL, E. : A fully implicit finite element method for bidomain models of cardiac electrophysiology. In: *Computer Methods in Biomechanics and Biomedical Engineering* 15 (2012), Nr. 6, S. 645–656

[32] DARCY, H. : *Les fontaines publiques de la ville de Dijon: exposition et application...* Victor Dalmont, 1856

[33] DIAS, C. ; MITRA, A. : Vitreal elimination kinetics of large molecular weight FITC-labeled dextrans in albino rabbits using a novel microsampling technique. In: *Journal of pharmaceutical sciences* 89 (2000), 05, S. 572–8. http://dx.doi.org/10.1002/(SICI)1520-6017(200005)89:5<572::AID-JPS2>3.0.CO;2-P. – DOI 10.1002/(SICI)1520–6017(200005)89:5<572::AID–JPS2>3.0.CO;2–P

[34] DISEASE STUDY 2013 COLLABORATORS, G. B.: Global, regional, and national incidence, prevalence, and years lived with disability for 301 acute and chronic diseases and injuries in 188 countries, 1990–2013: a systematic analysis for the Global Burden of Disease Study 2013. In: *The Lancet* 386 (2015), Nr. 9995, S. 743 – 800

[35] DÖRSAM, S. ; OLKHOVSKIY, V. ; STEIN, J. ; ZIRJACKS, P. ; AUFFARTH, G. ; FRIEDMANN, E. : The Virtual Eye-the basis of in silico treatments. In: *Investigative Ophthalmology & Visual Science* 59 (2018), Nr. 9, S. 5285–5285

[36] DOSTALÍK, M. ; PRŮŠA, V. ; TŮMA, K. : Finite amplitude stability of internal steady flows of the Giesekus viscoelastic rate-type fluid. In: *Entropy* 21 (2019), Nr. 12, S. 1219

[37] DOSTALÍK, M. ; PRŮŠA, V. ; RAJAGOPAL, K. R.: Unconditional finite amplitude stability of a fluid in a mechanically isolated vessel with spatially non-uniform wall temperature. In: *Continuum Mechanics and Thermodynamics* 33 (2021), Nr. 2, S. 515–543

[38] DOSTALÍK, M. ; PRŮŠA, V. ; STEIN, J. : Unconditional finite amplitude stability of a viscoelastic fluid in a mechanically isolated vessel with spatially non-uniform wall temperature. In: *Mathematics and Computers in Simulation* 189 (2021), S. 5–20

[39] DROBNY, A. ; FRIEDMANN, E. : Numerical Solution of Viscoelastic Fluid-Structure-Diffusion Systems with Applications in Ophthalmology. In: *PAMM* 19 (2019), Nr. 1, S. e201900348

[40] DROBNY, A. ; FRIEDMANN, E. : Numerical Simulation of Viscoelastic Fluid-Structure Interaction Problems and Drug Therapy in the Eye. In: *PAMM* 20 (2021), Nr. 1, S. e202000260

[41] DÖRSAM, S. ; FRIEDMANN, E. ; STEIN, J. : Modeling and Simulations of Drug Distribution in the Human Vitreous. In: ŠIMURDA, D. (Hrsg.) ; BODNÁR, T. (Hrsg.): *Topical Problems of Fluid Mechanics*. Prague, 2017, S. 95–102

[42] DURAIRA, C. ; SHA, J. C. ; SENAPATI, S. ; KOMPELLA, U. B.: Prediction of vitreal half-life based on drug physicochemical properties: quantitative structure-pharmacokinetic relationships (QSPKR). In: *Pharmaceutical Research* 26 (2009), Nr. 5, S. 1236–1260

[43] EBERWEIN, P. ; NOHAVA, J. ; SCHLUNCK, G. ; SWAIN, M. : Nanoindentation Derived Mechanical Properties of the Corneoscleral Rim of the Human Eye. In: *Local Mechanical Properties X* Bd. 606, Trans Tech Publications Ltd, 6 2014 (Key Engineering Materials), S. 117–120

[44] EDINGTON, M. ; CONNOLLY, J. ; CHONG, N. V.: Pharmacokinetics of intravitreal anti-VEGF drugs in vitrectomized versus non-vitrectomized eyes. In: *Expert opinion on drug metabolism & toxicology* 13 (2017), Nr. 12, S. 1217–1224

[45] EDWARDS, D. A.: Non-fickian diffusion in thin polymer films. In: *Journal of Polymer Science Part B: Polymer Physics* 34 (1996), Nr. 5, 981–997. http://dx.doi.org/10.1002/(SICI)1099-0488(19960415)34:5<981::AID-POLB16>3.0.CO;2-7. – DOI 10.1002/(SICI)1099–0488(19960415)34:5<981::AID–POLB16>3.0.CO;2–7. – ISSN 1099–0488

[46] EDWARDS, D. A. ; COHEN, D. S.: A mathematical model for a dissolving polymer. In: *AIChE Journal* 41 (1995), Nr. 11, S. 2345–2355

[47] ENGLER, C. ; SANDER, B. ; LARSEN, M. ; DALGAARD, P. ; LUND-ANDERSEN, H. : Fluorescein transport across the human blood-retina

barrier in the direction vitreous to blood. In: *Acta Ophthalmologica* 72 (1994)

[48] EVANS, L. : *Partial Differential Equations*. American Mathematical Society (Graduate studies in mathematics). https://books.google.de/books?id=Xnu0o_EJrCQC. – ISBN 9780821849743

[49] FATT, I. ; HEDBYS, B. : Flow of water in the sclera. In: *Experimental Eye Research* 10 (1970), Nr. 2, S. 243–249

[50] FERRARA, N. ; DAMICO, L. ; SHAMS, N. ; LOWMAN, H. ; KIM, R. : Development of ranibizumab, an anti–vascular endothelial growth factor antigen binding fragment, as therapy for neovascular age-related macular degeneration. In: *Retina* 26 (2006), Nr. 8, S. 859–870

[51] FERREIRA, J. ; GRASSI, M. ; GUDIÑO, E. ; OLIVEIRA, P. de: A new look to non-Fickian diffusion. 39 (2014), 06

[52] FERREIRA, J. ; OLIVEIRA, P. de ; SILVA, P. : Reaction–diffusion in viscoelastic materials. 236 (2012), 09, S. 3783–3795

[53] FERREIRA, J. ; BARBEIRO, S. ; PENA, G. ; WHEELER, M. : *Modelling and Simulation in Fluid Dynamics in Porous Media* (Springer Proceedings in Mathematics & Statistics). – ISBN 9781461450559

[54] FERREIRA, J. ; GONÇALVES, M. ; GUDIÑO, E. ; MAIA, M. ; OISHI, C. : Mathematical model for degradation and drug release from an intravitreal biodegradable implant. In: *Computers & Mathematics with Applications* 80 (2020), Nr. 10, S. 2212–2240

[55] FERREIRA, J. ; OLIVEIRA, P. de ; SILVA, P. da ; MURTA, J. : Numerical simulation of aqueous humor flow: From healthy to pathologic situations. In: *Applied Mathematics and Computation* 226 (2014), 777 - 792. http://dx.doi.org/https://doi.org/10.1016/j.amc.2013.10.070. – DOI https://doi.org/10.1016/j.amc.2013.10.070. – ISSN 0096–3003

[56] FERREIRA, J. ; OLIVEIRA, P. de ; SILVA, P. da ; SILVA, R. : Mathematics of aging: Diseases of the posterior segment of the eye. In: *Computers & Mathematics with Applications* 73 (2017), Nr. 1, 11 - 26. http://dx.doi.org/https://doi.org/10.1016/j.camwa.2016.10.013. – DOI https://doi.org/10.1016/j.camwa.2016.10.013. – ISSN 0898–1221

[57] FERREIRA, J. A. ; OLIVEIRA, P. de ; SILVA, P. da ; SIMON, L. : Flux tracking in drug delivery. In: *Applied Mathematical Modelling* 35 (2011), Nr. 10, S. 4684 – 4696

[58] FITT, A. D. ; GONZALEZ, G. : Fluid Mechanics of the Human Eye: Aqueous Humour Flow in the Anterior Chamber. In: *Bulletin of Mathematical Biology* 68 (2006), Nr. 1, S. 53–71

[59] FOLGAR, F. ; CHARLES L. TUCKER, I. : Orientation Behavior of Fibers in Concentrated Suspensions. In: *Journal of Reinforced Plastics and Composites* 3 (1984), Nr. 2, S. 98–119

[60] FRIEDMANN, E. ; DOERSAM, S. ; STEIN, J. ; AUFFARTH, G. U.: Effectiveness Analysis of Action of Drugs for the Treatment of Retinal Diseases. In: *2018 ASCRS ASOA Annual Meeting* ASCRS, 2018

[61] FRIEDRICH, S. ; CHENG, Y.-L. ; SAVILLE, B. : Drug distribution in the vitreous humor of the human eye: the effects of intravitreal injection position and volume. In: *Current Eye Research* (1997)

[62] FRIEDRICH, S. ; CHENG, Y.-L. ; SAVILLE, B. : FE modeling of drug distribution in the vitreous humor of the rabbit eye. In: *Annals of biomedical Engineering* (1997)

[63] FRIEDRICH, S. ; CHENG, Y.-L. ; SAVILLE, B. : Mathematical Modeling of Drug Distribution in the Vitreous Humor. In: *CRC Press* (2003), S. 181–221

[64] FRIEDRICHS, K. : Die Randwert- und Eigenwertprobleme aus der Theorie der elastischen Platten. (Anwendung der direkten Methoden der Variationsrechnung). In: *Mathematische Annalen* 98 (1928), S. 205–247

[65] In: GALDI, G. P.: *An Introduction to the Navier-Stokes Initial-Boundary Value Problem*. Birkhäuser Basel, 1–70

[66] *Kapitel* Mathematical Problems in Classical and Non-Newtonian Fluid Mechanics. In: GALDI, G. ; RANNACHER, R. ; ROBERTSON, A. ; TUREK, S. : *Hemodynamical Flows: Modeling, Analysis and Simulation*. Oberwolfach Seminars. Berlin : Birkhäuser Verlag, 2008, S. 121–274

[67] GOFF, M. L. ; BISHOP, P. : Adult vitreous structure and postnatal changes. In: *Eye* 22 (2008), S. 1214–1222

[68] GRASSELLI, M. ; LORENZI, A. : Abstract nonlinear Volterra integrodifferential equations with nonsmooth kernels. In: *Atti della Accademia Nazionale dei Lincei. Classe di Scienze Fisiche, Matematiche e Naturali. Rendiconti Lincei. Matematica e Applicazioni* 2 (1991), Nr. 1, S. 43–53

[69] GRASSI, M. ; GRASSI, G. : Mathematical Modelling and Controlled Drug Delivery: Matrix Systems. 2 (2005), 02, S. 97–116

[70] GREEN, A. E.: A continuum theory of anisotropic fluids. In: *Mathematical Proceedings of the Cambridge Philosophical Society* 60 (1964), Nr. 1, S. 123–128. http://dx.doi.org/10.1017/S0305004100037531. – DOI 10.1017/S0305004100037531

[71] GRYTZ, R. ; FAZIO, M. A. ; GIRARD, M. J. ; LIBERTIAUX, V. ; BRUNO, L. ; GARDINER, S. ; GIRKIN, C. A. ; DOWNS, J. C.: Material Properties of the Posterior Human Sclera. In: *Journal of the mechanical behavior of biomedical materials* 29 (2014), S. 1–29

[72] GUDIÑO ROJAS, E. A.: *Recent developments in non-Fickian diffusion: a new look at viscoelastic materials*, Diss., 2014

[73] GUILLOPÉ, C. ; SAUT, J. C.: Global existence and one-dimensional nonlinear stability of shearing motions of viscoelastic fluids of Oldroyd type. In: *ESAIM: Mathematical Modelling and Numerical Analysis-Modélisation Mathématique et Analyse Numérique* 24 (1990), Nr. 3, S. 369–401

[74] GURTIN, M. ; FRIED, E. ; ANAND, L. : *The Mechanics and Thermodynamics of Continua*. Cambridge University Press, 2010

[75] HAGHJOU, N. ; ABDEKHODAIE, M. J. ; CHENG, Y. L. ; SAADATMAND, M. : Computer Modeling of Drug Distribution after Intravitreal Administration. In: *World Academy of Science, Engineering and Technology* 53 (2011), S. 706–716

[76] HARTMANN, S. ; NEFF, P. : Polyconvexity of generalized polynomial-type hyperelastic strain energy functions for near-incompressibility. In: *International Journal of Solids and Structures* 40 (2003), Nr. 11, 2767 - 2791. http://dx.doi.org/https://doi.org/10.1016/S0020-7683(03)00086-6. – DOI https://doi.org/10.1016/S0020–7683(03)00086–6. – ISSN 0020–7683

[77] HEIDA, M. ; MÁLEK, J. ; RAJAGOPAL, K. R.: On the development and generalizations of Cahn–Hilliard equations within a thermodynamic framework. In: *Zeitschrift für angewandte Mathematik und Physik* 63 (2012), Nr. 1, S. 145–169

[78] HENEIN, C. ; AWWAD, S. ; IBEANU, N. ; VLATAKIS, S. ; BROCCHINI, S. ; TEE KHAW, P. ; BOUREMEL, Y. : Hydrodynamics of intravitreal injections into liquid vitreous substitutes. In: *Pharmaceutics* 11 (2019), Nr. 8, S. 371

[79] HEYS, K. R. ; CRAM, S. L. ; TRUSCOTT, R. J. W.: Massive increase in the stiffness of the human lens nucleus with age: the basis for presbyopia? In: *Molecular vision* 10 (2004), S. 956–963

[80] HEYWOOD, J. ; RANNACHER, R. ; TUREK, S. : Artificial boundaries and flux and pressure conditions for the incompressible Navier-Stokes equations. In: *International Journal for Numerical Methods in Fluids* 22 (1996), Nr. 5, S. 325–352

[81] HOLZAPFEL, G. : *Nonlinear Solid Mechanics: A Continuum Approach for Engineering*. Wiley, 2000

[82] HRON, J. ; MILOŠ, V. ; PRŮŠA, V. ; SOUČEK, O. ; TŮMA, K. : On thermodynamics of incompressible viscoelastic rate type fluids with temperature dependent material coefficients. In: *International Journal of Non-Linear Mechanics* 95 (2017), Oct, 193–208. http://dx.doi.org/10.1016/j.ijnonlinmec.2017.06.011. – DOI 10.1016/j.ijnonlinmec.2017.06.011. – ISSN 0020–7462

[83] HRON, J. ; RAJAGOPAL, K. ; TŮMA, K. : Flow of a Burgers fluid due to time varying loads on deforming boundaries. In: *Journal of Non-Newtonian Fluid Mechanics* 210 (2014), 08. http://dx.doi.org/10.1016/j.jnnfm.2014.05.005. – DOI 10.1016/j.jnnfm.2014.05.005

[84] HUTTER, K. ; JÖHNK, K. D.: Continuum methods of physical modeling. In: *JOURNAL OF FLUID MECHANICS* 526 (2005), Nr. 1, S. 377–378

[85] HUTTON-SMITH, L. ; GAFFNEY, E. ; BYRNE, H. ; MAINI, P. ; GADKAR, K. ; MAZER, N. : Ocular Pharmacokinetics of Therapeutic Antibodies Given by Intravitreal Injection: Estimation of Retinal Permeabilities Using a 3-Compartment Semi-Mechanistic Model. In: *Molecular Pharmaceutics* 14 (2017), 06. http://dx.doi.org/10.1021/acs.molpharmaceut.7b00164. – DOI 10.1021/acs.molpharmaceut.7b00164

[86] HUYNH, H. M.: *Improved Fiber Orientation Predictions for Injection-Molded Composites*, University of Illinois Urbana-Champaign, Diplomarbeit, 2001

[87] IGUCHI, Y. ; ASAMI, T. ; UENO, S. ; USHIDA, H. ; MARUKO, R. ; OIWA, K. ; TERASAKI, H. : Changes in Vitreous Temperature During Intravitreal Surgery. In: *Investigative Ophthalmology & Visual Science* 55 (2014), 04, Nr. 4, S. 2344–2349

[88] JEFFERY, G. B.: The Motion of Ellipsoidal Particles Immersed in a Viscous Fluid. In: *Proceedings of the Royal Society of London Series A* 102 (1922), S. 161–179

[89] JONGEBLOED, W. ; WORST, J. : The cisternal anatomy of the vitreous body. In: *Documenta Ophthalmologica* 67 (2004), S. 183–196

[90] JOSEPH, D. D.: Fluid Dynamics of Mixtures of Incompressible Miscible Liquids. In: *Applied and Numerical Partial Differential Equations*. Springer, 2010, S. 127–145

[91] KAISER, R. ; MAURICE, D. : The diffusion of fluorescein in the lens. In: *Experimental Eye Research* 3 (1964), Nr. 2, 156 - IN2. `http://dx.doi.org/https://doi.org/10.1016/S0014-4835(64)80030-0`. – DOI https://doi.org/10.1016/S0014–4835(64)80030–0. – ISSN 0014–4835

[92] KALONI, P. ; DESILVA, C. : A theory of oriented fluids. In: *The Physics of Fluids* 13 (1970), Nr. 7, S. 1708–1716

[93] KATHAWATE, J. ; ACHARYA, S. : Computational modeling of intravitreal drug delivery in the vitreous chamber with different vitreous substitutes. In: *International Journal of Heat and Mass Transfer* 51 (2008), Nr. 23-24, S. 5598–5609

[94] KAUFMAN, P. L. ; ALM, A. : *Adler's Physiology of the Eye*. 10th ed. Mosby Year book, 2003

[95] KIM, R. Y. ; KWON, S. ; RA, H. : Gravity influences bevacizumab distribution in an undisturbed balanced salt solution in vitro. In: *Plos one* 14, Nr. 10

[96] KLEINBERG, T. T. ; TZEKOV, R. T. ; STEIN, L. ; RAVI, N. ; KAUSHAL, S. : Vitreous substitutes: a comprehensive review. In: *Survey of ophthalmology* 56 (2011), Nr. 4, S. 300–323

[97] KORTEWEG, D. J.: Sur la forme que prennent les équations du mouvements des fluides si l'on tient compte des forces capillaires causées par des variations de densité considérables mais connues et sur la théorie de la capillarité dans l'hypothèse d'une variation continue de la densité. In: *Archives Néerlandaises des Sciences exactes et naturelles* 6 (1901), S. 1–24

[98] KOSTIN, ILYA ; MARION, MARTINE ; TEXIER-PICARD, ROZENN ; VOLPERT, VITALY A.: Modelling of Miscible Liquids with the Korteweg Stress. In: *ESAIM: M2AN* 37 (2003), Nr. 5, 741-753. `http://dx.doi.org/10.1051/m2an:2003042`. – DOI 10.1051/m2an:2003042

[99] KOTHA, S. ; MURTOMäKI, L. : Virtual pharmacokinetic model of human eye. In: *Mathematical Biosciences* 253 (2014), S. 11–18

[100] KUPPEL, L. : *Existence and uniqueness for a model of miscible liquids*. 2017

[101] LADYZHENSKAYA, O. A. ; SOLONNIKOW, W. A. ; URALTSEVA, N. : *Linear and Quasi-linear Equations of Parabolic Type*. American Mathematical Society, 1968

[102] LADYZHENSKAYA, O. A.: *Linear and Quasilinear Elliptic Equations*. Elsevier Science, 1968 (Mathematics in Science and Engineering). – ISBN 9780080955544

[103] LANDERS III, M. B. ; WATSON, J. S. ; ULRICH, J. N. ; QUIROZ-MERCADO, H. : Determination of retinal and vitreous temperature in vitrectomy. In: *Retina* 32 (2012), Nr. 1, S. 172–176

[104] LARSEN, J. ; LUND-ANDERSEN, H. ; KROGSAA, B. : Transient transport across the blood-retina barrier. In: *Bulletin of Mathematical Biology* 45 (1983), Nr. 5, 749 - 758. http://dx.doi.org/https://doi.org/10.1016/S0092-8240(83)80023-8. – DOI https://doi.org/10.1016/S0092–8240(83)80023–8. – ISSN 0092–8240

[105] LAX, P. : *Functional Analysis*. Wiley, 2014 (Pure and Applied Mathematics: A Wiley Series of Texts, Monographs and Tracts). – ISBN 9781118626740

[106] LEE, B. ; LITT, M. ; BUCHSBAUM, G. : Rheology of the vitreous body. Part I: Viscoelasticity of human vitreous. In: *Biorheology* 29 (1992), S. 521–533

[107] LEE, B. ; LITT, M. ; BUCHSBAUM, G. : Rheology of the vitreous body. Part 2: Viscoelasticity of bovine and porcine vitreous. In: *Biorheology* 31 (1994), S. 327–338

[108] LEI, Z. ; LIU, C. ; ZHOU, Y. : Global solutions for incompressible viscoelastic fluids. In: *Archive for Rational Mechanics and Analysis* 188 (2008), Nr. 3, S. 371–398

[109] LEI, Z. ; ; ZHOU, Y. : Global Existence of Classical Solutions for the Two-Dimensional Oldroyd Model via the Incompressible Limit. 37 (2005), Nr. 3, S. 797–814

[110] LEVIN, L. ; NILSSON, S. ; HOEVE, J. ; WU, S. ; KAUFMAN, P. ; ALM, A. : *Adler's Physiology of the Eye*. Elsevier Health Sciences, 2011

[111] LI, K. ; LIMJOCO, M. ; ZARATE, J. : *3D modeling of aflibercept transport in the vitreous humor*. BEE/MAE4530: Computer Aided Engineering: Applications to Biological Processes, May 11 2017

[112] LIONS, J. L. ; MAGENES, E. : *Non-Homogeneous Boundary Value Problems and Applications*. Springer-Verlag, 1972

[113] LIONS, P. L. ; MASMOUDI, N. : Global solutions for some Oldroyd models of non-Newtonian flows. In: *Chinese Annals of Mathematics* 21 (2000), Nr. 02, S. 131–146

[114] LITWILLER, D. V. ; LEE, S. J. ; KOLIPAKA, A. ; MARIAPPAN, Y. K. ; GLASER, K. J. ; PULIDO, J. S. ; EHMAN, R. L.: MR elastography of the ex vivo bovine globe. In: *Journal of magnetic resonance imaging : JMRI* 32 1 (2010), S. 44–51

[115] LIU, Q. ; WANG, X. ; KEE, D. D.: Mass transport through swelling membranes. In: *International Journal of Engineering Science* 43 (2005), Nr. 19, 1464 - 1470. `http://dx.doi.org/https://doi.org/10.1016/j.ijengsci.2005.05.010`. – DOI https://doi.org/10.1016/j.ijengsci.2005.05.010. – ISSN 0020–7225

[116] LUND-ANDERSEN, H. ; KROGSAA, B. ; COUR, M. la ; LARSEN, J. : Quantitative vitreous fluorophotometry applying a mathematical model of the eye. In: *Investigative Ophthalmology & Visual Science* 26 (1985), 05, Nr. 5, S. 698–710

[117] MÁLEK, J. ; PRŮŠA, V. : Derivation of Equations for Continuum Mechanics and Thermodynamics of Fluids. In: *Handbook of Mathematical Analysis in Mechanics of Viscous Fluids* (2018), S. 3–72

[118] MARIEB, E. N. ; HOEHN, K. : *Human Anatomy & Physiology*. 7th ed., Pearson Education Inc., 2006

[119] MARSDEN, J. ; HUGHES, T. : *Mathematical Foundations of Elasticity*. Dover, 1994 (Dover Civil and Mechanical Engineering Series). – ISBN 9780486678658

[120] MASON, M. ; WEAVER, W. : The Settling of Small Particles in a Fluid. In: *Phys. Rev.* 23 (1924), S. 412–426

[121] MASUD, A. ; HUGHES, T. J. R.: A stabilized mixed finite element method for Darcy flow. In: *Computer methods in applied mechanics and engineering* 191 (2002), S. 4341–4370

[122] MAURICE, D. : Review: Practical Issues in Intravitreal Drug Delivery. In: *Journal of Ocular Pharmacology and Therapeutics* 17 (2001), Nr. 4, S. 393–401

[123] MERAL, I. ; KARADENIZ BILGILI, M. : Diffusion Changes in the Vitreous Humor of the Eye during Aging. In: *AJNR. American journal of neuroradiology* 32 (2011), 07, S. 1563–6. http://dx.doi.org/10.3174/ajnr.A2543. – DOI 10.3174/ajnr.A2543

[124] MIKELIĆ, A. ; AGANOVIĆ, I. : Homogenization of stationary flow of miscible fluid in a domain with grained boundary. In: *SIAM Journal on Mathematical Analysis* 19 (1988), Nr. 2, S. 287–294

[125] In: MIKELIĆ, A. : *Regularity and Uniqueness Results for Two-Phase Miscible Flows in Porous Media*. Bd. 114. Basel : Birkhäuser Basel, 1993, S. 139–154

[126] MIKELIC, A. ; JÄGER, W. : On The Interface Boundary Condition of Beavers, Joseph, and Saffman. In: *SIAM Journal on Applied Mathematics* 60 (2000), Nr. 4, S. 1111–1127

[127] MISSEL, P. J.: Simulating Intravitreal Injections in Anatomically Accurate Models for Rabbit, Monkey, and Human Eyes. In: *Pharmaceutical Research* 29 (2012), Nr. 12, S. 3251– 3272

[128] MÁLEK, J. ; RAJAGOPAL, K. ; TŮMA, K. : On a variant of the Maxwell and Oldroyd-B models within the context of a thermodynamic basis. In: *International Journal of Non-Linear Mechanics* 76 (2015), 42 - 47. http://dx.doi.org/https://doi.org/10.1016/j.ijnonlinmec.2015.03.009. – DOI https://doi.org/10.1016/j.ijnonlinmec.2015.03.009. – ISSN 0020–7462

[129] MÁLEK, J. ; RAJAGOPAL, K. ; TŮMA, K. : Derivation of the Variants of the Burgers Model Using a Thermodynamic Approach and Appealing to the Concept of Evolving Natural Configurations. In: *Fluids* 3 (2018), 09, S. 69. http://dx.doi.org/10.3390/fluids3040069. – DOI 10.3390/fluids3040069

[130] MOLOKHIA, S. ; JEONG, E.-K. ; HIGUCHI, W. ; LI, S. : Transscleral iontophoretic and intravitreal delivery of a macromolecule: Study of ocular distribution in vivo and postmortem with MRI. In: *Experimental Eye Research* 88 (2009), 03, S. 418–425. http://dx.doi.org/10.1016/j.exer.2008.10.010. – DOI 10.1016/j.exer.2008.10.010

[131] MUNGALL, J. : Interfacial tension in miscible two-fluid systems with linear viscoelastic rheology. In: *Physical review letters* 73 (1994), Nr. 2, S. 288

[132] N. PLANGE, P. W.: *Basiswissen Augenheilkunde*. Springer, 2017

[133] NEURINGER, J. L.: Green's Function for an Instantaneous Line Particle Source Diffusing in a Gravitational Field and Under the Influence of a Linear Shear Wind. In: *SIAM Journal on Applied Mathematics* 16 (1968), Nr. 4, S. 834–842

[134] NICKERSON, C. S. ; PARK, J. ; KORNFIELD, J. A. ; KARAGEOZIAN, H. : Rheological properties of the vitreous and the role of hyaluronic acid. In: *Journal of Biomechanics* 41 (2008), Nr. 9, 1840 - 1846. http://dx.doi.org/https://doi.org/10.1016/j.jbiomech.2008.04.015. – DOI https://doi.org/10.1016/j.jbiomech.2008.04.015. – ISSN 0021–9290

[135] NISHIMURA, Y. ; HAYASHI, H. ; OSHIMA, K. ; IWATA, S. : The diffusion of fluorescein in the bovine vitreous. In: *Acta Ophthalmol. Jpn.* 90 (1986), S. 1313–1316

[136] NIWA, Y. ; KAKINOKI, M. ; SAWADA, T. ; WANG, X. ; OHJI, M. : Ranibizumab and aflibercept: intraocular pharmacokinetics and their effects on aqueous VEGF level in vitrectomized and nonvitrectomized macaque eyes. In: *Investigative ophthalmology & visual science* 56 (2015), Nr. 11, S. 6501–6505

[137] OHTORI, A. ; TOJO, K. : In Vivo/in Vitro Correlation of Intravitreal Delivery of Drugs with the Help of Computer Simulation. In: *Biological & Pharmaceutical Bulletin* 17 (1994), Nr. 2, S. 283–290. http://dx.doi.org/10.1248/bpb.17.283. – DOI 10.1248/bpb.17.283

[138] OLDROYD, J. G. ; WILSON, A. H.: On the formulation of rheological equations of state. In: *Proceedings of the Royal Society of London. Series A. Mathematical and Physical Sciences* 200 (1950), Nr. 1063, S. 523–541

[139] OLKHOVSKIY, V. : *Modeling and Simulation of the Aqueous Humor Flow for Healthy, Glaucomatous and Treated Eyes with Stokes and Darcy Equations*, Heidelberg University, Diss., 2020

[140] OSEEN, C. : The theory of liquid crystals. In: *Transactions of the Faraday Society* 29 (1933), Nr. 140, S. 883–899

[141] OUMER, A. N. ; ALI, A. M. S. ; MAMAT, O. B.: Numerical simulation of fiber orientation in simple injection molding processes. In: *International Journal of Mechanical & Mechatronics Engineering IJMME-IJENS* 9 (2009), Nr. 9, S. 18–24

[142] PARK, J. ; BUNGAY, P. M. ; LUTZ, R. J. ; AUGSBURGER, J. J. ; MILLARD, R. W. ; ROY, A. S. ; BANERJEE, R. K.: Evaluation of coupled convective–diffusive transport of drugs administered by intravitreal injection and controlled release implant. In: *Journal of Controlled Release* 105 (2005), Nr. 3, S. 279 – 295

[143] PENKOVA, A. N. ; MARTINEZ, J. C. ; HUMAYUN, M. ; TADLE, A. ; GALESIC, A. ; CALLE, A. ; THOMPSON, M. ; PRATT, M. ; SADHAL, S. S.: BEVACIZUMAB DIFFUSION COEFFICIENT IN VIVO MEASUREMENT OF RABBIT VITREOUS HUMOR WITH FLUORESCEIN LABELING. In: *Investigative Ophthalmology & Visual Science* 60 (2019), Nr. 9, S. 1552–5783

[144] PITKÄNEN, L. ; RANTA, V. ; MOILANEN, V. H. ; URTTI, A. : Permeability of retinal pigment epithelium: effects of permeant molecular weight and lipophilicity. In: *Investigative Ophthalmology and Visual Science* 46 (2005), Nr. 2, S. 641–646

[145] QUINTANILLA, R. ; RAJAGOPAL, K. R.: On Burgers fluid. In: *Mathematical Methods in the Applied Sciences* 29 (2006), S. 2133–2147

[146] QUINTANILLA, R. ; RAJAGOPAL, K. R.: Further mathematical results concerning Burgers fluids and their generalizations. In: *Zeitschrift für angewandte Mathematik und Physik* 63 (2012), S. 191–202

[147] RAJAGOPAL, K. ; SRINIVASA, A. : A thermodynamic frame work for rate type fluid models. In: *Journal of Non-Newtonian Fluid Mechanics* 88 (2000), Nr. 3, S. 207 – 227

[148] RAJAGOPAL, K. ; SRINIVASA, A. : Modeling anisotropic fluids within the framework of bodies with multiple natural configurations. In: *Journal of Non-Newtonian Fluid Mechanics* 99 (2001), Nr. 2-3, S. 109–124

[149] RANNACHER, R. : *Numerik 1: Numerik gewöhnlicher Differentialgleichungen*. Heidelberg University, 2017

[150] RANNACHER, R. : *Numerik 2: Numerik partieller Differentialgleichungen*. Heidelberg University, 2017

[151] RATTANAKIJSUNTORN, K. ; PENKOVA, A. ; SADHA, S. : Mass diffusion coefficient measurement for vitreous humor using FEM and MRI. In: *IOP Conference Series: Materials Science and Engineering* 297 (2018), 01, S. 012024. http://dx.doi.org/10.1088/1757-899X/297/1/012024. – DOI 10.1088/1757–899X/297/1/012024

[152] REID, R. C. ; PRAUSNITZ, J. M. ; POLING, B. E.: The properties of gases and liquids. (1987)

[153] REPETTO, R. ; SIGGERS, J. ; STOCCHINO, A. : Mathematical model of flow in the vitreous humor induced by saccadic eye rotations: effect of geometry. In: *Biomechanics and Modeling in Mechanobiology* 9 (2010), S. 65–76

[154] SAFFMAN, P. G.: On the Boundary Condition at the Surface of a Porous Medium. In: *Studies in Applied Mathematics* 50 (1971), Nr. 2, S. 93–101

[155] In: SANG, D. N.: *Embryology of the Vitreous. Congenital and Developmental Abnormalities*. New York, NY : Springer New York, 1987, S. 11–35

[156] SAPOSNIKOVA, T. ; MAZ'YA, V. : *Sobolev Spaces*. Springer Berlin Heidelberg, 2013 (Springer Series in Soviet Mathematics)

[157] SCHNEIDER, L. ; HUTTER, K. : *Solid-Fluid Mixtures of Frictional Materials in Geophysical and Geotechnical Context: Based on a Concise Thermodynamic Analysis*. Springer Science & Business Media, 2009

[158] SCOVAZZI, G. ; WHEELER, M. F. ; MIKELIĆ, A. ; LEE, S. : Analytical and variational numerical methods for unstable miscible displacement flows in porous media. In: *Journal of Computational Physics* 335 (2017), S. 444–496

[159] SEBAG, J. : *Vitreous in Health and Disease*. Springer, 2014

[160] SEBAG, J. ; BALAZS, E. A.: Morphology and Ultrastructure of Human Vitreous Fibers. In: *Investigative Ophthalmology & Visual Science* 30 (1989), S. 1867–1871

[161] SEBAG, J. ; GREEN, W. : Vitreous and Vitreoretinal Interface. In: *Retina Fifth Edition* 1 (2012), 12, S. 482–516. http://dx.doi.org/10.1016/B978-1-4557-0737-9.00021-7. – DOI 10.1016/B978–1–4557–0737–9.00021–7. ISBN 9781455707379

[162] SHAFAIE, S. ; HUTTER, V. ; BROWN, M. ; COOK, M. ; CHAU, D. : Diffusion through the ex vivo vitreal body - Bovine, porcine, and ovine models are poor surrogates for the human vitreous. In: *International Journal of Pharmaceutics* 550 (2018), 07

[163] SHAH, N. S. ; BEEBE, D. C. ; LAKE, S. P. ; FILAS, B. A.: On the Spatiotemporal Material Anisotropy of the Vitreous Body in Tension and

Compression. In: *Annals of Biomedical Engineering* 44 (2016), Nr. 10, S. 3084–3095

[164] SHARIF-KASHANI, P. ; HUBSCHMAN, J.-P. ; SASSOON, D. ; PIROUZ KAVEHPOUR, H. : Rheology of the vitreous gel: Effects of macromolecule organization on the viscoelastic properties. In: *Journal of Biomechanics* 44 (2011), Nr. 3, S. 419–423

[165] SHOKRI, H. ; KAYHANI, M. ; NOROUZI, M. : A Numerical Study on Miscible Viscoelastic Fingering Instability. (2017)

[166] SILVA, A. ; ALVES, M. ; OLIVEIRA, M. : Rheological behaviour of vitreous humour. In: *Rheologica Acta* 56 (2017), 02, S. 1–10. http://dx.doi.org/10.1007/s00397-017-0997-0. – DOI 10.1007/s00397–017–0997–0

[167] SIMO, J. ; TAYLOR, R. ; PISTER, K. : Variational and projection methods for the volume constraint in finite deformation elasto-plasticity. In: *Computer Methods in Applied Mechanics and Engineering* 51 (1985), Nr. 1, 177 - 208. http://dx.doi.org/https://doi.org/10.1016/0045-7825(85)90033-7. – DOI https://doi.org/10.1016/0045–7825(85)90033–7. – ISSN 0045–7825

[168] SMITH, D. W. ; GARDINER, B. S.: Estimating outflow facility through pressure dependent pathways of the human eye. In: *PloS one* 12 (2017), Nr. 12, S. e0188769

[169] SPITZER, M. S. ; ZIEMSSEN, F. ; BARTZ-SCHMIDT, K. U. ; GELISKEN, F. ; SZURMAN, P. : Treatment of age-related macular degeneration: focus on ranibizumab. In: *Clinical ophthalmology (Auckland, NZ)* 2 (2008), Nr. 1, S. 1

[170] STAY, M. ; XU, J. ; RANDOLPH, T. ; BAROCAS, V. : Computer Simulation of Convective and Diffusive Transport of Controlled-Release Drugs in the Vitreous Humor. In: *Pharmaceutical research* 20 (2003), 02, S. 96–102. http://dx.doi.org/10.1023/A:1022207026982. – DOI 10.1023/A:1022207026982

[171] STEFFANSEN, B. ; BRODIN, B. ; NIELSEN, C. U.: *Molecular Biopharmaceutics - Aspects of drug characterisation, drug delivery and dosage form evaluation*. Pharmaceutical Press, 2010

[172] STEIN, J. ; PRŮŠA, V. : Viscoelastic rate type fluids with temperature dependent material parameters - Stability of the rest state. In: *AIP Conference Proceedings* Bd. 1843, 2017. – ISBN 9780735415133

[173] STEIN, J. ; TŮMA, K. ; AUFFARTH, G. U. ; PRŮŠA, V. ; FRIEDMANN, E. : Finite Element Numerical Simulation of Motion of Vitreous Humor in a Deforming Eye. In: *2018 ASCRS ASOA Annual Meeting* ASCRS, 2018

[174] STEIN, S. ; BOGDAHN, M. ; ROSENBAUM, C. ; WEITSCHIES, W. ; SEIDLITZ, A. : Distribution of fluorescein sodium and triamcinolone acetonide in the simulated liquefied and vitrectomized Vitreous Model with simulated eye movements. In: *European Journal of Pharmaceutical Sciences* 109 (2017), S. 233–243

[175] STEWART, M. : What are the half-lives of ranibizumab and aflibercept (VEGF Trap-eye) in human eyes? Calculations with a mathematical model. In: *Eye Reports* 1 (2011), 06. `http://dx.doi.org/10.4081/eye.2011.e5`. – DOI 10.4081/eye.2011.e5

[176] SU, X. ; VESCO, C. ; FLEMING, J. ; CHOH, V. : Density of Ocular Components of the Bovine Eye. In: *Optometry and Vision Science* 86 (2009), Nr. 10, S. 1187–1195

[177] TAN, L. E. ; ORILLA, W. ; HUGHES, P. M. ; TSAI, S. ; BURKE, J. A. ; WILSON, C. G.: Effects of vitreous liquefaction on the intravitreal distribution of sodium fluorescein, fluorescein dextran, and fluorescent microparticles. In: *Investigative ophthalmology & visual science* 52 (2011), Nr. 2, S. 1111–1118

[178] TEMAM, R. : *Navier-Stokes Equations: Theory and Numerical Analysis* (AMS/Chelsea publication). – ISBN 9780821827376

[179] TRAM, N. K. ; MAXWELL, C. J. ; SWINDLE-REILLY, K. E.: Macro-and Microscale Properties of the Vitreous Humor to Inform Substitute Design and Intravitreal Biotransport. In: *Current Eye Research* (2020), S. 1–16

[180] TRAM, N. K. ; SWINDLE-REILLY, K. E.: Rheological Properties and Age-Related Changes of the Human Vitreous Humor. In: *Frontiers in Bioengineering and Biotechnology* 6 (2018), Nr. 199, S. 1–12

[181] TŮMA, K. : *Identification of rate type fluids suitable for modelling geomaterials*, Charles University, Diss., 2013

[182] TŮMA, K. ; STEIN, J. ; PRŮŠA, V. ; FRIEDMANN, E. : Motion of the vitreous humour in a deforming eye–fluid-structure interaction between a nonlinear elastic solid and viscoleastic fluid. In: *Applied Mathematics and Computation* 335 (2018), S. 50 – 64

[183] UCHIO, E. ; OHNO, S. ; KUDOH, J. ; AOKI, K. ; TOMASZ KISIELEWICZ, L. : Simulation model of an eyeball based on finite element analysis on a supercomputer. In: *The British journal of ophthalmology* 83 (1999), 11, S. 1106–11

[184] VARELA-FERNÁNDEZ, R. ; DÍAZ-TOMÉ, V. ; LUACES-RODRÍGUEZ, A. ; CONDE-PENEDO, A. ; GARCÍA-OTERO, X. ; LUZARDO-ÁLVAREZ, A. ; FERNÁNDEZ-FERREIRO, A. ; OTERO-ESPINAR, F. J.: Drug delivery to the posterior segment of the eye: Biopharmaceutic and pharmacokinetic considerations. In: *Pharmaceutics* 12 (2020), Nr. 3, S. 269

[185] VOLPERT, V. A. ; POJMAN, J. A. ; TEXIER-PICARD, R. : Convection induced by composition gradients in miscible systems. In: *Comptes Rendus - Mecanique* 330 (2002), Nr. 5, S. 353–358. http://dx.doi.org/10.1016/S1631-0721(02)01467-5. – DOI 10.1016/S1631–0721(02)01467–5. – ISSN 16310721

[186] VOROTNIKOV, D. A.: Dissipative solutions for equations of viscoelastic diffusion in polymers. In: *Journal of mathematical analysis and applications* 339 (2008), Nr. 2, S. 876–888

[187] WANG, J. ; O'GARA, J. F. ; TUCKER, C. L.: An objective model for slow orientation kinetics in concentrated fiber suspensions: theory and rheological evidence. In: *Journal of Rheology* 52 (2008), Nr. 5, S. 1179–1200

[188] WHITAKER, S. : Flow in Porous Media I: A Theoretical Derivation of Darcy's Law. In: *Transport in Porous Media* 1 (1986), S. 3–25

[189] WILDE, G. ; BURD, H. ; JUDGE, S. : Shear modulus data for the human lens determined from a spinning lens test. In: *Experimental Eye Research* 97 (2012), Nr. 1, S. 36 – 48

[190] WINEMAN, A. ; RAJAGOPAL, K. : *Mechanical Response of Polymers: An Introduction*. Cambridge University Press, 2000 (Mechanical Response of Polymers: An Introduction)

[191] WLOKA, J. : *Partielle Differentialgleichungen: Sobolevräume und Randwertaufgaben* (Mathematische Leitfäden). – ISBN 9783519022251

[192] XU, J. ; HEYS, J. ; BAROCAS, V. ; RANDOLPH, T. : Permeability and Diffusion in Vitreous Humor: Implications for Drug Delivery. In: *Pharmaceutical research* 17 (2000), 07, S. 664–9. http://dx.doi.org/10.1023/A:1007517912927. – DOI 10.1023/A:1007517912927

[193] XU, Q. ; BOYLAN, N. J. ; SUK, J. S. ; WANG, Y.-Y. ; NANCE, E. A. ; YANG, J.-C. ; MCDONNELL, P. J. ; CONE, R. A. ; DUH, E. J. ; HANES, J. : Nanoparticle diffusion in, and microrheology of, the bovine vitreous ex vivo. In: *Journal of Controlled Release* 167 (2013), Nr. 1, S. 76 – 84

[194] YOON, S. ; AGLYAMOV, S. ; KARPIOUK, A. ; EMELIANOV, S. : The Mechanical Properties of Ex Vivo Bovine and Porcine Crystalline Lenses: Age-Related Changes and Location-Dependent Variations. In: *Ultrasound in Medicine & Biology* 39 (2013), Nr. 6, S. 1120 – 1127. – ISSN 0301–5629

[195] ZEIMER, R. C. ; BLAIR, N. P. ; CUNHA-VAZ, J. G.: Pharmacokinetic interpretation of vitreous fluorophotometry. In: *Investigative Ophthalmology & Visual Science* 24 (1983), 10, Nr. 10, S. 1374–1381